2022

The Chemical Characterization of Microplastic Polymer Composition from Various Littoral Environments on Cape Cod, Massachusetts

Leah Kosovsky

The Chemical Characterization of Microplastic Polymer Composition from Various Littoral Environments on Cape Cod, Massachusetts

Leah Kosovsky

Connecticut College, Department of Chemistry

New London, Connecticut 06320

Spring 2022

Advisor: Professor Marc Zimmer

“Can anyone believe it is possible to lay down
such a barrage of poisons on the surface of the Earth
without making it unfit for all life?”
– Rachel Carson, Silent Spring

Table of Contents

Acknowledgements

I would like to firstly thank my family and friends for their continuous love and support. Specifically, thank you to those who sent me every microplastic article they came across and listened to me go on and on about my research. I do not know where I would be without such a caring and encouraging support system. I would like to thank Professor Marc Zimmer for advising me on this thesis. Since my first semester at Connecticut College, he has inspired my love for chemistry. Thank you also to my academic advisor, Professor Stanton Ching. I am grateful for my time in his first-year seminar as both a student and an advisor. Throughout my time at college, they have both been valuable mentors and wonderful teachers, and I am extremely grateful. I would also like to thank Dr. Ashok Deshpande for welcoming me into his lab and teaching me so much about microplastics, analytical chemistry, and what it means to be a true scientist. Additionally, thank you to my wonderful lab team at the National Oceanic and Atmospheric Administration - thank you to Kathryn Zic, Shyui Lin, Aishwarya Rao, Kyra Freeney, and Audrey Kennelley. It was a pleasure to work on such a cohesive and supportive team. I am grateful for the positive and productive environment we cultivated to collaborate on the analysis of our microplastic samples. Thank you also to my mentors and peers at the Goodwin-Niering Center for the Environment for the ongoing support and community. Specifically, thank you to Jennifer Lamb, Keleigh Wagner, Professor Derek Turner, and Professor Julia Flagg. If it were not for GNCE, I would not have even dreamed of starting a project like this. Finally, thank you to whoever takes the time to read this thesis, I appreciate your attention and consideration. This work has truly shaped me into the student that I am as I graduate from Connecticut College.

Abstract

The increasing abundance of microplastic pollution in marine environments is a rising concern, and it has the potential to negatively affect the health and sustainability of marine organisms and ecosystems. Microplastics can harm organisms through a variety of chemical, biological, and physical mechanisms. The extent to which they are harmful varies greatly and is significantly dependent on the chemical and physical makeup of the plastic polymer. Due to this variability, it is important to characterize microplastic samples in various environments to better understand the risks associated with the debris in certain areas. Through field research, a spatial analysis of the nature of this plastic pollution was conducted across Cape Cod, Massachusetts. Samples were collected from shorelines on the Bass River, the Nantucket Sound, the Outer Cape, and the Cape Cod Bay. The microplastic samples were then run through a pyrolysis-GC-MS instrument to determine their chemical composition. The resulting mass spectra were analyzed to identify unique peak patterns and marker compounds, which confirmed the identity of the plastic polymers and additives that make up the various samples. Polypropylene made up most of the samples collected, at about 29% of the total sample pool. Polyethylene followed close behind at about 20%. Polyethylene terephthalate and resins both made up about 14%, cellulose made up 9%, polyvinyl chloride and polystyrene both made up made up 6%, and polyamides made up about 3%. The characterization of microplastic polymers from various locations on Cape Cod provides a glimpse into what types of plastics are polluting certain coastal environments. As microplastic research is a developing field, this component of polymer identification will add to the understanding of potential sources and risks of plastic pollution, paving the way for more in-depth hypotheses to be tested.

Introduction

i. The Story of Plastics

Plastics are made of a variety of synthetic and semi-synthetic compounds that can be melted down and molded to form the hard or flexible solids that we use every day (da Costa et al., 2017). The physical features of plastics are reflected in their name, which is derived from the Greek words *plastikos*, meaning 'capable of being shaped,' and *plastos*, meaning 'molded' (da Costa et al., 2017). Plastics were first derived during the industrial revolution, when the fossil fuel extraction and petroleum use from which they originate dramatically increased. It wasn't until 1950 when plastic products infiltrated society, and their production and use rapidly inflated (Geyer et al., 2017). Following World War II, the world moved into what is termed, "the age of plastics" (Avio et al., 2017; Geyer et al., 2017). This "throwaway society" provided sanitary and convenient plastic products to households across America, in addition to allowing new lifesaving medical advancements. Approximately 6.3 billion tons of plastics were produced from 1950 to 2015 worldwide, followed by a consistent increase in annual production (Jeon et al., 2021). Many characteristics of plastics make them a desirable material, including their versatility, durability, and resistance to degradation (Avio et al., 2017). Their low cost and versatility enable plastics to be used in a vast array of applications (Stevens, 2002). However, the same characteristics that make plastics useful also cause them to be harmful to the environment (Geyer et al., 2017). Although there are some biodegradable plastics, none of the most common polymers fall within this category, causing them to accumulate in landfills and the environment (Geyer et al., 2017). Their accumulation in natural areas for long periods of time has allowed plastics to be seen primarily as an aesthetic issue. However, concerns surrounding plastic

pollution have expanded due to the newly recognized dangers associated with their degradation (Gola et al., 2021).

ii. Microplastics

a) Formation

Microplastics are defined as any plastic fragment less than 5 mm in size (Hayes et al., 2021). They are separated into two categories, primary and secondary, based on their size at the point of production (Hayes et al., 2021). Primary microplastics are within the definable size range when they are produced (Rillig, 2012). These microplastics are manufactured for a variety of purposes, such as cosmetic abrasives, engineering, industrial applications, and drug vectors (Ahmed et al., 2022; Auta et al., 2017). Primary microplastics also include nurdles, which are pre-production plastic pellets formed in industrial settings (Avio et al., 2017). As cosmetic abrasives, primary microplastics can be found in personal hygiene products, such as facial cleansers, toothpaste and exfoliants. After these products are used, the microplastics can enter the environment relatively easily through wastewater collection and treatment systems (da Costa et al., 2017). Less commonly, as drug vectors, primary microplastics can be found in medicines (Ahmed et al., 2022; da Costa et al., 2016; da Costa et al., 2017). They can also be found in household items, drilling fluids and air-blasting media (da Costa et al., 2017). In addition to postproduction pollution, accidental loss from improper handling at processing facilities and manufacturing plants leads to runoff, and ultimately the accumulation of primary microplastics and nurdles in the environment (da Costa et al., 2017). Since primary microplastics are already less than 5 mm when they enter the environment (Hayes et al., 2021), they move much faster through ecosystems because they do not require time to degrade.

Secondary microplastics, however, are formed when larger plastic products break down in the environment. The majority of the microplastics in the ocean are formed in this way, through the degradation and fragmentation of larger plastics (Andrady, 2011; Avio et al., 2017). When plastics are exposed to the elements, they undergo a combination of physical, biological, and chemical processes that greatly reduce the structural integrity of the debris (da Costa et al., 2017). In addition to polymer fragmentation in the environment, the breakdown of plastics can occur before they are released into the environment. For example, synthetic plastic fibers are readily released when clothes are run through a washing machine (da Costa et al., 2017). In this case, the particles are broken down prior to their entrance into the natural environment. More examples of how secondary microplastics can enter the environment include general littering, abrasion in landfills and recycling facilities, carelessly handled fishing gear, plastics in organic waste, paints containing plastics, and more (da Costa et al., 2017). There is a new avenue for secondary microplastics to enter the environment that has arisen since the start of the COVID-19 pandemic in 2020. As disposable face masks have been shown to slow down the transmission rate of the virus between people, there has been a dramatic increase in their global production (Fadare and Okoffo, 2020). These masks often contain polypropylene, polyester, polyethylene, and cellulose fibers (Fadare and Okoffo, 2020). Polymer-based face coverings present a new environmental threat, as they are a rising source of secondary microplastic pollution. The samples collected during this study were primarily secondary microplastics. Although primary microplastics were also collected, most of the samples were slightly larger than 5 mm at the point of collection and were analyzed under the assumption that they would degrade into secondary pollutants.

Microplastics have been detected in most aquatic, terrestrial, and even atmospheric environments (Ahmed et al., 2022). They have even been found in ice and sea salt (Auta et al., 2017). Microplastics have traditionally been seen as a marine pollution issue, however their effect on soil is becoming more widely recognized as well (Sarker et al., 2020; Wang et al., 2020; Xu et al., 2020). Microplastic pollution has been detected in various terrestrial environments, including agricultural, greenhouse, home garden, coastal, industrial and floodplain soils (Xu et al., 2020). One paper discusses how they can be found readily in agricultural fields where plastic mulching is practiced (Rillig, 2012). Additionally, incidental plastic debris from pollution or washing machines can produce secondary microplastic fibers that may end up in fields or other land systems (Rillig, 2012). Another way that microplastics may enter terrestrial and soil systems is through atmospheric deposition of airborne fibers (Rillig, 2012). There is a research group at the University of California, San Diego studying the sorption of microplastics out of the ocean and into aerosol particles at ocean-air interfaces (Slade, 2021). The possibility of aerosols up-taking and transporting microplastics could explain how they have been found in remote places, including on top of mountains (Bian et al., 2022; Free et al., 2014; Padha et al., 2022). The prevalence of microplastic pollution in a wide variety of environments is a cause for concern, as these plastic polymers can clearly travel far and wide, further increasing the areas they are able to impact. As a result of the littoral collection sites in this study, marine microplastics are the primary focus of this paper.

b) Properties

There are many diverse types of microplastics, which vary in size, shape, color, composition, and chemical properties. Some common shape categories they are placed into include fibers, pellets, fragments, films, foams, particles, ellipses, lines, and flakes (Ahmed et al.,

2022; Lares et al., 2018). Their sizes vary drastically depending on region and point in degradation. Although microplastics are typically defined as particles ranging from 1-5 mm, there is a lack of unanimity regarding this definition. The most prevalent microplastic polymers include polyethylene (PE), polypropylene (PP), polyvinyl chloride (PVC), polystyrene (PS), polyethylene terephthalate (PET), polyester (PES), polyamide (PA), polyurethane (PUR), and resins (Ahmed et al., 2022; Andrady, 2011; Avio et al., 2017; Geyer et al., 2017). The differing compositions of these various polymers determine their unique physiochemical properties, including crystallinity, density, molecular weight distribution and surface chemistry. The crystallinity is significant due to its effect on density (Ahmed et al., 2022). The higher the crystallinity, the more rigid the polymer (McKeen, 2012). Since polypropylene and polyethylene (the most abundantly produced polymers) are semi-crystalline polymers (Ahmed et al., 2022), their densities are less than that of water, causing them to float. This characteristic dramatically alters the way these polymers behave in the environment and which organisms they have a greater likelihood of impacting. It is also important to understand how the crystallinity of the polymer can change when microplastics experience weathering and aging. These processes impact size, shape, additive leaching, and pollutant sorption (Ahmed et al., 2022). The properties of microplastics evolve over time as the particle breaks down both chemically and physically.

c) Degradation

Plastics break down in the environment in a variety of ways, including physical disintegration, abiotic degradation, and biodegradation. These various processes can happen simultaneously or sequentially, depending on the specific substance and its environment (da Costa et al., 2017). Physical degradation, or mechanical disintegration (da Costa et al., 2017), consists of waves and other forces breaking down the plastics. Some sources do not consider the

physical breakdown of plastics degradation, because the molecular bonds of the polymer do not change, but rather the material undergoes morphological modifications (da Costa et al., 2017).

Abiotic degradation consists of the chemical breakdown of polymers without the aid of biological microorganisms, as an abiotic process is not associated with or derived from living organisms. Some common abiotic mechanisms of degradation include photodegradation, thermal degradation, oxidation, and hydrolytic degradation (da Costa et al., 2017). Photodegradation, which is one of the most efficient routes of abiotic degradation in the environment, occurs when plastic polymers are exposed to visible and high energy UV radiation (da Costa et al., 2017). When the polymers absorb this radiation, at wavelengths ranging from 290-700 nm, their electrons become highly reactive and their break down is mediated by chain scission and cross-linking reactions (da Costa et al., 2017). Chain scission is a common mechanism of polymer degradation that reduces the molecular weight of macromolecules (Chapiro, 2004). The scission, or division/point of splitting, particularly occurs at sites of high reactivity (Bai, 2013). When all the repeating units of the polymer are equally reactive (which is common in plastic polymers), the scission sites on the polymer are randomly distributed. This process is known as "random chain scission." Although thermal degradation also leads to bond scissions and physical changes of the material, high enough temperatures for it to take place are not as common in the environment (da Costa et al., 2017). Following physical and abiotic breakdown, the polymers are typically more amenable to the microbial colonization that takes place during biodegradation.

Plastics can biodegrade when microorganisms on their surface release degrading enzymes, such as lipase and dehydrogenase (Jeon et al., 2021). These enzymes attack the polymer substrate, cleave the polymer chains by hydrolytic processes, and degrade them into smaller molecules, including oligomers, dimers, and monomers (da Costa et al., 2017). As the

molecular weight of the polymers decrease, the smaller molecules are ultimately degraded into carbon dioxide and water (Jeon et al., 2021). Biodegradation can take place in different environments, including aquatic and terrestrial. Plastic polymers such as polyethylene, polypropylene, and polyethylene terephthalate consist of short and regular repeating monomers that limit the accessibility of enzymes due to their compact structures (da Costa et al., 2017). Due to this hinderance, these polymers are less susceptible to breakdown via biomolecules (da Costa et al., 2017).

The biodegradation of plastic products is much more environmentally friendly than alternative methods of disposal, such as incineration, which releases toxic and carcinogenic contaminants into the atmosphere. For example, one study found that the controlled incineration of polyethylene, polypropylene, and polyvinyl chloride released over twenty individual polycyclic aromatic hydrocarbons (PAHs) (Li et al., 2001), which have been shown to be carcinogenic (Speizer, 1986). Although these dangers make the natural biodegradation of plastic appealing, this process occurs concerningly slowly, as the polymers are very durable, especially when they contain additives that enhance these properties. The degradation of plastics into microplastics in the environment has increased the concern surrounding plastic pollution. It is now recognized as an ecological and public health threat, due to the many toxic impacts of microplastics and the additives they readily leach (Gola et al., 2021).

d) Health and Ecosystem Impacts

Microplastics are a known threat to ecosystems, marine organisms, and even human health. This risk is growing, as there is expected to be more plastic (by mass) in the ocean than fish by 2050 (New Plastics Economy, 2016). Due to their small size, microplastics can be ingested by filter feeders at the bottom of the food chain, as well as by many organisms including

plankton, fish, marine mammals, and birds (da Costa et al., 2017). They can enter organisms through a variety of pathways, including ingestion, inhalation, and digestion (Ahmed et al., 2022). Once they enter the food chain, microplastics are known for bioaccumulating and biomagnifying up the food chain, eventually allowing them to threaten human health (Ahmed et al., 2022). A recent study found microplastic particles in infant and adult feces (Zhang et al., 2021). In fact, their research revealed that infants are exposed to much higher concentrations than adults. Despite these findings, it was unclear for a long time whether plastic particles were isolated in the digestive system in humans, or if they could cross into other parts of the body. This question was recently addressed, when the first report of internal microplastic exposure in human blood was published (Leslie et al., 2022). This new research utilized the pyro-GC-MS analytical technique to identify various polymers, including polyethylene terephthalate, polyethylene, and polystyrene, among others (Leslie et al., 2022). The results revealed microplastics in the blood of 80% of people (from the public) who were tested (Leslie et al., 2022). The ability of microplastics to enter human blood raises new questions about the public health risks associated with these particles.

In the environment, organism's ingestion of microplastics is harmful and toxic for a variety of reasons. The first is the physical stress of ingestion. This includes the energy expenditure the organism uses to consume the plastics, blockage, and false satiety (da Costa et al., 2017). For example, if fish are overconsuming microplastics, they may "think" they are eating their normal prey and feel full, which can lead to malnutrition and death. Many laboratory experiments have revealed a wide variety of organisms who readily ingest microplastics, including cnidarians, rotifers, ciliates, annelids, copepods, mysids, amphipods, euphausiids, mussels, barnacles, tunicates, birds, and fish (da Costa et al., 2017). Studies have shown that

likelihood of microplastic ingestion depends not only on shape and size of the fragment, but also on the color. The uptake of duller colors that resemble prey is much higher than that of bright and unnatural colors (Shaw and Day, 1994). In addition to starvation, ingestion of microplastics can obstruct digestive tracts and lead to internal injuries (Lambert et al., 2014). Another physical concern raised by microplastics includes entanglement of fragments in gills, which disrupts respiration da Costa et al., 2017). As seen by these examples, the presence of microplastic particles in aquatic environments leads to a variety of ecosystem threats by disrupting organisms physically.

Another mechanism by which microplastics harm organisms is through the toxic additives and plasticizers incorporated into the plastics during manufacturing to bolster the thermal and mechanical properties of plastic products. These compounds can leak and transfer from the plastic to the organism, leading to many negative health effects such as endocrine disruption (Avio et al., 2017; da Costa et al., 2017). The reasons these additives can readily leach away from the plastic materials is because they are usually not chemically bound to the polymer (da Costa et al., 2017). Many additives are lipophilic, or have a high affinity for fats, which enables them to penetrate cell membranes and alter biochemical reactions that alter the behavior and reproduction of effected organisms (da Costa et al., 2017). The polymerization reactions during plastic production are often incomplete, so the unreacted monomers, solvents and additives in the plastics are free to interact with the body of the organism. Some polymers contain or are made of particularly toxic monomers. These include polyvinyl chloride (PVC), polystyrene (PS), and polycarbonate (PC), which cause reproductive abnormalities and are carcinogenic in invertebrates, rodents, and humans (da Costa et al., 2017). The toxic additives

and monomers that are incorporated into plastics during production to ensure desirable properties are one of the main reasons microplastics are so dangerous in the environment.

Additionally, organisms can be exposed to organic contaminants that were absorbed by the microplastic (Avio et al., 2017; da Costa et al., 2017), such as persistent organic pollutants (POPs) (Koelmans et al., 2013). These organic pollutants include polychlorinated biphenyls (PCBs), polycyclic aromatic hydrocarbons (PAHs), and organochlorine pesticides (such as DDT). These types of compounds are termed "persistent" due to their ability to resist environmental degradation. Some POPs, including PCBs, have been shown to mimic natural hormones and cause reproductive disorders (da Costa et al., 2017; Daouk et al., 2011; Smits-van Prooije et al., 1993). For example, one study found that several reproductive traits of zebrafish were altered after they were exposed to a PCB-contaminated diet (Daouk et al., 2011). The dynamics of POP sorption into microplastics varies greatly depending on the POP and the plastic polymer. Factors such as density, molecular weight, and hydrophobicity all play a role in how likely it is for a microplastic to absorb a specific pollutant (da Costa et al., 2017). Particularly hydrophobic molecules have the concerning tendency to bioaccumulate (da Costa et al., 2017). Due to all the listed ecosystem and health risks of microplastics, there is a need to study and characterize plastic polymers to learn more about their geographic distribution, chemical compositions, and subsequent dangers.

iii. Analyzing Microplastics

Before more advanced instrumental techniques were applied to the analysis of microplastics, characterization was not an option. Microplastics could only be quantified using visual and microscopic recognition. As features of small samples are not very distinctive, the use

of more reliable identification methods is essential (Fischer and Scholz-Böttcher, 2017). Now, microplastic compositions can be determined using a variety of analytical techniques, including Raman Spectroscopy, FT-IR, and Pyrolysis-Gas Chromatography-Mass Spectrometry, which was utilized in this study.

Pyrolysis-Gas Chromatography-Mass Spectrometry (pyro-GC-MS) enables the systematic and sequential identification of marker peaks. Pyrolysis consists of heating samples at high enough temperatures that they fragment into smaller molecules and become a gaseous mixture of these heat degradation products. These molecules are then separated in a GC column and can be identified to determine the composition of the sample using the mass spectra of each compound.

When the sample is first run in the instrument, it is exposed to extremely high heat, so it disintegrates into small particles. The characteristic thermal degradation products can be analyzed to determine the polymer identity (Fischer and Scholz-Böttcher, 2017). This fragmentation upon heating consists of the breaking of carbon-carbon bonds at different sites along the polymer chain due to the intense heat, which yields a variety of short chain molecules that are separated in the GC column. As seen in figure 1, the sample is pyrolyzed with a high heat coil filament, and the resulting mixture travels through the gas chromatography (GC) column.

In this study, the gaseous mixture was carried through a 0.25 mm thick and 60 m long fused silica column with hydrogen gas. Helium gas can also be used as a carrier gas, but this study utilized hydrogen due to its low cost and availability. In the GC column, the mixture is separated into its various constituent compounds based on a variety of chemical and physical properties. As polymerization results in a variety of short chain molecules, each of the

compounds spreads out across a chromatogram based on the molecular weight of the fragment. Thus, each peak on the chromatogram represents a different compound. The resulting chromatogram shows the peaks in chronological order, as more time goes on and the sample is exposed to higher heat. The heavier hydrocarbons come out slower, while the light molecules come out first since they move faster. Since molecules with smaller molecular masses come through faster, their peaks appear first on the chromatogram. So, moving from left to right across the chromatogram, the peaks will represent fragments of increasing large molecular masses. It is important to note that for the pyrolysis-GC-MS technique, this chromatogram is technically called a pyro-gram. The gas chromatogram is really an ion chromatogram because the resulting peaks are not just peaks, they are a combination of all the *ions*.

By focusing on one peak at a time, mass spectrometry (MS) can be used to identify what each compound is by matching the fragmentation pattern with that of a known compound. So, after the mixture passes through this GC column, the newly separated compounds move towards the MS. Mass spectrometry consists of the compound being ionized (ionization method), the ions being separated based on their mass to charge (m/z) ratio (ion separation method), and the detection and quantification of each of the ions (Silverstein et al., 2005). Electron impact (EI) ionization, which is a widely used method for generating ions for mass spectrometry, was utilized as the ionization method in this study. This method consists of bombarding molecules in the vapor phase with a high energy electron beam (generally 70 eV), which eject an electron from a sample molecule to produce a radical cation, known as the molecular ion (Silverstein et al., 2005). This step can be seen in the area labeled “electron ionization” in figure 1. The result of EI is recorded as a spectrum, separated by m/z ratios, of the series of positive ions that have been formed (Silverstein et al., 2005).

The mass analyzer, which follows ionization, is the heart of the mass spectrometer. This step, which is labeled in the schematic in figure 1, separates the mixture of ions generated during ionization by their m/z ratios to obtain the final spectrum. There are many different types of mass analyzers, including magnetic sector, quadrupole, ion trap, time of flight, and Fourier transform mass analyzers. The quadrupole mass analyzer was utilized in this study and is shown in the schematic in figure 1. A quadrupole consists of four cylindrical rods of about 100-200 mm in length (Silverstein et al., 2005). These rods are mounted parallel to each other, each forming the corner of a square. Essentially, a *constant* direct current (DC) voltage is modified by a radio frequency voltage to create various overall voltages that are applied to the rods (Silverstein et al., 2005). When the voltages are applied, ions are introduced to the space between the four rods, which forms a sort of tunnel that they travel down. For any different total voltage, which is formed by combining the DC voltage with a modified voltage at a specific frequency, only ions with a certain and exact m/z ratio can pass through the tunnel. Ions with different m/z ratios have unstable trajectories at that voltage, causing them to miss the tunnel (Silverstein et al., 2005). This specificity in which m/z ratio ions can pass through the quadrupole allows for the detection and quantification of each of the ions. In practice, this filtering of ions happens so quickly that the entire mass range can be scanned in less than a second (Silverstein et al., 2005). It is important to note that when the charge of the ion is +1, which is typical in this technique since one electron is removed, the m/z ratio is the same as the molecular mass of the fragment since it is divided by the charge of one. This means that when it comes to analysis, the m/z ratios of the prominent MS peaks are typically the same numerical value as the molecular weight of the compound they represent.

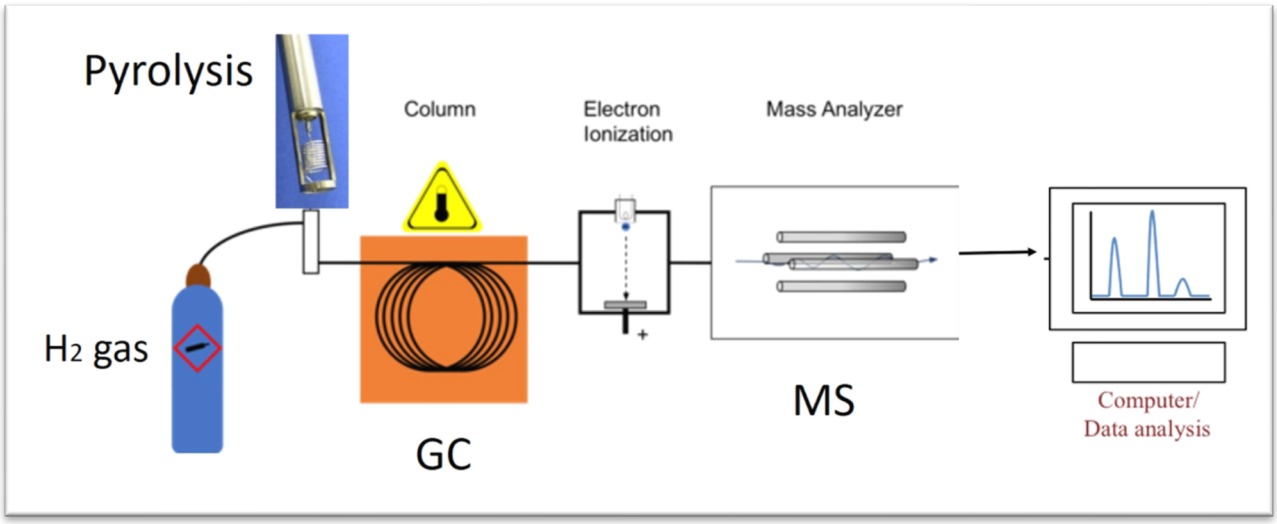

Figure 1: A schematic diagram of the pyrolysis-GC-MS instrument (Cwszot, 2018). Sample is pyrolyzed in filament and carried with hydrogen gas. The pyrolyzed gaseous mixture moves through the GC column where it is separated, then to electron ionization chamber, and mass analyzer (quadrupole) where it is fragmented. The spectral results are sent to the computer for analysis.

By combining the GC with the MS, this study utilizes tandem data analysis, which allows for more reliable confirmation of the polymer characterization. This analytical system, like most mass specs today, is interfaced with a computer. The resulting pyro-gram spectra and mass spectrum are finally sent to the computer for analysis.

An example of the characterization analysis that occurs once the data is sent to the computer is outlined below. The ion chromatogram depicted in figure 2 shows multiple ion chromatogram peaks, each representative of a compound from the fragmentation of the polymer. The spectrum displays the retention time (in minutes) on the x-axis, and the peak abundance on the y-axis. During analysis, the tallest and most prominent peak is assessed first. In this example, the tallest peak lies a little bit after the 5-minute retention time marker, as seen at the bottom of

the spectra. By double right clicking on this peak, which is pointed out by an arrow, the mass spectrum for that fragment is revealed beneath, which is shown in figure 3.

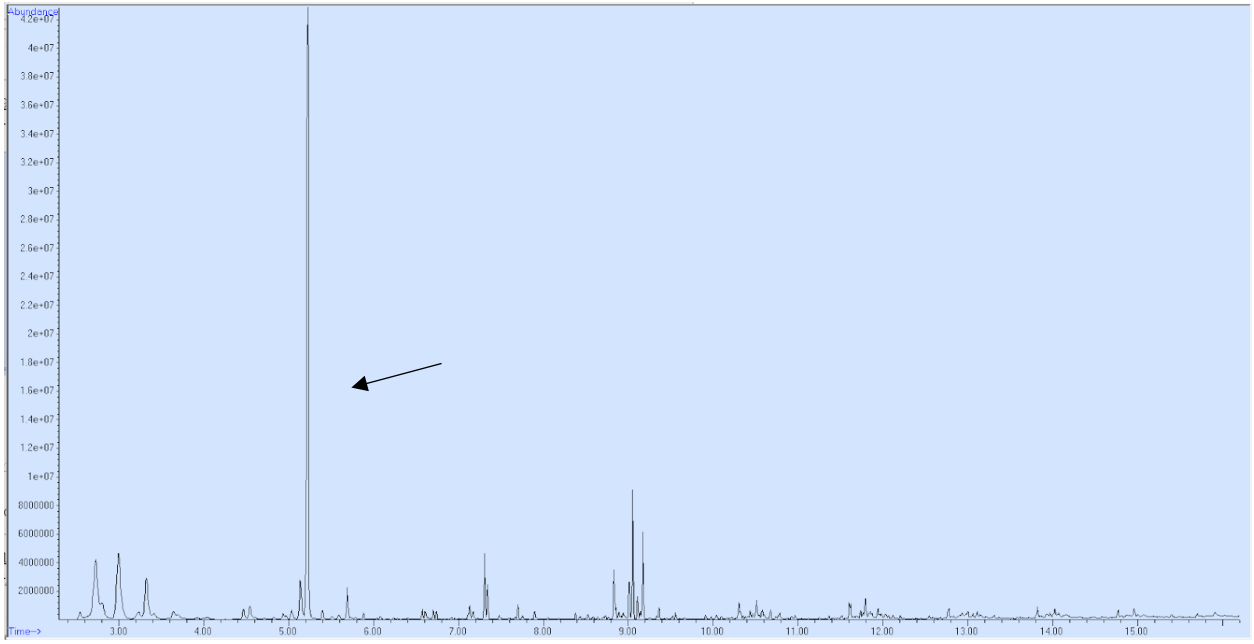

Figure 2: An example of the chromatogram of a polypropylene sample. The peaks at earlier retention times on the left represent lighter fragment compounds while peaks emerging later represent heavier fragments. The tallest and most prominent peaks are identified first. In this example, such peak is marked with an arrow.

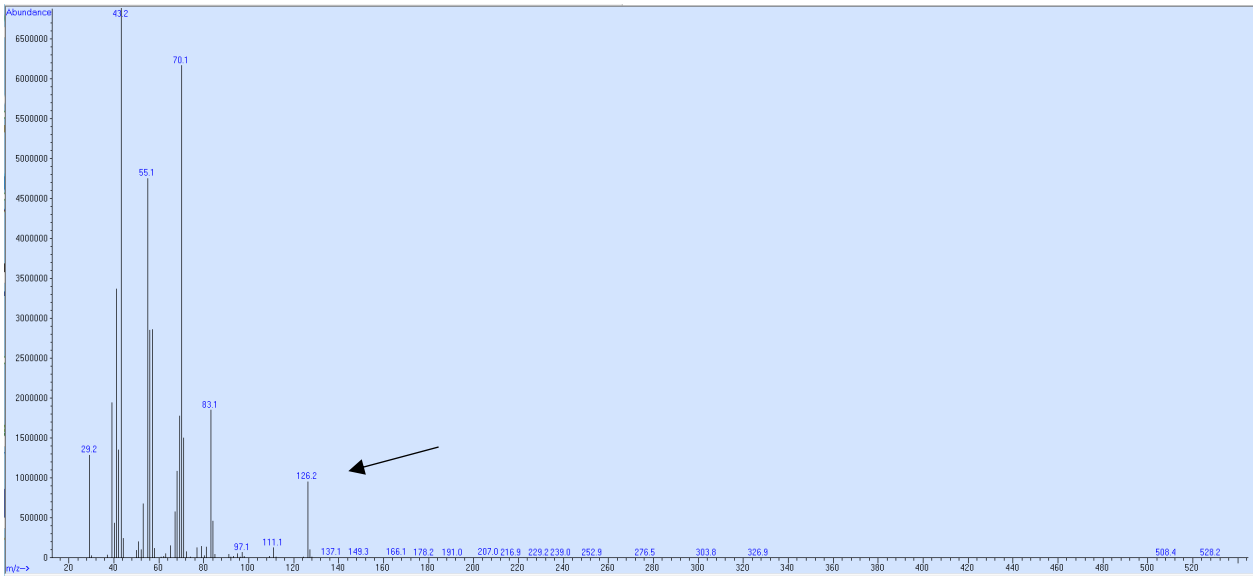

Figure 3: An example of the mass spectra of the tallest peak in figure 2. The MS peak highlighted by the arrow displays a m/z ratio of 126.2, which aligns with the molecular mass of the suggested compound, 2,4-dimethyl-1-heptene.

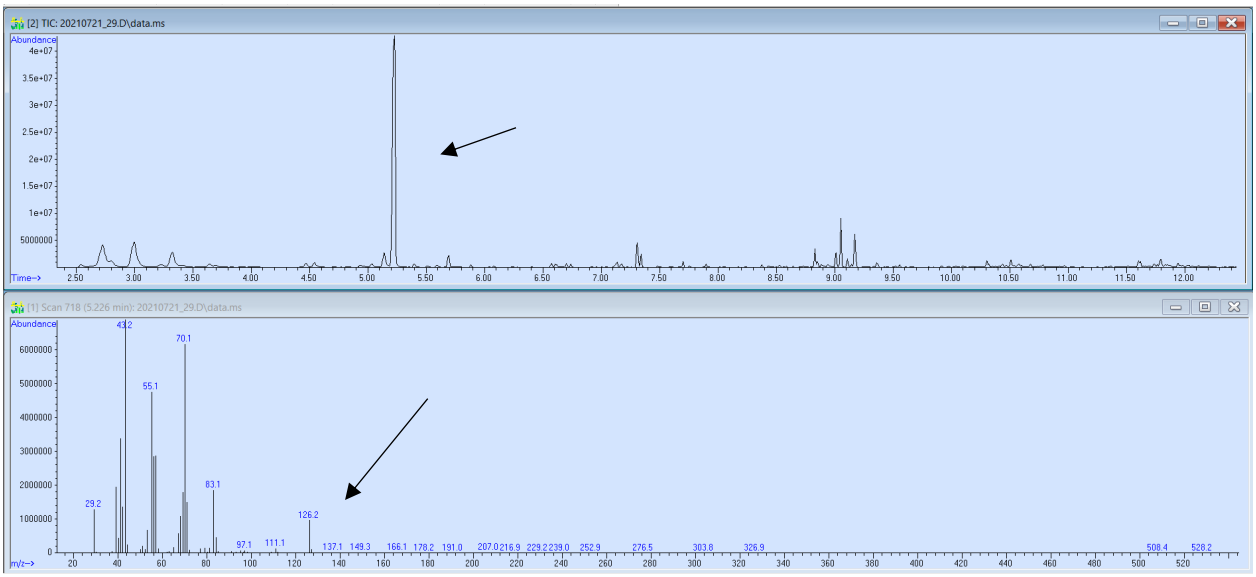

Figure 4: The ion chromatogram peaks are shown on the top and the mass spectra of the tallest peak, depicted by an arrow, is shown beneath.

The mass spectra for the tallest peak in the chromatogram of figure 1 is shown in figures 2 and 3 above. The mass spectrum shows abundance on the y-axis (vertical peak intensity) versus m/z ratio on the x-axis. This spectrum can be compared to the mass spec data in the NIST EI-MS database that was linked to the ChemStation software (National Institute of Standards and Technology, 2021), and ultimately be matched with a probable fragment compound. In this case, the peak was determined to be 2,4-dimethyl-1-heptene, which is a known marker for polypropylene. The MS peak pointed out by the arrow has the number “126.2” above it. This is the m/z ratio, which is the same as the molecular mass of the fragment in this case. The 2,4-dimethyl-1-heptene polypropylene marker has a molecular mass of about 126 g/mol, so this MS peak further confirms the polymer identification. Matching to m/z value of the MS peak to the expected molecular weight of the fragment compound enables confirmation beyond the suggestion from the NIST database matching. The NIST database proposes a compound that it finds to be the best match for the given mass spectra, as seen in figure 5. There are different

compounds associated with the fragmentation of each plastic polymer. As demonstrated, the mass spectra can be used to identify the compounds associated with peaks in the chromatogram, allowing marker peaks to be recognized and matched to known standard polymers.

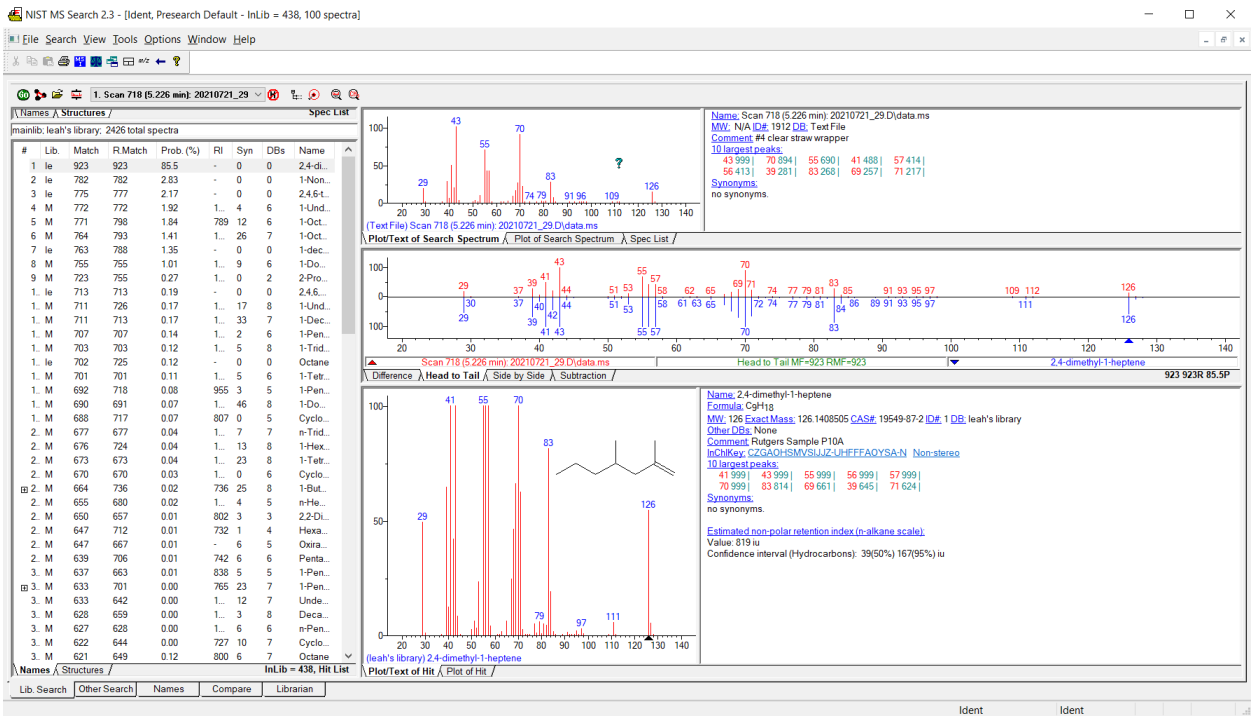

Figure 5: An example of the proposed compound from the NIST database that accompanies the mass spectra shown in figure 3. Different probable compounds are attributed to each GC peak from the NIST database.

iv. Plastic Polymer Fragmentation

a) Synthetic Polymer Background

The desirable properties and characteristics of plastics, like their durability, often come from the polymers and additives that make them up. Polymers are larger molecules that are composed of repeating subunits, called monomers. The length of polymer chains drastically ranges from hundreds to hundreds of thousands of units long. These repeating monomers form a chain linked together by carbon-carbon bonds. It is these bonds that make plastics durable and resistant to degradation (Jeon et al., 2021). Monomer compositions influence the functional groups and properties of each polymer chain (Ouellette and Rawn, 2015). Additionally,

intermolecular forces between polymer chains can determine the physical properties of the plastic (Ouellette and Rawn, 2015). These forces include hydrogen bonding, dipole-dipole, and London dispersion forces (Ouellette and Rawn, 2015). The properties of the plastic polymers also depend on the length of the chains (Ouellette and Rawn, 2015). Longer chains are typically stronger and more viscous when heated, while shorter chains are softer. Crosslinking, which essentially adds bridges between polymer chains, can also strengthen plastic polymers (Ouellette and Rawn, 2015). A variety of alterations can be made to plastic polymers to ensure the manufacturer creates desired properties for their products.

As mentioned, the most common synthetic polymers include polyethylene (PE), polypropylene (PP), polyvinyl chloride (PVC), polystyrene (PS), polyethylene terephthalate (PET) and resins (Ahmed et al., 2022; Andrady, 2011; Avio et al., 2017; Geyer et al., 2017). Polyethylene and polypropylene are the most abundantly produced polymers, and they account for more than 50% of total plastic usage (Jeon et al., 2021). Most plastics, including these two abundantly produced polymers, are made up of monomers derived from fossil hydrocarbons (Geyer et al., 2017).

b) Polyethylene

Polyethylene (PE) is the most abundantly produced plastic polymer (Jeon et al., 2021), and it is also one of the simplest. PE is typically used in the production of plastic bags, six-pack rings, bottles, netting, drinking straws, and milk jugs (Andrady, 2011). It consists of repeating ethylene monomers, which are two carbons connected by a double bond, as seen in figure 6. Although its name ends with "-ene," the polyethylene polymer is an alkane composed of an alkene monomer. Its' name can be confusing, but

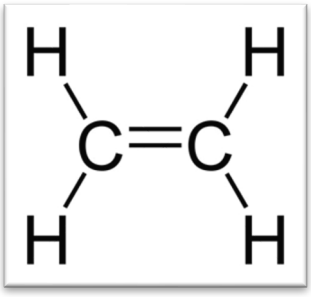

Figure 6: The chemical makeup of an ethylene monomer. Two carbons connected by a double bond.

polymers are typically named by adding the “poly-“prefix before the original name of the monomer. The typical high-density PE (HDPE) polymer consists of a long chain of carbon atoms with two hydrogen atoms attached to each one. When these hydrogens are replaced by other PE chains, the polymer is considered low-density PE (LDPE), which is less rigid. The standard fragmentation of polyethylene contains a pattern of triplet hydrocarbon clusters with increasing carbon chain lengths. This fragmentation is the result of a random chain scission (Fischer and Scholz-Böttcher, 2017). During this process, the carbon backbone is split apart to produce various smaller hydrocarbons with terminal free radicals (Kusch, 2017). These radicals are stabilized by abstraction of a hydrogen or beta scission, which often produce more free radicals on the smaller fragments (Kusch, 2017). Hydrogen abstraction, which is shown in figure 7, occurs when a hydrogen atom is removed from the polymer to form a free radical (Diaz et al., 2018), whereas beta scission involves the splitting of a carbon-carbon bond to form the free radical. The process continues and produces saturated, doubled bonded, and single bonded hydrocarbon fragments of various chain lengths (Kusch, 2017).

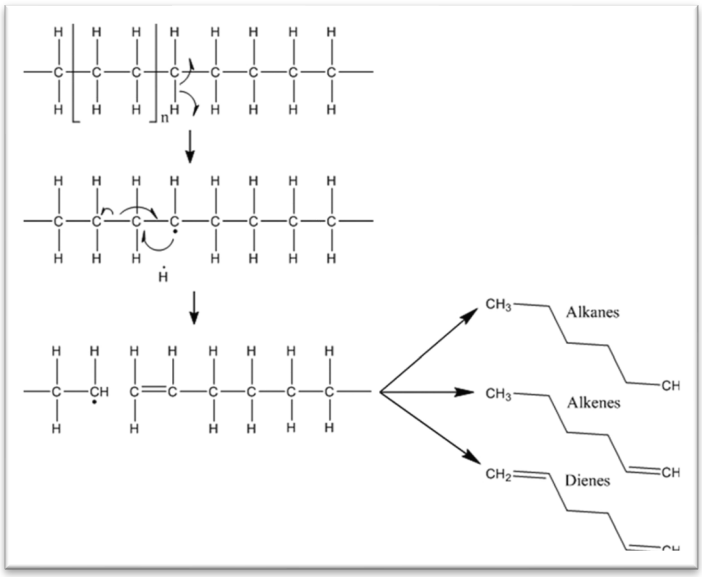

Figure 7: A schematic of the random chain scission mechanism that is responsible for the fragmentation of polyethylene (Diaz et al., 2018). In this figure, hydrogen abstraction produces a free radical, which leads to scission and the formation of various fragment compounds.

As these three types of compounds are formed at each carbon chain length, the resulting pyro-gram contains serial triplet peaks (Kusch, 2017). As mentioned, each triplet cluster contains a single bonded, double bonded, and saturated hydrocarbon with the groups specified number of carbons. So, the standard pyro-GC-MS signal for polyethylene consists of multiple signals of *n*-alkanes, *n*-alkenes and *n*-alkadienes (Fischer and Scholz-Böttcher, 2017). For example, one triplet may consist of a nine-carbon chain. The compounds attributed to these three peaks would be 1,8-nonadiene (the saturated hydrocarbon), 1-nonene (the double bonded hydrocarbon), and nonane (the single bonded hydrocarbon) (Tsuge et al., 2011). Instead of specific compounds with specific mass to charge ratios, this overall pattern of multiple *n*-alkane, *n*-alkene, and *n*-alkadiene signals was the determinant marker for polyethylene in this study. A sequence of smaller fragments following this pattern is shown in figure 8 below.

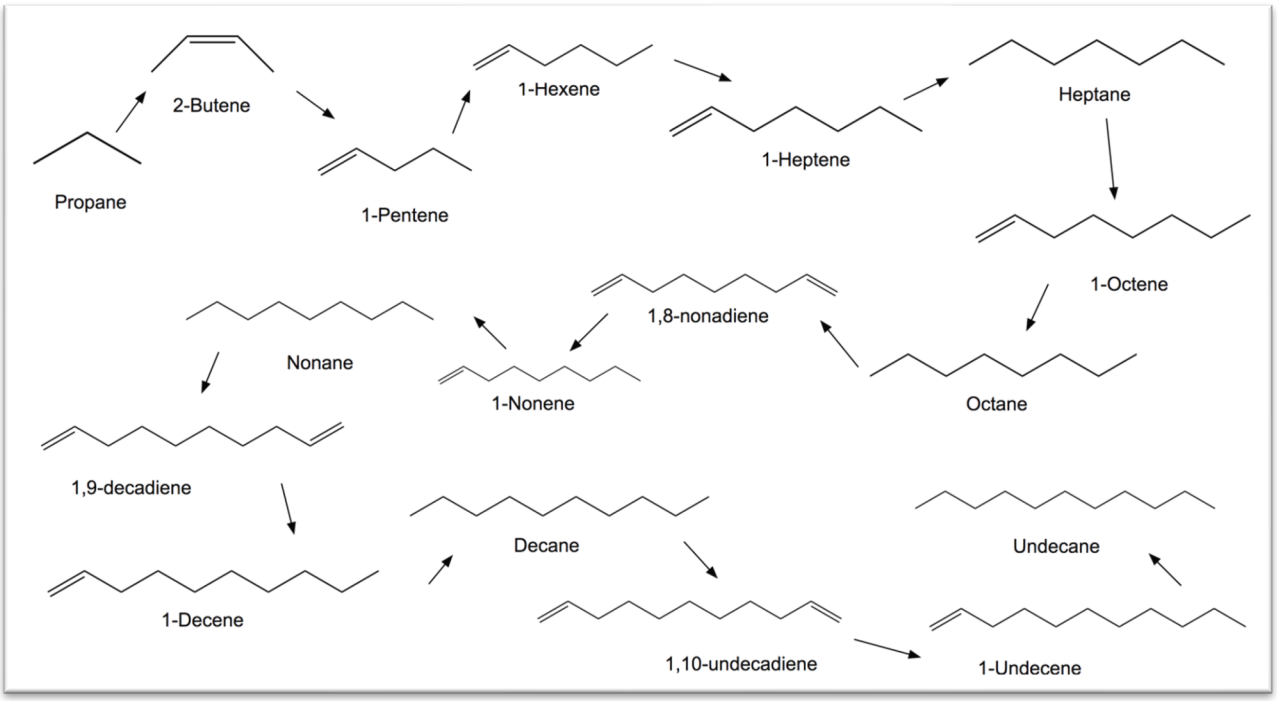

Figure 8: A portion of the expected pyro-GC-MS fragmentation of the polyethylene polymer. The fragments spread out across the spectra according to their molecular weight. The arrows move in the direction of smaller MW compounds to larger MW compounds, since the lighter fragments come out of the column first and are found at earlier retention times in the spectra. When looking for the structure of polyethylene, it is typical to see single bonded, double bonded, and saturated hydrocarbon fragments of each carbon chain length.

c) Polypropylene

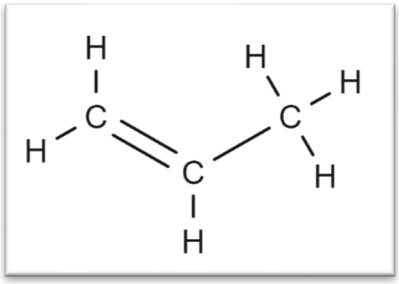

Figure 9: The propylene monomer is essentially ethylene with a methyl group in place of one of the hydrogens.

Polypropylene (PP) is the second most abundantly produced plastic polymer (Jeon et al., 2021). This polymer is made up of repeating propylene monomers, which are similar to ethylene, but contain an additional carbon from a methyl group in the place of one of the hydrogens. The three-carbon chain consists of one double bond and one single bond, as seen in figure 9. This monomer forms a polymer with a methyl group on every other backbone carbon. This simple structure leads to a remarkably versatile polymer (Calhoun, 2016). The fragmentation of this polymer consists of propene, pentane, 2-methyl-1-pentene (84 m/z), 2,4-dimethyl-1-heptene (126 m/z), 2,4,6-trimethyl-1-nonene (168 m/z), and 2,4,6,8-tetramethyl-1-undecene (210 m/z) (Tsuge et al., 2011). Like polyethylene, this fragmentation is the result of a random chain scission (Fischer and Scholz-Böttcher, 2017). The standard pyro-GC-MS marker used for identifying PP consists of multiple signals of methyl alkenes and alkadienes (Fischer and Scholz-Böttcher, 2017). Part of the typical fragmentation of PP is shown in figure 10 below. In this study, the 2,4-dimethyl-1-heptene compound (126 m/z) was the initial marker for polypropylene, followed by confirmation of the other standard signals. This 2,4-dimethyl-1-heptene compound is a propylene trimer, and it typically appears at around the 8-minute retention time on the ion chromatogram. Likewise, the 2-methyl-1-pentene dimer appears at around the 6-minute retention time, while the 2,4,6-trimethyl-1-nonene tetramer and 2,4,6,8-tetramethyl-1-undecene pentamer come out less consistently and later (Kusch, 2017). Polypropylene plastics are typically clear and transparent items (Rodríguez-Seijo and Pereira, 2017), although they can be treated with dyes.

Polypropylene is typically used to produce rope, bottle caps, netting, carpeting, laboratory equipment, drinking straws, packaging, and a variety of disposable products (Andrady, 2011; Jeon et al., 2021; Kusch, 2017).

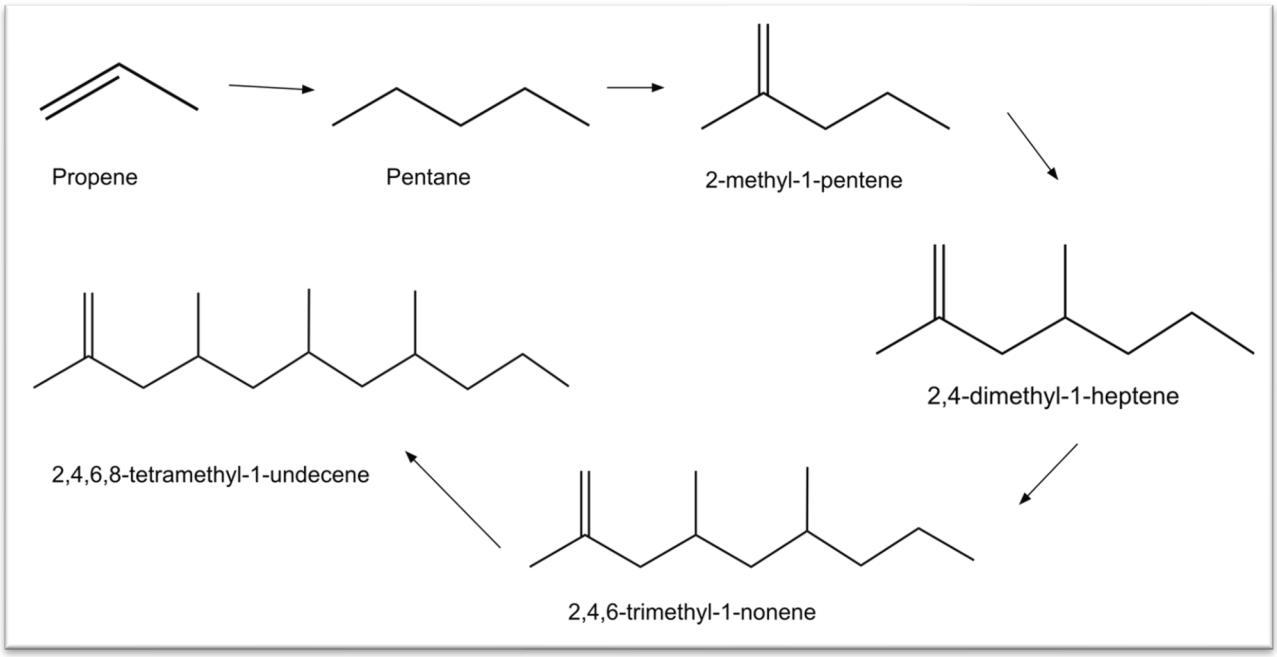

Figure 10: A portion of the expected pyro-GC-MS fragmentation of the polypropylene polymer. The fragments spread out across the spectra according to their molecular weight. The arrows move in the direction of smaller MW compounds to larger MW compounds, since the lighter fragments come out of the column first and are found at earlier retention times in the spectra. When looking for the structure of polypropylene, it is typical to see methyl alkene and alkadiene fragments of various sizes.

d) Polystyrene

Polystyrene is comprised of repeating styrene monomers. Ethylene and propylene, the monomers that make up common two of the most abundantly produced polymers (polyethylene and polypropylene), are much simpler and less toxic than the styrene monomer. As seen above, ethylene and propylene are simple monomers composed of carbon-carbon single and double bonds. The styrene monomer, depicted in

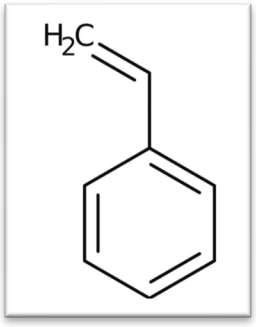

Figure 11: The styrene monomer is essentially ethylene with a phenol group in place of one of the hydrogens.

figure 11, is more complex because it contains an aromatic ring. The presence of this cyclic ring in the polymer leads to the formation of many volatile compounds during its degradation (Kusch, 2017; Tsuge et al., 2011). Out of all the commonly produced microplastic polymers, polystyrene is of particular concern due to is higher levels of toxicity (Green et al., 2001; Kogevinas et al., 2018; National Toxicology Program, 2011).

Polystyrene comes in many forms, including the general purpose, high impact, and expanded polymers (Kusch, 2017). The general purpose, or crystalline polymer, is in the form of a hard and brittle solid (Kusch, 2017). Polystyrene is a thermoplastic polymer and is a glassy clear solid at room temperature. Although it is naturally transparent (National Toxicology Program, 2011), it can be colored with colorants. The high impact polymer is formed by the addition of dienes and exists as a tough plastic that is easy to thermoform and fabricate (Kusch, 2017). Expanded polystyrene is made from pre-existing polystyrene beads or nurdles and is formed using a blowing agent that enables their expansion into a tough foam (Kusch, 2017). This foam is commonly used in food packaging, protection of products during transport (packing peanuts), storage, and insulation of external walls and foundations. Expanded polystyrene is commonly and inaccurately referred to as “Styrofoam,” which is a trademarked brand of specific polystyrene products. The trademarked term is used generically to refer to expanded polystyrene foam products, including coffee cups and food containers. Polystyrene is typically used to produce plastic utensils and food containers, while foamed polystyrene can be found in floats, bait boxes, and foam cups (Andrady, 2011). In aquatic and littoral environments, such as the sampling sites in this study, a common source of polystyrene is from the foams that make up floats. Although this aromatic hydrocarbon is relatively chemically inert, it is more concerning than more simple polymers due to its toxic degradation products.

Polystyrene particles have been shown to induce oxidative stress in various organisms. One study assessed the effect of polystyrene particles on *Caenorhabditis elegans (C. elegans),* a nematode that is often used as a model organism (Shang et al., 2021). This study found that polystyrene exposure induced oxidative stress, resulting in cellular damage and neurodevelopmental toxicity (Shang et al., 2021). Another study looked at the effects of polystyrene particles on the marine mussel *Mytilus galloprovincialis* (Gonçalves et al., 2022). This study also found that exposure led to oxidative damage, in addition to the fact that particle toxicity is tissue and time dependent (Gonçalves et al., 2022). The oxidative stress that is caused by polystyrene is likely a result of its volatile organic degradation products, including ethylbenzene, benzene, toluene, and styrene (Kusch, 2017; Tsuge et al., 2011). Various studies have linked aromatic volatile compounds to oxidative stress. One study determined that toluene, benzene, and styrene led to oxidative stress in human epithelial (skin) cells (Mögel et al., 2011). The CDC's glossary of volatile organic compounds mentions health concerns for ethylbenzene, benzene, xylenes, toluene, and styrene (Centers for Disease Control and Prevention, 2003). The styrene compound is of particular interest in the discussion of polystyrene.

One of the main reasons the polystyrene polymer is more dangerous than other polymers is because the styrene molecule (104 g/mol) is its main thermal decomposition product. The styrene monomer alone has established toxic effects (Simmonds, 2004), included that it has been demonstrated to be carcinogenic (Green et al., 2001; Kogevinas et al., 2018). Styrene is also frequently used as an additive in other types of polymers or plastics to enhance their thermal and mechanical properties (Eben et al., 2020). According to the 12th Report on Carcinogens from the National Toxicology Program, styrene can reasonably be considered carcinogenic due the combination of studies on exposed humans, reasonable evidence from animal studies, and

supporting data from the mechanisms of carcinogenesis (National Toxicology Program, 2011). The studies on humans consist of surveying workers that have been exposed to styrene, such as individuals from the reinforced-plastics industry or the styrene-butadiene rubber industry (National Toxicology Program, 2011). These studies have revealed increased levels of mortality from or instance of cancer in these exposed workers, as well as increased levels of genetic damage (National Toxicology Program, 2011). These surveys are significant especially as they reinforce the intentional manipulation of styrene levels used in animal studies. Styrene has been shown to cause lung cancer in several strains of mice by various routes of exposure (National Toxicology Program, 2011). One study revealed that styrene caused an increase in lung tumor instances in mice that were exposed orally (Green et. al, 2001; National Toxicology Program, 2011). Styrene has been shown to induce DNA damage, gene mutations, and chromosomal aberrations, among other effects (Kogevinas et al., 2018). Additionally, this compound is quickly absorbed, widely distributed, and extensively metabolized in the body, increasing the danger of the additive (Kogevinas et al., 2018). The reason polystyrene is deemed safe by the FDA to be used as a food wrapper is because styrene is found in such low levels of polystyrene products that it is safe for the consumer (National Toxicology Program, 2011). Styrene becomes more of a concern in the environment when the polystyrene polymer begins to degrade.

Polystyrene is recognized by its mass spectral fragmentation containing toluene (92 m/z), styrene (104 m/z), α-methyl styrene (118 m/z), and a styrene dimer (208 m/z) and trimer (312 m/z) (Tsuge et al., 2011). The fragment compounds are shown in the order of their retention in figure 13 below. This fragmentation is the result of random chain scission and end chain scission signals (Fischer and Scholz-Böttcher, 2017). Potential mechanisms for this fragmentation are

shown in parts (a) and (b) of figure 12. Part (c) of this figure depicts a plausible fragmentation of polystyrene that leads to its volatile organic fragment compounds.

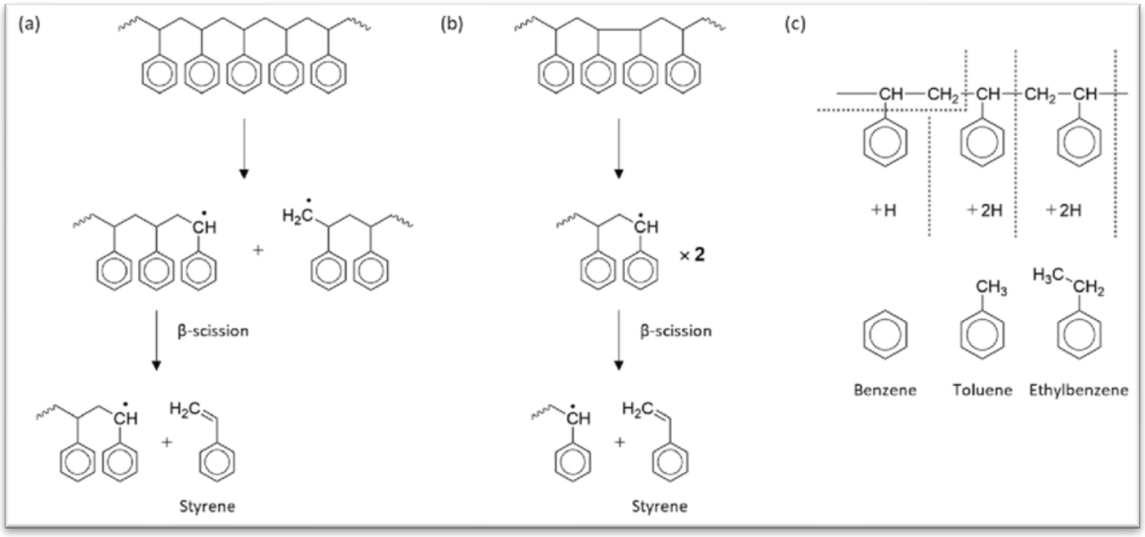

Figure 12: Schematics of the random chain scission mechanisms that are responsible for the fragmentation of polystyrene (Kim et al., 2021). In this figure, beta scission splits the C-C bond and produces a free radical, forming various fragment compounds. a) heat-to-tail scission b) heat-to-head scission c) plausible mechanism for the formation of volatile fragment compounds.

The standard pyro-GC-MS markers for polystyrene are the mono-, di-, tri- and tetramer signals of styrene (Fischer and Scholz-Böttcher, 2017), as well as its other expected fragmentation products, including benzene, toluene, and ethylbenzene. The products of polystyrene's fragmentation are shown in figure 13 below. The styrene monomer typically appears around the 9.6-minute retention time, the dimer (3-butene-1,3-diyldibenzene) typically appears around the 25-minute retention time, and the trimer (5-hexene-1,3,5-triyltribenzene) typically appears around the 37-minute retention time (Kusch, 2017). These components were utilized in this study to characterize polystyrene polymers. Styrene on its own was not an indicator of the polystyrene polymer because the molecule is commonly used as an additive in other plastics.

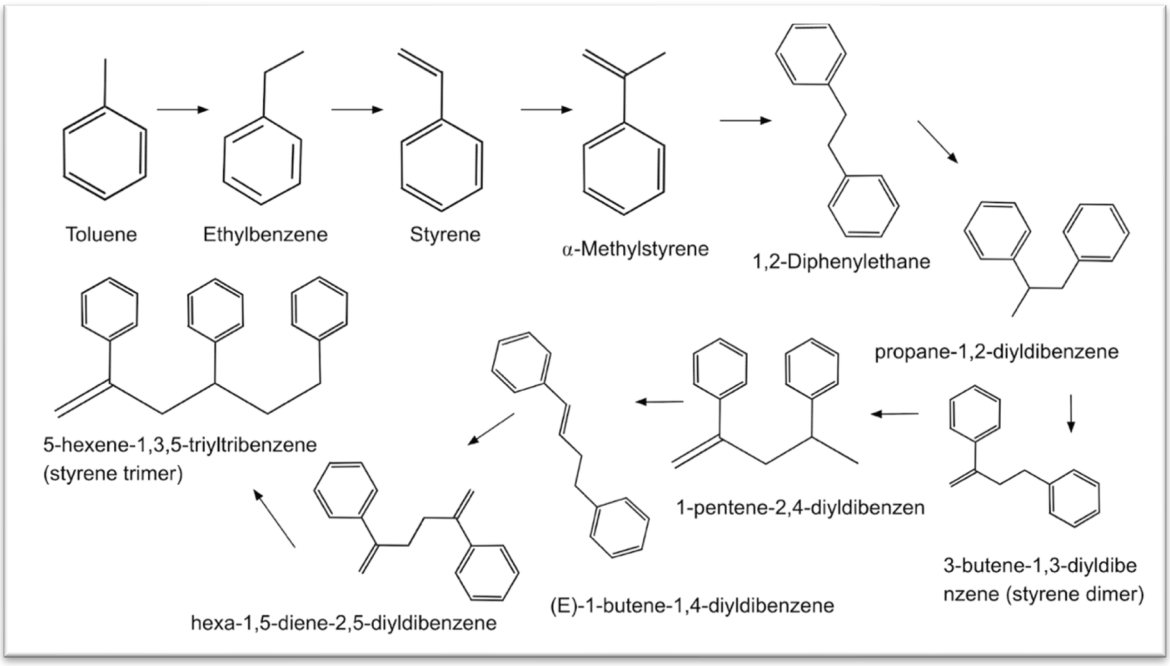

Figure 13: A portion of the expected pyro-GC-MS fragmentation of the polystyrene polymer. The fragments spread out across the spectra according to their molecular weight. The arrows move in the direction of smaller MW compounds to larger MW compounds, since the lighter fragments come out of the column first and are found at earlier retention times in the spectra. When looking for the structure of polystyrene, it is typical to see mono-, di-, tri- and tetramer signals.

e) Polyethylene terephthalate

Polyethylene terephthalate, or PET, is the most important thermoplastic terephthalate (Kusch, 2017). Thermoplastics are polymers that can be softened and melted to become pliable (Mallick, 2010). PET is often referred to as polyester and is produced in the form of fibers, films, or granules (Kusch, 2017; Lanaro et al., 2018). As seen in figure 14, the PET monomer contains the terephthalate molecule attached to a carbon on one side. This monomer is very complex compared to other polymers, as it contains a cyclic ring and two esters (each containing two oxygen atoms). Although this monomer is more chemically complex, PET is like PE and PP because they all consist of regular

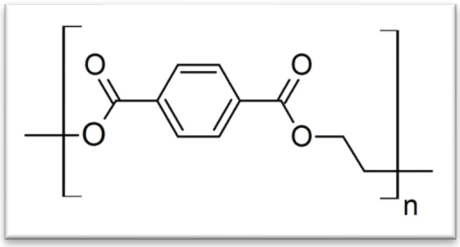

Figure 14: Monomer of PET.

and symmetric repeating units (da Costa et al., 2017). The crystalline form of PET is obtained from ethylene glycol with dimethyl terephthalate (DMT) by a transesterification reaction, or with terephthalic acid by an (trans)esterification reaction (Fischer and Scholz-Böttcher, 2017; Kusch, 2017). PET is typically characterized as having good chemical resistance, high mechanical properties, excellent transparency, and high barrier properties, particularly for oxygen and CO2 (Kusch, 2017). The characteristic "high barrier properties" refers to the materials permeability of gases, and thus their strong ability to keep things in. High barrier properties make PET a desirable polymer for food and beverage packaging, as the quality of the packaged goods can be maintained. PET is used for soft drink bottles, food packaging, thermal insulation, clothing fibers, and blister packs (da Costa et al., 2017). PET is also often used in industrial applications due to its excellent moisture and oxygen barrier characteristics (Lanaro et al., 2018).

The standard pyro-GC-MS signal for PET consists of multiple signals of benzoate and terephthalate derivatives and oligomers (Fischer and Scholz-Böttcher, 2017). A typical PET fragmentation, which is shown in figure 15, contains carbon dioxide, acetaldehyde, benzene (78 m/z), vinyl benzoate (148 m/z), benzoic acid (122 m/z), diphenyl (154 m/z), divinyl terephthalate (218 m/z), 4-(vinyloxycarbonyl) benzoic acid, ethan-1,2-diyldibenzoate, 2-(benzoyloxy)ethyl vinyl terephthalate, ethan-1,2-diyl divinyl diterephthalate, bis(2-(benzoyloxy)ethyl) terephthalate, and 2-(4-((2 (benzoyloxy)ethoxy)carbonyl)benzoyloxy) ethylvinyl terephthalate (Tsuge et al., 2011). The fragmentation of PET is the result of the chain scission and secondary reactions (Fischer and Scholz-Böttcher, 2017). In this study, benzene, vinyl benzoate, benzoic acid, and divinyl terephthalate were primarily utilized to identify this polymer, while the larger expected compounds were used to confirm the characterization.

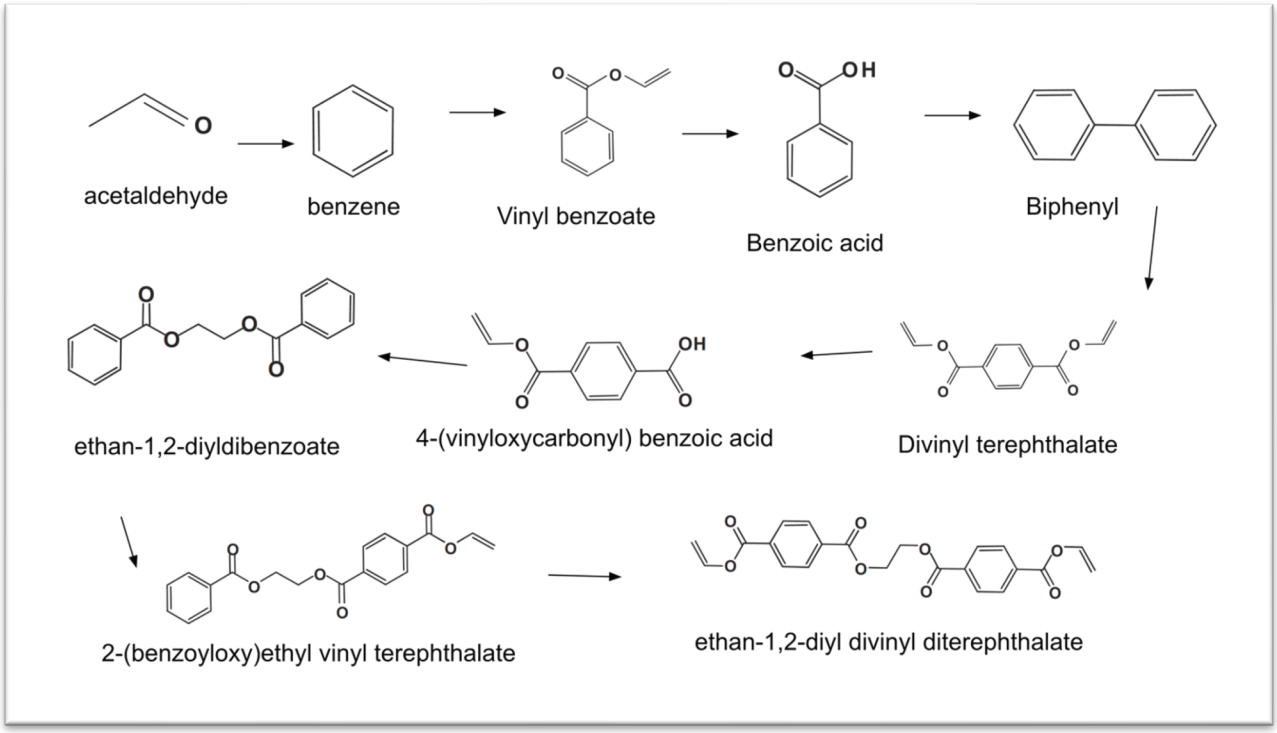

Figure 15: A portion of the expected pyro-GC-MS fragmentation of the polyethylene terephthalate (PET) polymer. The fragments spread out across the spectra according to their molecular weight. The arrows move in the direction of smaller MW compounds to larger MW compounds, since the lighter fragments come out of the column first and are found at earlier retention times in the spectra. When looking for the structure of PET, it is typical to see benzoate and terephthalate derivatives and oligomers fragments.

f) Polyvinyl chloride

Polyvinyl chloride (PVC) is a polymer comprised of repeated vinyl chloride monomer units. The vinyl chloride monomer, showin in figure 16, is an ethylene monomer with a chlorine in place of one hydrogen. After PE and PP, PVC is the third most produced polymer. In fact, the vinyl chloride monomer is very similar to ethylene, as its base is two carbons attached by a double bond, but a chlorine replaces one of the four hydrogens. PVC has a wide variety of uses that are dependent on its flexibility, as PVC can come in both rigid and flexible forms (Kusch, 2017). In general, PVC is

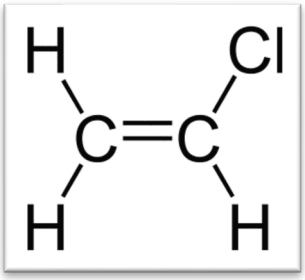

Figure 16: The vinyl chloride monomer is essentially ethylene with a chlorine in place of one of the hydrogens.

commonly known for its use in plastic films, as well as bottles and cups (Andrady, 2011). Records are made from PVC, which is why they are commonly referred to as "vinyl." Rigid PVC (RPVC) can be found in pipes, doors, windows, bottles, packaging, and bank/membership cards (Kusch, 2017). RPVC is also used in plumbing, electrical cable insulation, inflatable products, and imitation materials (such as rubber and leather). For these uses, rigid PVC is made softer using plasticizers like phthalates (Kusch, 2017).

The fragmentation of PVC consists of hydrogen chloride and a variety of aromatic hydrocarbons (Kusch, 2017), such as benzene and subsequent cyclic products. PVC fragmentation has cyclic compounds because of the pyrolytic conversion of PVC to benzene. The fragmentation of PVC, as show in figure 17, is the result of the chain stripping mechanism (Fischer and Scholz-Böttcher, 2017). The mechanism for the cyclization of PVC involves the removal of HCl, rearrangement and cyclization, and finally the elimination of side chains. The standard pyro-GC-MS marker for PVC consists of HCl, benzene, and multiple small signals of aromatic compounds (Fischer and Scholz-Böttcher, 2017). Toluene and polycyclic aromatic hydrocarbons are present in the fragmentation of PVC due to the double bonds formed during the elimination of HCl (Kusch, 2017). Specifically, known markers consist of hydrogen chloride (36 m/z), benzene (78 m/z), toluene (92 m/z), ethylbenzene (106 m/z), xylene (106 m/z), styrene (104 m/z), indene (116 m/z), 1-methylindene (130 m/z), 3-methylindene (130 m/z), naphthalene (128 m/z), 2-methylnaphthalene (142 m/z), 1-methylnaphthalene (142 m/z), acenaphthene (154 m/z), fluorene (166 m/z), and anthracene (178 m/z) (Tsuge et al., 2011). These compounds were utilized as to identify PVC polymers in this study.

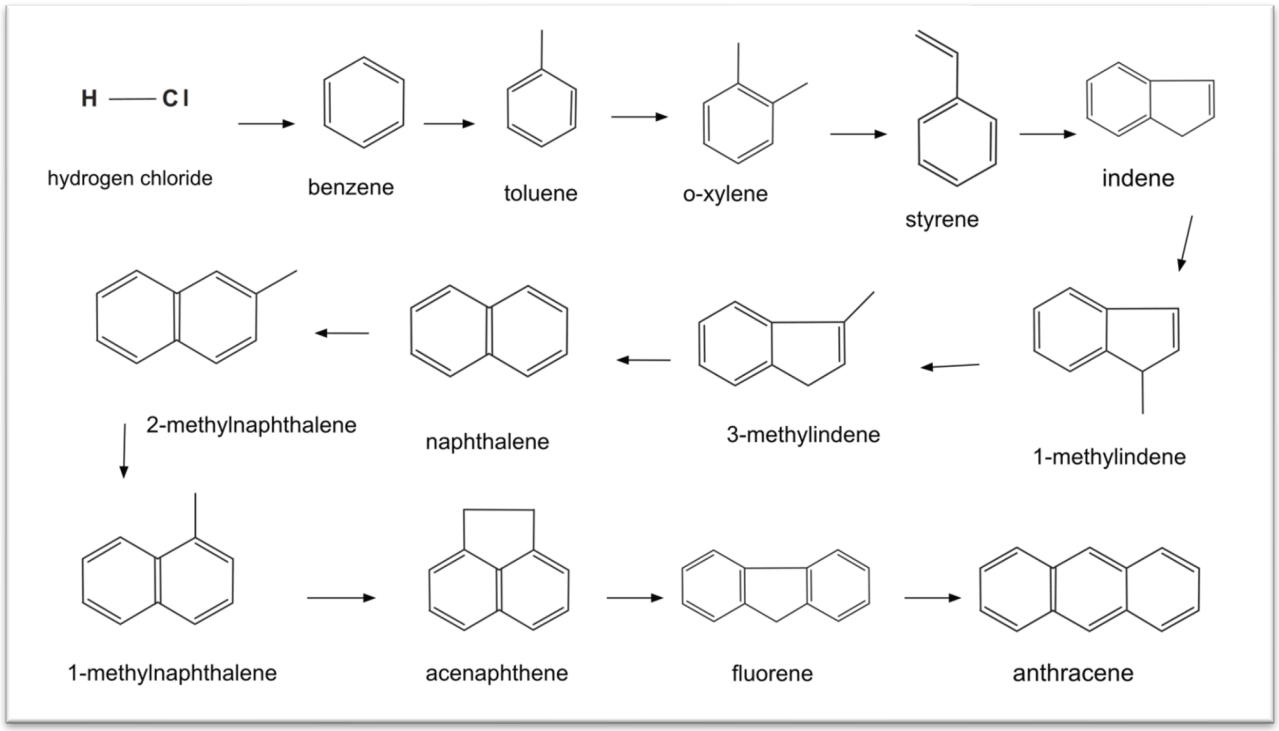

Figure 17: A portion of the expected pyro-GC-MS fragmentation of the polyvinyl chloride (PVC) polymer. The fragments spread out across the spectra according to their molecular weight. The arrows move in the direction of smaller MW compounds to larger MW compounds, since the lighter fragments come out of the column first and are found at earlier retention times in the spectra. When looking for the structure of PVC, it is typical to see benzene and other cyclic aromatic fragment compounds.

g) Resins

Various synthetic resins were characterized in this study. For example, the fragmentation of an epoxy resin is depicted below. Resins include a broad category of substances from plant or synthetic origin that can be converted into polymers relatively easily. They are a very useful material due to their strength, versatility, and excellent adhesion to a variety of surfaces. Resin's molecular structure consists of condensed aromatic rings surrounded by cycloalkanes and alkyl chains, with nitrogen, oxygen, sulfur, and other elements (Xie et al., 2022). The epoxy resin, whose fragmentation is shown below in figure 18, is one of the most common and widely used thermosetting resins (Du et al., 2022), or thermoset. Thermosets are polymers that set into a hard

shape via heat or radiation. This setting, or curing, process creates a polymer network that is cross-linked by covalent chemical bonds, making the hardening of the material irreversible. The presence of the epoxy ring functional group is responsible for epoxy resin's name. They are classified as molecules containing epoxy groups and capable of being converted to a thermoset form (Takeichi and Furukawa, 2012). Prior to their curing, epoxy resins are reactive and must be cross-linked by polymerization via epoxide or hydroxyl groups (Massingill and Bauer, 2000). The traditional epoxy resin composition contains bisphenol A (BPA) and accounts for 90% of these resins (Du et al., 2022). This version of the epoxy resin is not ideal because it relies on the limited petrochemical resource, and it is a threat to human health due to the presence of BPA, which is an xenoestrogen that can interfere with the endocrine system (Du et al., 2022). Due to these negative environmental and public health impacts, there is a push for the development of bio-based raw materials as epoxy resin alternatives (Du et al., 2022).

Epoxy resins have many industrial and manufacturing advantages, such as their resistance to corrosion, electrical resistance, low shrinkage, and low price (Du et al., 2022). They are utilized for a wide array of applications, including adhesives, coatings, electronics, vehicle materials, casting resins, composites, building materials, railway, and aerospace (Du et al., 2022). A typical epoxy resin fragmentation, shown in figure 18, contains acetaldehyde, phenol, cresol, p-isopropylphenol, p-isopropenylphenol, p-hydroxy-2,2-diphenylpropane, 2-(4'-hydroxyphenyl)-2-(4'-methoxyphenyl) propane, and BPA (Tsuge et al., 2011). In epoxy resins, BPA is not an additive or flame retardant, but rather an intermediate product in the formation of the polymeric material (Rios Mendoza et al., 2017).

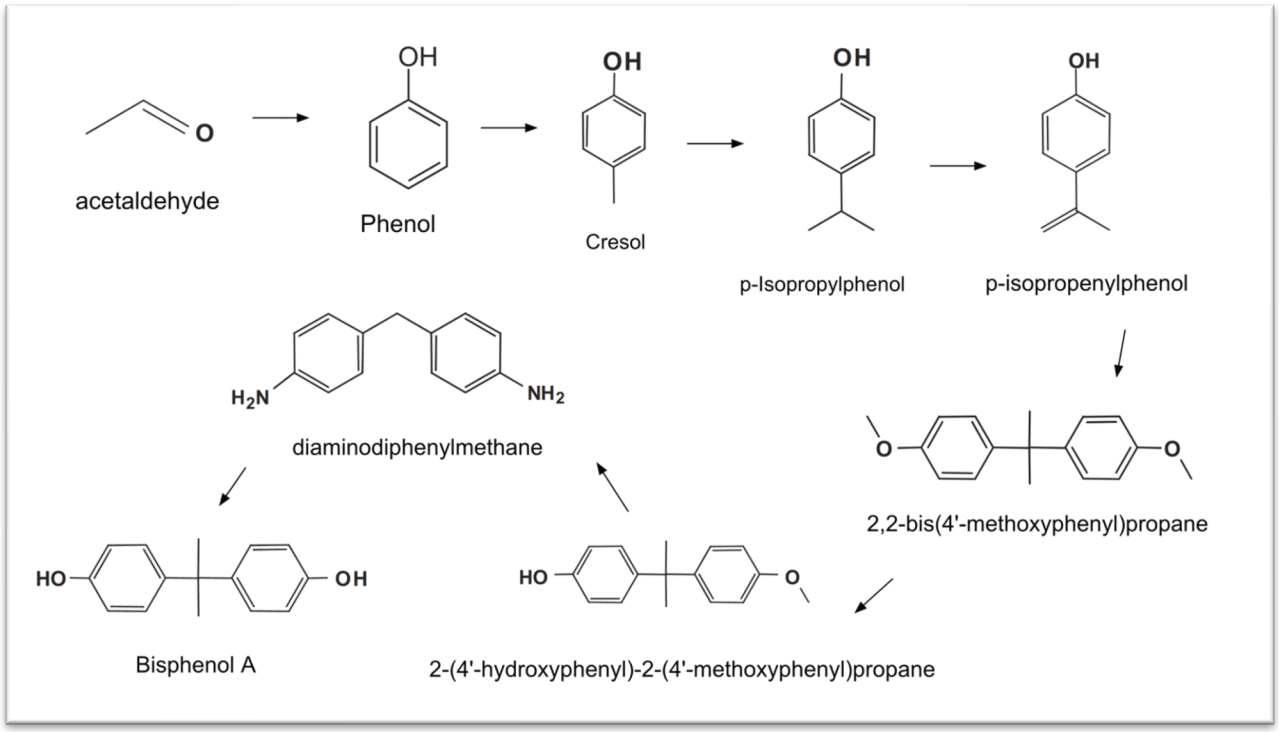

Figure 18: A portion of the expected pyro-GC-MS fragmentation of the epoxy resin polymer. The arrows move in the direction of smaller MW compounds to larger MW compounds, since the lighter fragments are found at earlier retention times in the spectra. When looking for the structure of the epoxy resin, it is typical to see many cyclic compounds, including bisphenol A as an intermediate.

v. Relevant Plastic Additives

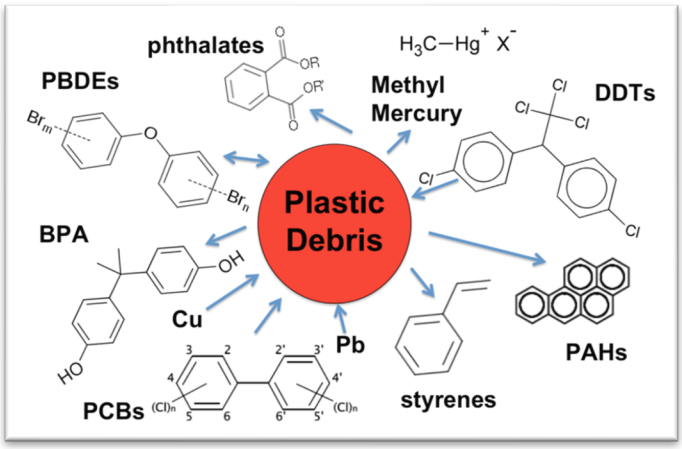

Figure 19: "Cocktail" of chemical contaminants (Rochman, 2015).

As mentioned in the "Health and Ecosystem Impacts" section, various additives and plasticizers are incorporated into all kinds of polymers during manufacturing processes. These additives, some of which are shown in figure 19, enhance the thermal and mechanical properties of plastics, and extend their

resistance to heat (Avio et al., 2017; Eben et al., 2020). Some examples of additives that were present in this study's samples include bisphenol A, or BPA (228 m/z), 2,4-Ditertbutylphenol (10.45 retention), methyl methacrylate (100 m/z), styrene (104 m/z), and various phthalate plasticizers. These additives contribute to the concern of microplastic pollution because they are shown to have numerous toxic effects in marine organisms and humans. Additives also increase the time it takes for plastics to degrade (Avio et al., 2017). Phthalates and bisphenol A are known endocrine disruptors, as they can disrupt, mimic, and compete with endogenous hormones (Avio et al., 2017). Phthalates can constitute about 50% of PVC products (Avio et al., 2017). In addition to being established endocrine disruptors, phthalates have been associated with adverse pregnancy outcomes (Meeker et al., 2009). It has been shown that blending resins with styrene and methyl methacrylate creates the desired enhanced thermal and mechanical properties sought out by additive incorporation (Eben et al., 2020). Methyl methacrylate has been shown to have toxic health effects (Bereznowski, 1995). However, the toxicity of this additive is not ubiquitously agreed upon. One study found methyl methacrylate to be less toxic in the nasal epithelium of humans than in rats (Mainwaring et al., 2001). Although the toxic effects of methyl methacrylate in humans is not as well established as other additives, its ability to enhance its plastic properties is a cause for concern, because the impacted polymers will persist for longer in the environment. Styrene, on the other hand, has well established toxic effects (Simmonds, 2004), including the fact that it is likely carcinogenic (Green et al., 2001; Kogevinas et al., 2018). Styrene has been shown to induce DNA damage, gene mutations, and chromosomal aberrations, among other effects (Kogevinas et al., 2018). Additionally, this compound is quickly absorbed, widely distributed, and extensively metabolized in the body, increasing the danger of the additive (Kogevinas et al., 2018). Another significant additive in this study, 2,4-ditertbutylphenol, is part

of a group of compounds called synthetic phenolic antioxidants (SPAs), which are known for their toxicity and environmental contamination (Liu and Mabury, 2019). This additive is shown to be a toxic lipophilic phenol in animals (Zhao et al., 2020), and acts as an endocrine disruptor in humans (Bach et al., 2013). This study was able to recognize these additives using the pyro-GC-MS, which provides insight into which dangerous compounds are present in certain products and areas.

vi. Background on the study

In this study, plastic samples were collected from four littoral environments on Cape Cod, MA. To encompass a wide variety of shorelines surrounding this area, the chosen sampling locations included the Bass River, the Nantucket Sound, the Outer Cape, and the Cape Cod Bay. These sites are distinctly shown in figure 22 below. It was predicted that most of the samples collected would fall within the polyethylene or polypropylene categories because these polymers are more abundantly produced than other common polymers. In addition to their abundant production, they were also expected to collect more abundantly on the littoral sampling sites of this study since they are more buoyant than other polymers. As seen in figure 20, polyethylene (0.93-0.98 g/cm³) and polypropylene (0.89-0.91 g/cm³) are less dense than sea water (1.025 g/cm³), which causes them to float. Polymers denser than sea water, such as polystyrene and PVC, are expected to sink in the ocean, while lower density polymers were

Matrix	Density (g/cm^3)
Distilled water	1
Sea water	1.025
Polyethylene (PE)	0.93–0.98
Polypropylene (PP)	0.89–0.91
Polystyrene (PS)	1.04–1.11
Polyvinylchloride (PVC)	1.20–1.45
Polyamide (PA)	1.13–1.5
Polyethylene terephthalate (PET)	1.38–1.39
Polyvinyl Alcohol (PVA)	1.19–1.35

Figure 20: Polymer densities in comparison to seawater (Avio et al., 2017). PE and PP are the least dense and can float in seawater.

shown to float in a water column (Avio et al., 2017). While denser polymers are more likely to collect in the depths or floor of the ocean, low density microplastics that float on the surface of the water would be more likely to wash onto the shores and be collected during this study.

To predict where the plastic samples that were collected in this study may have come from, it is important to understand the tides and currents surrounding Cape Cod, MA. Two major Atlantic currents converge at Cape Cod: The Gulf Stream current running from South to North and the Maine Coastal Current running from North to South. With these two currents colliding in addition to the presence of the Martha's Vineyard and Nantucket Islands, and the Cape Cod Canal, the flow of the currents can get messy (Lloret, 2022). These major currents are depicted in figure 21 below. The Northern Shore of Cape Cod likely receives debris from the Boston area that is carried down by the Maine Coastal Current (Lloret, 2022). As the Northern Shore falls within the Cape Cod Bay, a portion of the debris on those shores likely accumulates from pollution in the areas surrounding the Bay. The Southern Shore of Cape Cod may receive debris from areas further south along the East Coast of the U.S. that are carried up by the Gulf Stream Current (Lloret, 2022). The Nantucket Sound is partially protected by the Nantucket and Martha's Vineyard islands, which are shown in figure 21, so not all the debris flowing up in the Gulf Stream Current would feasibly make it to the Southern Shore. It is expected for the Eastern coast of Cape Cod to be cleaner because of its proximity to the open Atlantic and strong currents (Lloret, 2022). As a result, debris found on the Outer Cape collection site likely arose from pollution on the land, rather from the ocean. Although these currents may reveal how microplastics travel around the waters of Cape Cod, it is important to note that many of the samples collected in this study likely came from litter and pollution on the beach. With a littoral

collection site, it cannot be said with certainty whether the samples emerged from the water itself.

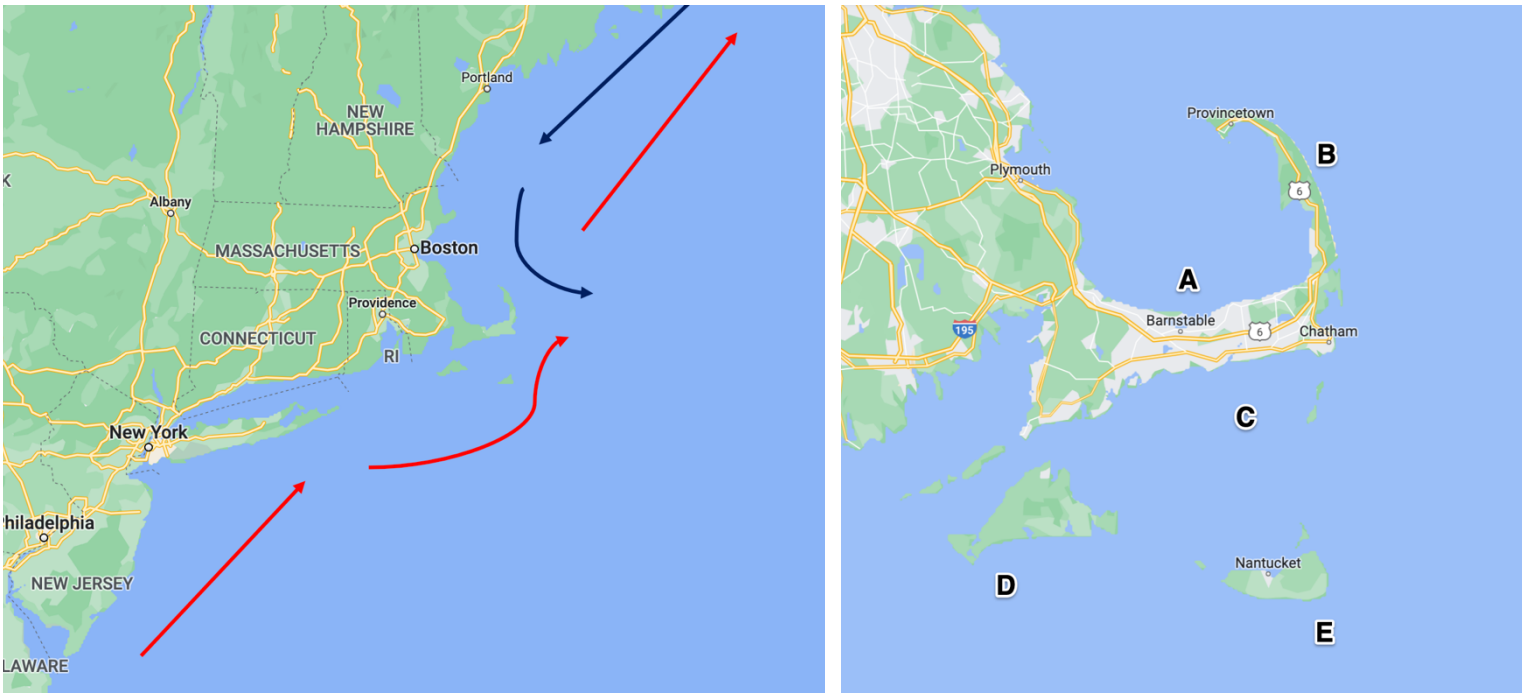

Figure 21: The image on the left shows the Gulf Stream Current flowing North (in red) and the Maine Coastal Current flowing South (in blue). The image on the right shows the Cape Cod Bay (point A), the Outer Cape (point B), the Nantucket Sound (point C), Martha's Vineyard Island (point D), and Nantucket Island (point E).

Materials and Methods

Materials. The sampling procedure required glass jars for collection, a tide calendar, scoops, sieves, and GPS device for determining latitude and longitude locations. The analytical technique used for this project required the *Agilent 6890 GC* and *Agilent 5973 MS* instruments that are made by Agilent Technologies, the *CDS-2000 pyro-probe*, the *CDS-1500 GC-MS interface*, the quartz tubes, quartz wool, tweezers, and a scalpel. ChemStation software was used to acquire and

process the data. This analytical program could only run on a Windows-10 based computer. The mass spectral database library from NIST was required to see what molecular fragments the peaks from the spectra could correlate to. This database provided compounds that were potentially present in the pyrolyzed mixture, which could be verified with logic and used to identify patterns. The marker compounds in the pyrolyzed product mixture served as the different pieces of a puzzle that were used to put the puzzle back together, ultimately leading to the characterization of the polymer composition.

i. Sample Collection

Plastic samples were collected from four littoral environments across Cape Cod, Massachusetts: The Bass River, the Nantucket Sound, the Outer Cape, and the Cape Cod Bay. Collection sites are depicted in figure 22. Samples were collected from the last week of June 2021 through the first week of July 2021. Samples were collected within a few hours before or after low tide so that plastics washing up on the shore from the water were accessible. Local tides were checked each day to accommodate this procedure. Date, time, tide, coordinates, temperature, weather conditions, air pressure, and any other factors were noted. Samples were typically collected by walking along the shore about five feet from the tide line, paying close attention to accumulations of seaweed or rocks where plastics could get caught. Samples within the microplastic size range were initially targeted, but larger plastics (up to about 20 cm) were

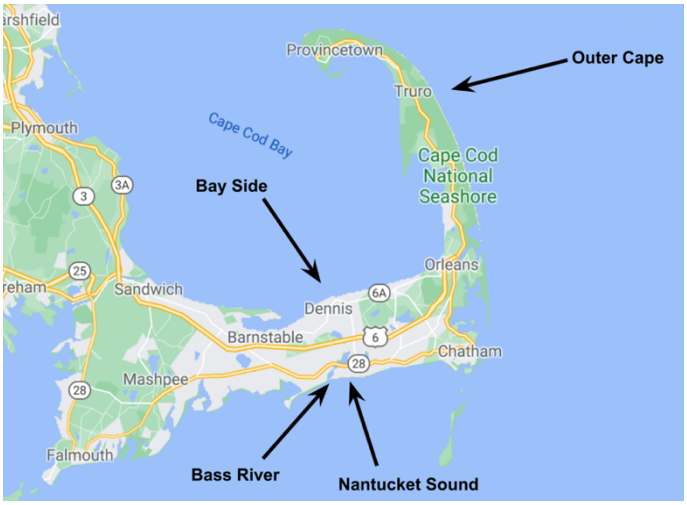

Figure 22: Map of the four sampling locations on Cape Cod, Massachusetts.

also collected and analyzed under the assumption that they would break down into secondary microplastics.

Samples were collected from the Bass River at Windmill Beach in South Yarmouth on June 27, 2021. Collection occurred from 7:52 pm to 8:04 pm, a little bit before low tide, which occurred at 8:25 pm. The conditions were partly sunny and humid with a chance of rain. The temperature was 22℃, and the pressure was 765 mmHg. Samples were collected in the area around latitude 41.65462 and longitude -70.196369.

Samples were collected from the Nantucket Sound at South Middle Beach in South Yarmouth on June 29, 2021. Collection occurred from 6:13 pm to 6:30 pm, before low tide, which occurred at 9:57 pm. The conditions were sunny and nice, the temperature was 28℃, and the pressure was 763 mmHg. Samples were collected in the area around latitude 41.643019 and longitude -70.205339.

Samples were collected from the Outer Cape at the Head of the Meadow Beach in Truro on July 5, 2021. Collection occurred from 4:00 pm to 4:15 pm, about an hour after low tide, which occurred at 2:47 pm. The conditions were partly cloudy, the temperature was 21℃, and the pressure was 763 mmHg. Samples were collected in the area around latitude 42.052298 and longitude -70.077659.

Samples were collected from Cape Cod Bay on two occasions, both on July 7, 2021. The first was at Howes Street Beach in Dennis from 3:44 pm to 4:05 pm, before low tide, which occurred at 4:20 pm. Samples were collected in the area around latitude 41.750766 and longitude -70.183905. The second was at Corporation Beach in Dennis from 6:09 pm to 6:29 pm, after low tide, which occurred at 4:20 pm. Samples were collected in the area around latitude 41.751567 and longitude -70.187794. During both collections, the conditions were sunny, and the pressure

was 758 mmHg. The temperature during the first collection was 31℃, and the temperature during the second collection was 28℃.

ii. Analytical Technique

The samples were analyzed using the pyrolysis-gas chromatography-mass spectrometry analytical technique. To begin this process, a quartz tube was prepared to contain the sample. Quartz tubes were used due to their ability to withstand the levels of high heat necessary for this procedure. First, a small amount of quartz wool was inserted into the middle of the tube for the sample to rest on. The wool plug was compacted in with a probe, making it ready for cleaning. The quartz tube was then heated and cleaned three times in the pyro-probe before the sample was inserted. Each time, the quartz tube was heated at 1200℃ for 20 seconds. To carry out the cleaning, the quartz tube was inserted into the platinum filament of the CDS-2000 pyro-probe. The "clean" button on the control pad was then pressed, and the platinum filament glowed orange, confirming the heating of the quartz tube at an extremely hot temperature. This thorough cleaning minimized disruptions to the resulting spectra by removing organic contaminants that could interfere with the sample. Once the tube was cleaned, it was only handled with forceps.

A small piece of plastic sample was then cut using a scalpel to fit into the quartz tube, typically about 1mm in size. The plastic sample was then inserted into the clean quartz tube using forceps. Before running the sample, the settings were confirmed on the computer and the file location for the data was set. The desired settings consisted of an oven temperature of 45℃, an GC-inlet temperature of 320℃, a GC-MS interface temperature of 320℃, a column flow rate of 1.2 mL/min, a turbo-speed of 100 (100% vacuum pulling capacity), and an MS ion source temperature of 230℃. Information about the sample was then entered, including operator name, sample name, and data file name and location. The "start run" button was then pressed on the

computer. When the program indicated that the instrument was ready, it was time to insert the sample into the GC-MS interface. To prepare for manual injection, the "prep-run" button on the instrument was pressed. Then, the valve on the CDS-1500 GC-MS interface was opened by switching it from "run" to "load." A wet paper towel was then used to safely remove the hot cap from the entry point for the pyro-probe, the pyro probe was inserted, and the valve was switched back from "load" to "run." The following three buttons were then pressed consecutively and rapidly: "START" on the instrument, "PREP RUN" on the remote, and "RAMP/SINGLE" on the remote. Once these buttons were pressed, the sample was heated to 650℃ for 5 seconds. After one minute passed, the valve was closed by switching the dial from "run" to "load," and the pyro-probe was removed. If the valve was left open when the pyro-probe was removed, oxygen could enter the chamber and cause oxidative damage to the GC column. The knob was placed back over the opening for the pyro-probe using a wet paper towel. The pyrolyzed mixture was automatically carried through the chromatography process via the hydrogen carrier gas. The sample continued to run through the GC-MS as the peaks were resolved over time, which took about 40 minutes. The resulting pyro-gram was then sent to the computer for analysis.

iii. Peak Analysis

The resulting spectra were analyzed using the ChemStation software program. Through this program, each file produced from a pyrolysis-GC-MS run could be opened to reveal the ion chromatogram. Each peak in this chromatogram, representing a compound, could be double right clicked to open the mass spectral fragmentation peaks associated with that compound. Double right clicking on the mass spectrum peaks brought up a suggested list of compounds from the NIST database, which was connected to the ChemStation program. Using the suggestions from this database and a book of known standards, the compound associated with each peak was

determined and noted. This process occurred in sections at a time by zooming in on portions of the chromatogram, starting with the larger and more prominent peaks. Once the compounds associated with the major peaks in the spectra were identified, standard marker compounds and peak patterns could be recognized and lead to the characterization of the sample.

Results and Discussion

i. Polymer Characterization

Based on the characterization of all the polymers from this study, the samples were placed into one of the following five categories: polyethylene, polypropylene, PET, PVC, styrene, cellulose, and resin-based polymers. Each individual piece of plastic collected was considered a sample. As shown in figure 23, ten polypropylene samples made up 28.57% of the entire dataset. Seven polyethylene samples made up 20.00%, five PET samples made up 14.29%, five resin samples made up 14.29%, three cellulose samples made up 8.57%, two polystyrene samples made up 5.71%, and two PVC samples also made up 5.71%. Additionally, one polyamide made up 2.86% of the dataset. It was expected for most of the samples to be polyethylene and polypropylene, as these are the most produced polymers (Jeon et al., 2021).

The microplastic polymers in this study were characterized based on the ion chromatogram and related mass spectra that resulted from the pyrolysis-GC-MS analysis depicted in figure 1. Each sample was pyrolyzed to form a gaseous mixture of the polymer's specific heat degradation products. These fragment compounds were separated in the gas chromatography column. Each peak in a sample's resulting ion chromatogram represented one of the fragment compounds from the mixture. The chemical compound associated with each peak was determined using the related mass spectra. Once all the heat degradation products were

determined and labeled on the ion chromatogram, the peak patterns were compared to known standards to determine the polymer composition.

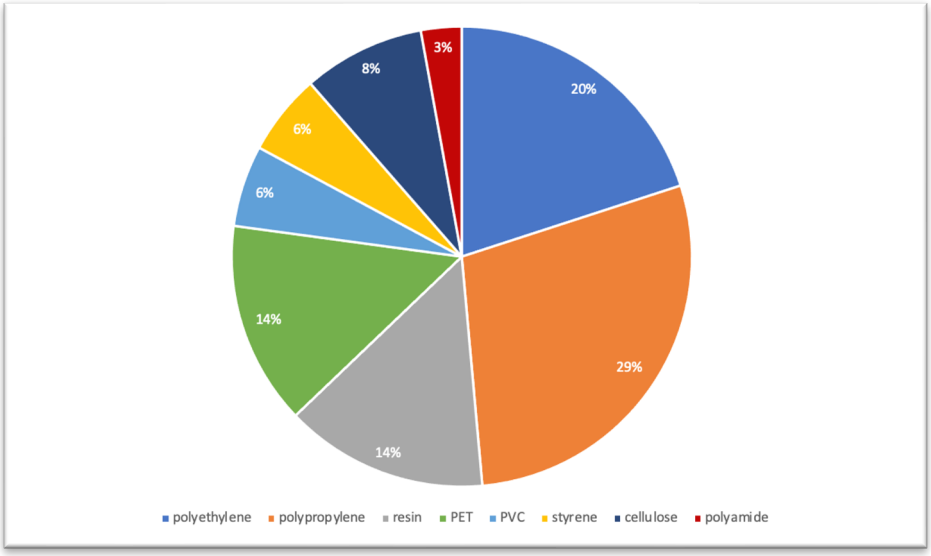

Figure 23: Polymer characterization of the total sample pool from all four locations across Cape Cod, Massachusetts. Charts organized by number of samples in each category divided by the total number of samples from the area specific to the section.

---

a) Bass River

From the Bass River collection location, five samples were analyzed, numbered BR1 through BR5. As seen in figure 24, the sample pool from this location consisted of the following polymer characterizations: 40% polystyrene, 20% polyethylene, 20% PVC, and 20% polypropylene. The abundance of polystyrene pollution from this location can reasonably be accounted for by the large number of boats and buoys in the Bass River estuary. Ship's hull scrapings and marine coatings are a plausible source of microplastic pollution (Gaylarde et al., 2021). The durable protective coatings of boats often contain synthetic polymers such as polystyrene (Gaylarde et al., 2021). Various buoyant boat parts and buoys can also be comprised of polystyrene foam (Chen et al., 2018; Mukai et al., 2020), which more likely explain the

resulting statistical prevalence of polystyrene, since the later described samples were predominantly foams.

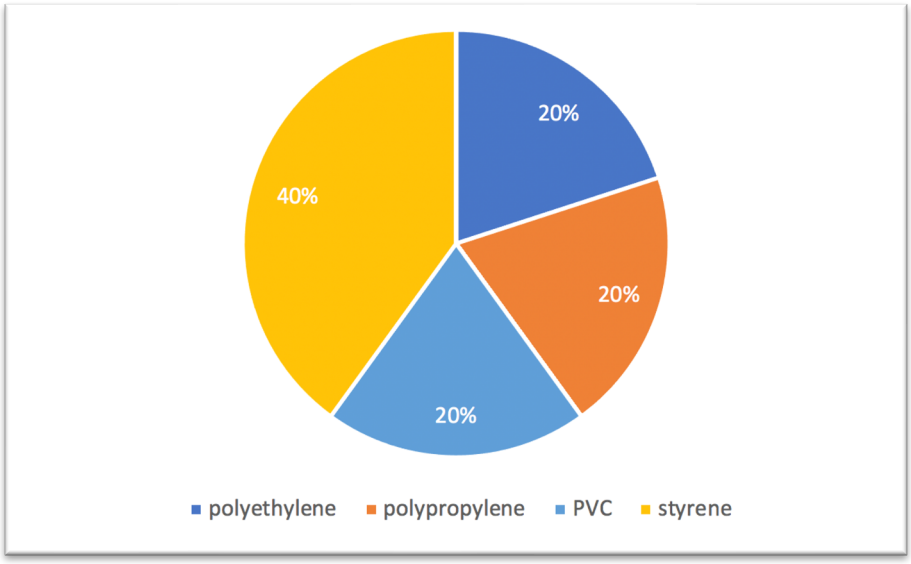

Figure 24: Polymer characterization of the Bass River samples.

Sample BR1, shown in figure 25, was a small purple microplastic collected from a rocky area about ten feet from the Bass River. Despite being firm, the sample was somewhat pliable. It was less than 1 mm at the time of collection, so it was unclear whether it was a primary or secondary microplastic. This sample was identified by its' ion chromatogram, which exhibited a pattern of triplet hydrocarbon clusters with increasing carbon chain lengths. Each triplet contained a single bonded, double bonded, and saturated hydrocarbon with its specified number of carbons. For example, the triplet peaks around 6.50 minutes consisted of 1,9-decadiene, 1-decene, and

Figure 25: An image of sample BR1, which was a tiny purple rubbery pellet at the time of collection.

decane, in that order. This triplet contained a single bonded, double bonded, and saturated hydrocarbon, each with a ten-carbon chain. The next set of triplet peaks, around 7.50 minutes, consisted of 1,10-undecadiene, 1-undecene, and undecane, which each had an eleven-carbon chain. As shown by the ion chromatogram in figure 26, this pattern began with the three-carbon chain molecule propane at around 2.50 minutes and continued through the twenty-six-carbon chain, hexacosane, at about 15.80 minutes. This peak pattern is standard for the polyethylene polymer (Tsuge et al., 2011). This sample did not contain styrene, acetic acid, 2,4-ditertbutyl-phenol, phthalate, or bisphenol A additives. The standard pattern of triplet hydrocarbon clusters with no additives is very typical for polyethylene polymers This peak pattern is standard for the polyethylene polymer (Tsuge et al., 2011). The sample was ultimately characterized as polyethylene and was placed in the polyethylene category.

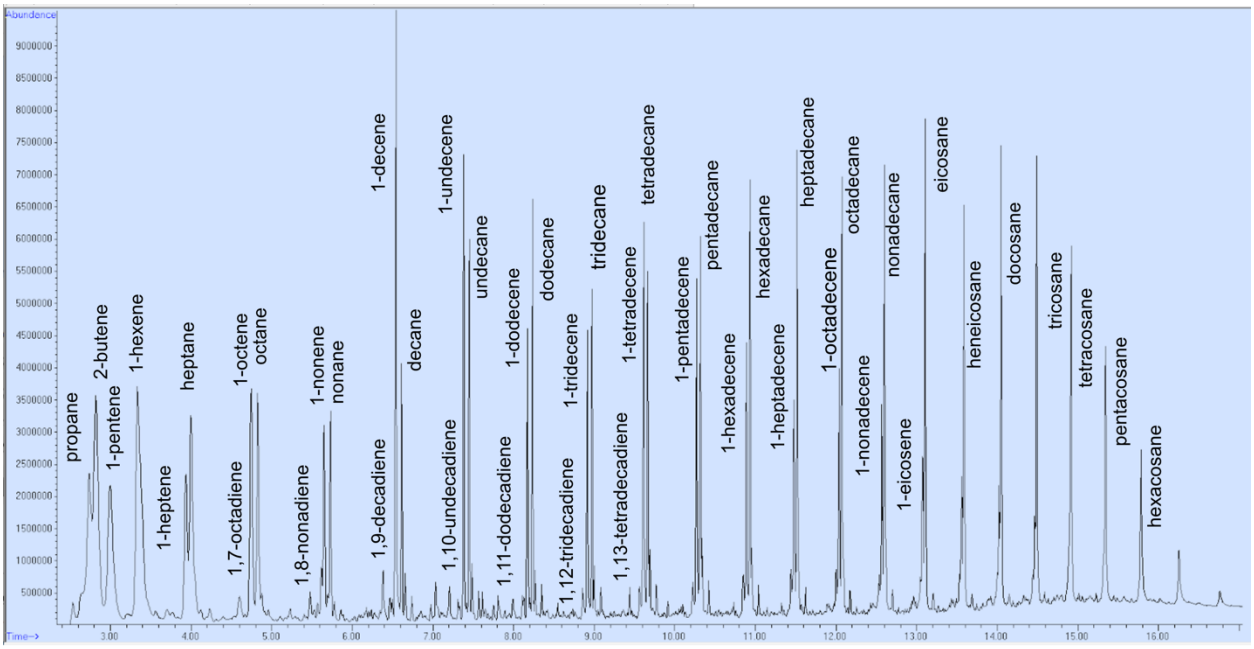

Figure 26: Labeled pyro-gram peaks of sample BR1, which was determined to be polyethylene due to the exhibited pattern of triplet hydrocarbon clusters with increasing carbon chain lengths. Sample was run at previously stated instrumental conditions (650 C pyrolysis).

Figure 27: An image of sample BR2.

Sample BR2, shown in figure 27, was a particle of teal foam. This sample was about 1 mm wide at the time of collection, but it appeared to be a part of a larger foam, making it a secondary microplastic. As seen in the ion chromatogram from figure 28, this sample contained toluene, styrene, α-methylstyrene, 1,2-diphenylethane, propane-1,2-diyldibenzene, 3-butene-1,3-diyldibenzene (which is also known as a styrene dimer), and 5-hexene-1,3,5-triyltribenzene (a styrene trimer). These compounds are known indicators of the polystyrene polymer (Tsuge et al., 2011), so this sample was characterized as polystyrene and placed in the styrene category. Styrene is sometimes used as an additive in other polymers to enhance their thermal and mechanical properties (Eben et al., 2020). Since styrene was a main component of the polymer, it is not considered an additive in this sample. There was no methyl methacrylate, bisphenol A, 2,4-ditertbutylphenol or phthalate additives detected in this sample. It

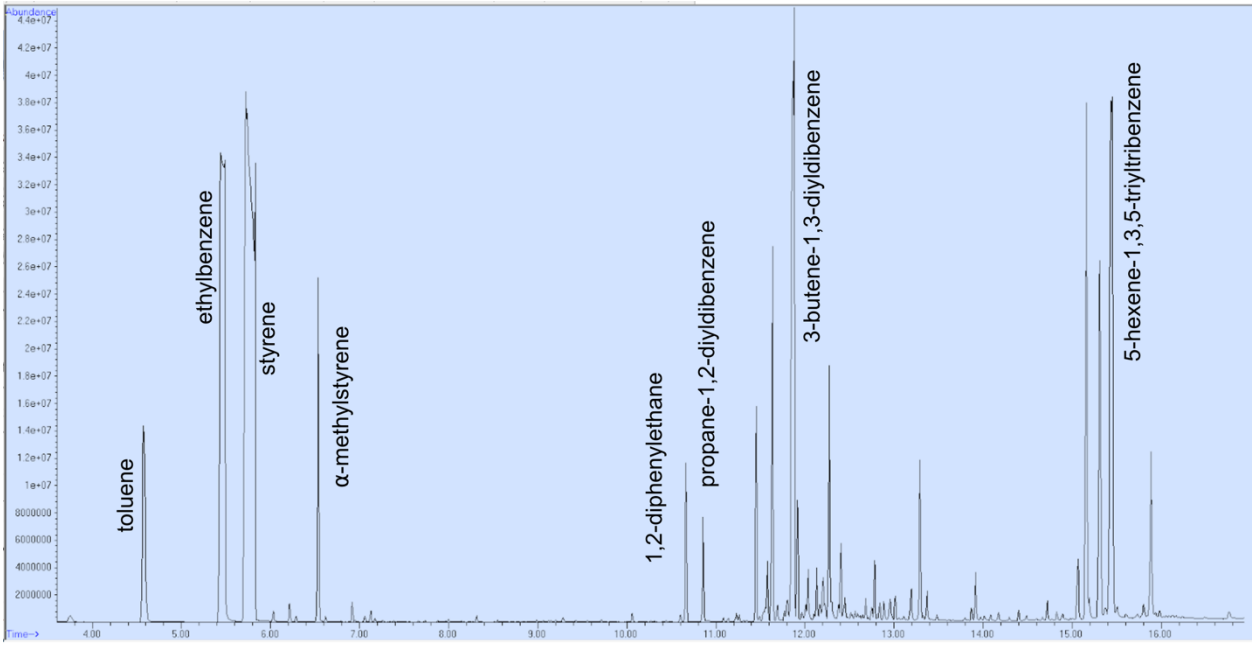

Figure 28: Labeled pyro-gram peaks of sample BR2, which was determined to be polystyrene.

is expected that foam samples would fall within the styrene category, which can be dangerous as styrene-based polymers are known to harm human health (Canesi et al., 2015; Chiu et al., 2015; Rahman et al., 2021), and foam samples can easily break down and spread, especially in littoral environments (Fok et al., 2017; Zhang et al., 2021).

Figure 29: An image of sample BR3.

Sample BR3, depicted in figure 29, was also a particle of teal foam. This sample was slightly larger than the definable microplastic size, but the foam was clearly breaking apart and creating secondary microplastics. Like sample BR2, this sample also contained many compounds typical to polystyrene (Tsuge et al., 2011), including toluene, styrene, α-methylstyrene, 3-butene-1,3-diyldibenzene, and 5-hexene-1,3,5-triyl-tribenzene. In addition, this sample contained many nitrile compounds, which alluded to the fact that it may be something more than solely polystyrene. As shown in the ion chromatogram depicted in figure 30, the presence of nitrile groups such as acrylonitrile, 2-methylene-4-phenylbutanenitrile, 4-phenylpent-4-enenitrile, 2-methylene-4,6-diphenyl-hexanenitrile, 2-methylene-4,6-diphenyl-hexanenitrile, 4,6-diphenyl-hept-6-enenitrile, and 2-phenethyl-4-phenylpent-4-enenitrile all aligned with the expected standard acrylonitrile-styrene alternating copolymer peaks (Tsuge et al., 2011). With the combination of styrene and these nitrile peaks, this sample was characterized as an acrylonitrile-styrene alternating copolymer and placed in the styrene category. This sample was likely part of a floatation device associated with boating or other recreational activities that take place in the Bass River. Since styrene was part of the polymer, it was not considered an additive in this sample. No additional additives, including methyl methacrylate, bisphenol A, 2,4-ditertbutylphenol or phthalates, were detected.

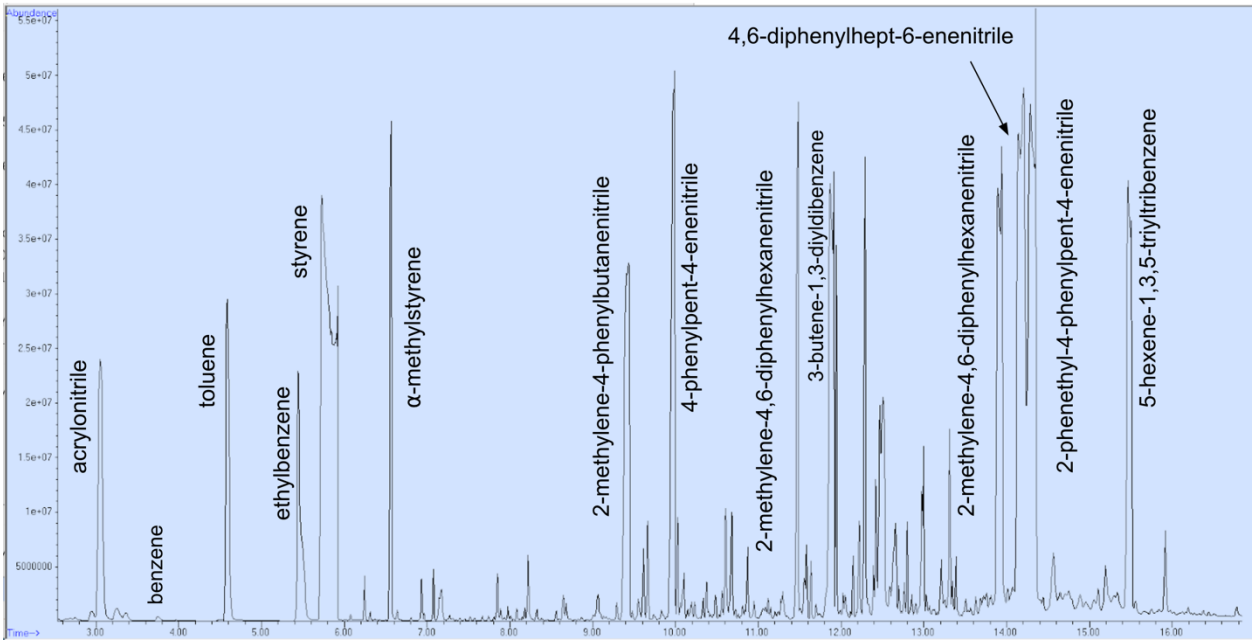

Figure 30: Labeled pyro-gram peaks of sample BR3, which was determined to be an acrylonitrile-styrene alternating copolymer.

Figure 31: An image of sample BR4.

Sample BR4, which is shown in figure 31, was a fragment of a clear straw wrapper. The fragment was about 4.5 mm long, and the wrapper was breaking down into smaller pieces, forming secondary microplastics. This sample was identified as polypropylene by the 2,4-dimethyl-1-heptene marker compound. This identification was confirmed as other compounds present in the ion chromatogram (displayed in figure 32) further aligned with the reference polypropylene standard, including 2-methyl-1-pentene, 2,4,6-trimethyl-1-nonene, and 2,4,6,8-tetramethyl-1-undecene (Tsuge et al., 2011). This sample also contained the 2,4-ditert-butylphenol additive, which is commonly found in polypropylene samples (Oliveira et al., 2020). No methyl methacrylate, bisphenol A, or phthalate additives were detected. This polymer was placed in the polypropylene category.

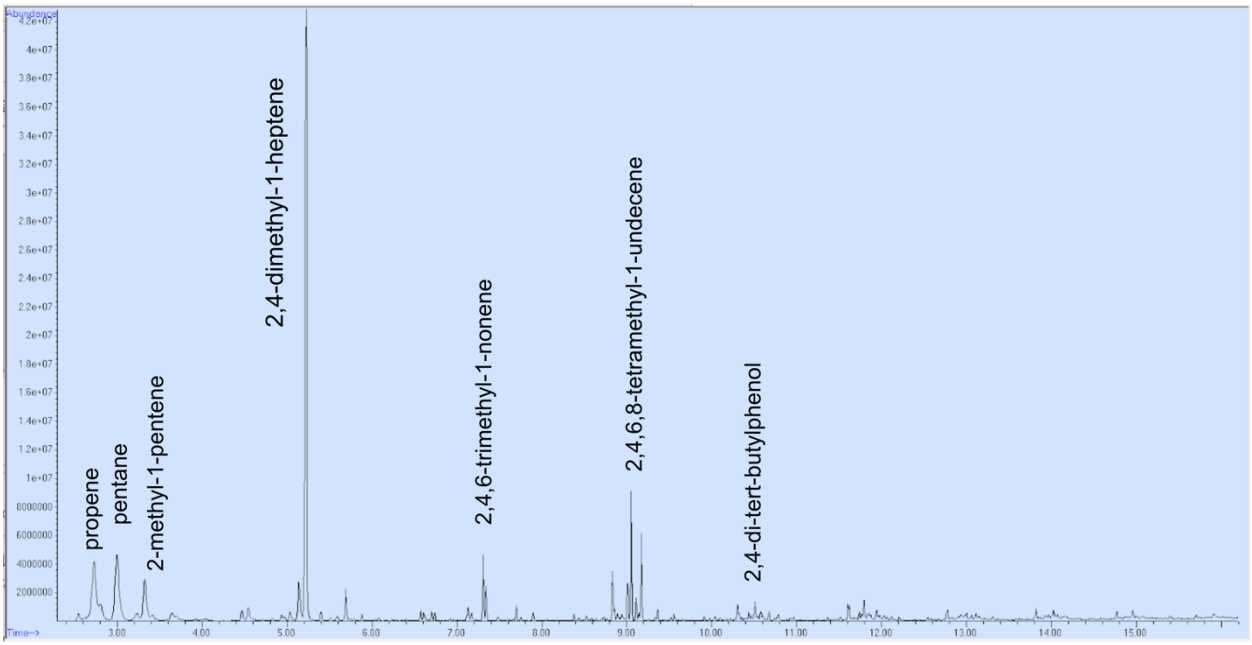

Figure 32: Labeled pyro-gram peaks of sample BR4, which was determined to be polypropylene.

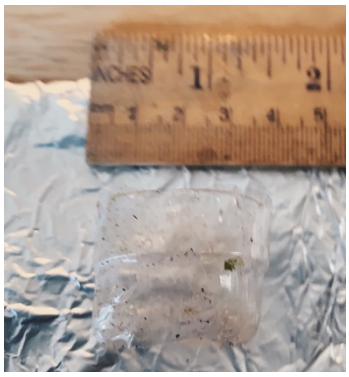

Figure 33: An image of sample BR5.

Sample BR5, depicted in figure 33, was part of a plastic lid wrapper, which was determined to be some sort of PVC due to the presence of benzene and subsequent cyclic fragmentation products. This sample was about 4 mm tall and small pieces were breaking off to form secondary microplastics. The sample was firm but flimsy, as the wrapper could be bent easily. This polymer was more specifically characterized as a vinyl chloride-vinyl acetate copolymer, or P(VC-VAc). This sample was identified based on the presence of many marker compounds of P(VC-VAc) that were identified in the ion chromatogram shown in figure 34, including hydrogen chloride, benzene, toluene, styrene, xylene, indene, and naphthalene (Tsuge et al., 2011). Since styrene was a component of the polymer, it was not considered an additive. No bisphenol A or 2,4-ditertbutyl-phenol additives were detected. Additives present included methyl methacrylate, and bis(2-ethylhexyl)

phthalate, which is a known plasticizer (Kang et al., 2021). It makes sense that more plasticizer additives would be present in a co-polymer, as the producer is aiming to make an effective mix of ingredients for their desired product (Jafferson and Chatterjee, 2021). Although many markers of P(VC-VAc) were present, the lack of an acetic acid peak lead to uncertainty about the presence of vinyl acetate, so the sample was placed in the PVC category.

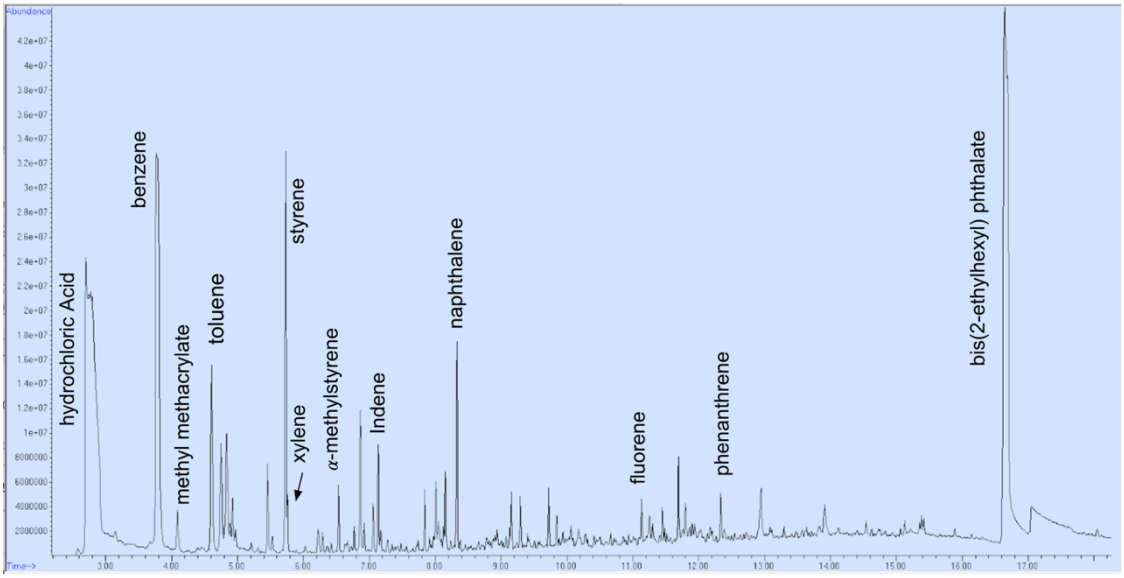

Figure 34: Labeled pyro-gram peaks of sample BR5, which was determined to be vinyl chloride-vinyl acetate copolymer, or P(VC-VAc).

---

b) Nantucket Sound

From the Nantucket Sound collection location, five samples were analyzed, numbered NS1 through NS5. As displayed in figure 35, the sample pool from this location consisted of the following polymer characterizations: 40% polypropylene, 40% PET, and 20% cellulose.

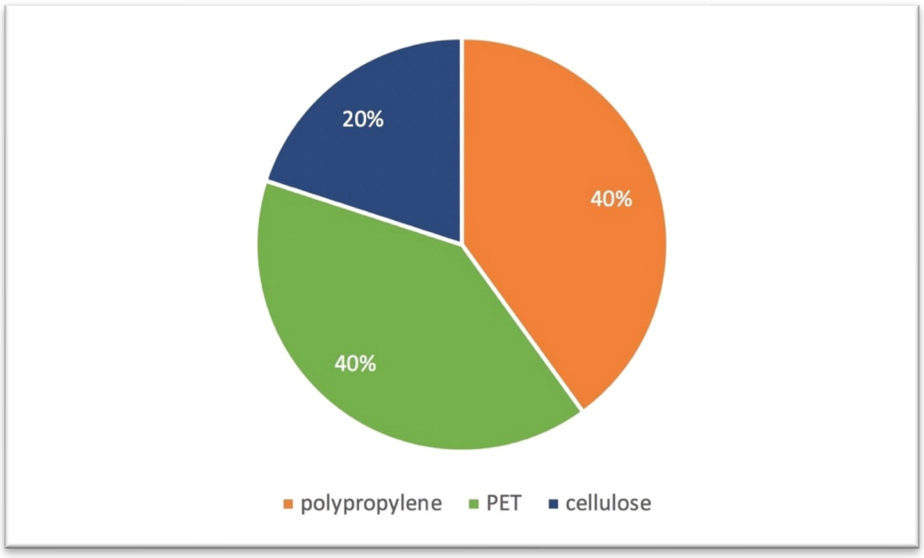

Figure 35: Polymer characterization of the Nantucket Sound samples.

Sample NS1 was a fragment of a clear plastic cup, which is shown in figure 36. It contained CO2 and acetic acid, which alluded to some sort of cellulose acetate (Tsuge et al., 2011). The sample's most prominent peak was acrolein, which is present in cellulose acetate-propionate (Tsuge et al., 2011). The spectra for this sample, shown in figure 37, contained many other markers for this polymer, including propanoic acid, hydroxy-2-butanone, and propionic anhydride, which further confirmed this characterization (Tsuge et al., 2011). Some of the peaks towards the end of the chromatogram, around 18.00 minutes, have similar mass spectra peaks to three plasticizers that are commonly expected to be found in cellulose acetate-propionate (Tsuge et al., 2011). Although the spectra did not perfectly align, these three peaks are likely dibutyl phthalate, butyl palmitate, and butyl stearate. All the compounds labeled on the ion chromatogram in figure 37 below are expected to be found in cellulose acetate-propionate (Tsuge et al., 2011). This sample was placed in the cellulose category. Many additives were found in this sample. There were no bisphenol A or 2,4-

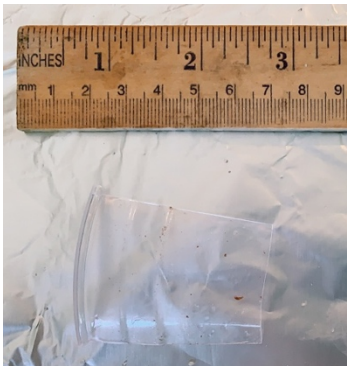

Figure 36: An image of sample NS1.

ditert-butylphenol detected. The most obvious additives were the phthalates, like the dibutyl phthalate plasticizer at the end of the spectra. There did appear to be methyl methacrylate at about 4.00 minutes, as this peak had mass spectral peaks relevant to methyl methacrylate, including a prominent peak at 100 m/z. A peak at about 6.00 minutes also appeared to be styrene, due to the prominent mass spectra peak at 104 m/z. There were also some furans present in the spectra. This complex mixture of additives and plasticizers was unexpected in a plastic cup, which are typically comprised of a basic polymer like polypropylene, as seen in sample NS5. The mixture of plasticizers in a drinking cup is concerning, as many of these additives have potential health threats.

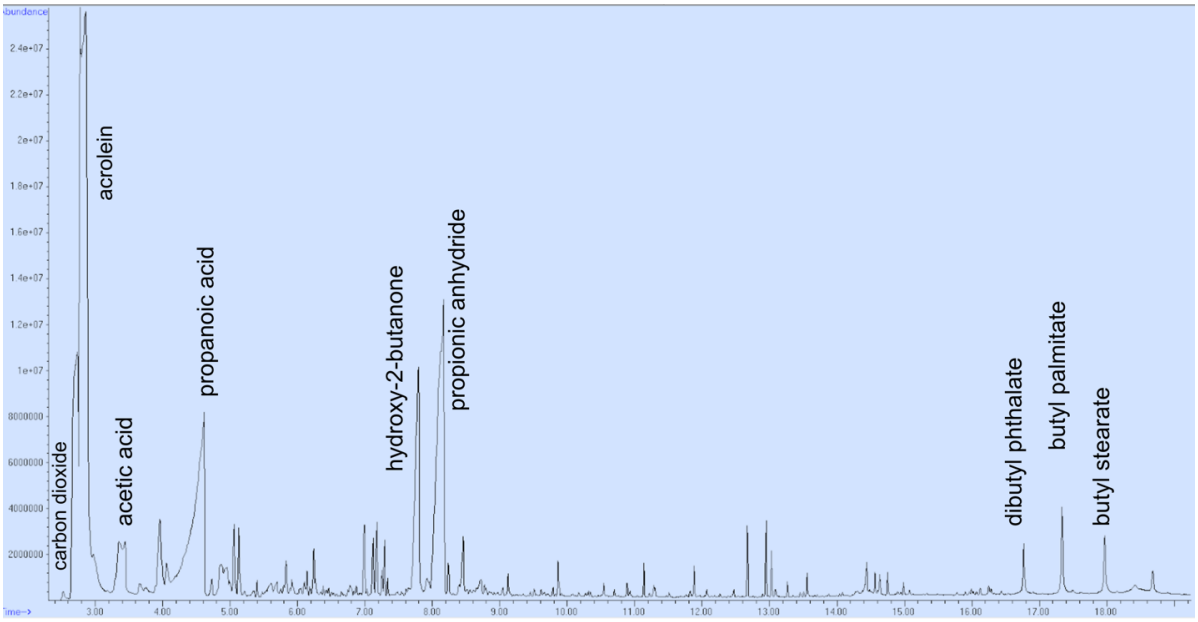

Figure 37: Labeled pyro-gram peaks of sample NS1, which was characterized as cellulose acetate-propionate.

Sample NS2, shown in figure 38, was a blue piece of what appeared to be from a plastic food wrapper. It was determined to be a copolymer of polypropylene and poly(ethylene terephthalate), or PET. Its largest and most prominent peak was 2,4-dimethyl-1-heptene, which

Figure 38: An image of sample NS2.

indicated polypropylene (Tsuge et al., 2011). This possibility was further confirmed due to the presence of pentane, 2-methyl-1-heptene, 2,4,6-trimethyl-1-nonene and 2,4,6,8-tetramethyl-1-undecene peaks in the chromatogram shown in figure 39, which are all expected in a standard polypropylene sample (Tsuge et al., 2011). However, the sample could not solely be classified as polypropylene due to the presence of many PET markers (Tsuge et al., 2011), including acetaldehyde, benzene, vinyl benzoate, benzoic acid, biphenyl, and divinyl terephthalate. Although it can be difficult to see in the figure, vinyl benzoate was located at about 7.80 minutes, benzoic acid appeared shortly after at about 8.00 minutes, biphenyl appeared at about 9.70 minutes, and divinyl terephthalate appeared at about 10.81 minutes. Other PET marker compounds were identified in the chromatogram (Tsuge et al., 2011), including 4-(vinyloxycarbonyl) benzoic acid (11.10 minutes), ethan-1,2-diyl divinyl diterephthalate (~14.00 minutes), and ethan-1,2-diyldibenzoate (~14.00 minutes). Although the PET marker peaks were smaller than the polypropylene peaks, this sample was categorized as a PET polymer. Since these PET polymers were less common in the samples from this study, the presence of PET in this sample needed to be reflected in the resulting statistics. The two peaks just after 2,4-dimethyl-1-heptene were interesting, as they did not fit directly into the expected spectra for polypropylene or PET. At 5.43 minutes was either xylene or ethyl benzene, and at about 5.70 minutes was styrene. Although these cyclic compounds are not highlighted as standard of PET polymers (Tsuge et al., 2011), they make sense in the fragmentation of PET and are likely not separate additives. With regards to additives, phthalates were clearly present. Methyl methacrylate, bisphenol A, and 2,4-ditert-butylphenol were not located. This polymer was

ultimately classified as a polypropylene and poly(ethylene terephthalate) copolymer. The sample was a very flimsy wrapper, which is expected of PET, since PET is commonly used to create sheets and films (Hatami et al., 2021).

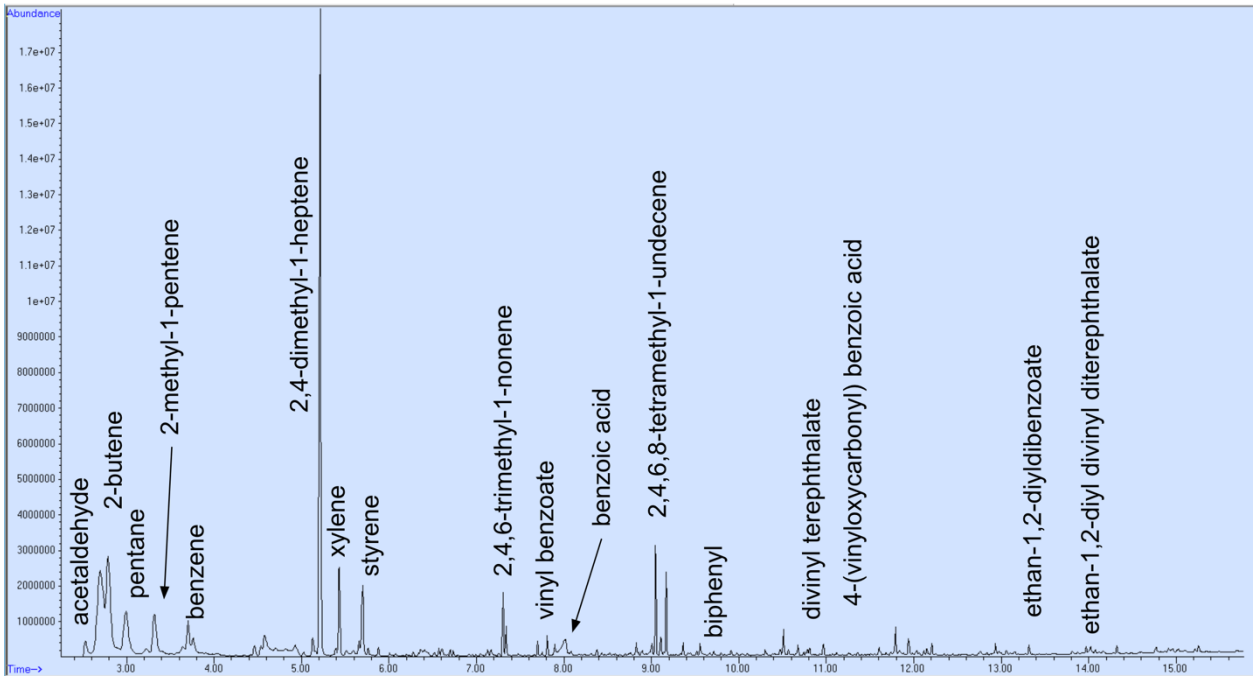

Figure 39: Labeled pyro-gram peaks of sample NS2, which was characterized as a polypropylene and PET copolymer.

Sample NS3, which was a piece of plastic clothing size label that is shown in figure 40, was characterized as poly(ethylene terephthalate), or PET. This characterization makes sense since it is a flimsy and bendable plastic, which is expected for commonly produced PET films (Hatami et al., 2021). The sample was characterized based on many relevant marker compounds expected in a PET sample, which were identified in the ion chromatogram shown in figure 41 (Tsuge et al., 2011), including benzene (3.78 minutes), vinyl benzoate (7.83 minutes), benzoic acid (8.43 minutes), divinyl terephthalate (10.85 minutes), 4-(vinyloxycarbonyl) benzoic acid (11.58

Figure 40: An image of sample NS3.

minutes), and 2-(benzoyloxy)ethyl vinyl terephthalate (16.06 minutes). Many phthalates are expected in a standard sample of PET, such as divinyl terephthalate, 2-(benzoyloxy)ethyl vinyl terephthalate, ethan-1,2-diyl divinyl diterephthalate, bis(2-(benzoyloxy)ethyl) terephthalate, and 2-(4-((2 (benzoyloxy)ethoxy)carbonyl)benzoyloxy) ethyl vinyl terephthalate (Tsuge et al., 2011). Consequently, although phthalates were present in the sample, they cannot necessarily be considered additives. There were no 2,4-ditert-butylphenol or bisphenol A additives detected in the sample, but the methyl methacrylate additive was present at 4.07 minutes on the ion chromatogram. Styrene was detected in the sample at about 5.73 minutes, but this cyclic compound makes sense as part of the PET fragmentation (Tsuge et al., 2011) and is not necessarily an additive. Additionally, the amount of styrene present could arguably be negligible, as the peak could only be detected when specially searching for styrene molecular mass in the chromatogram. This sample was ultimately determined to be poly(ethylene terephthalate) with a methyl methacrylate additive, and was placed in the PET category.

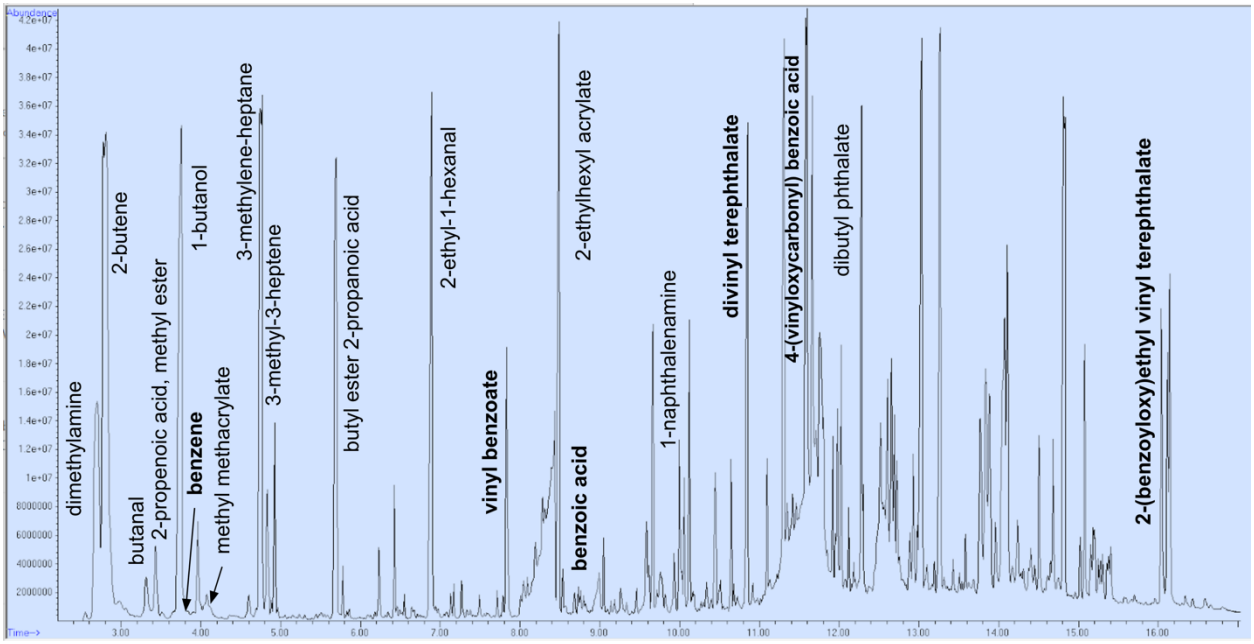

Figure 41: Labeled pyro-gram peaks of sample NS3, which was determined to be PET.

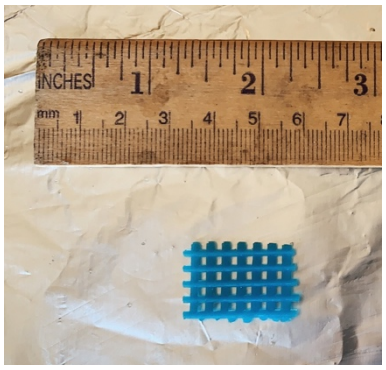

Figure 42: An image of sample NS4.

Sample NS4, which is shown in figure 42, was a hard blue plastic fragment that likely came from a beach toy. This sample was characterized as polypropylene with a 2,4-ditert-butylphenol additive. It was identified based on the presence of expected polypropylene marker compounds in the ion chromatogram shown in figure 43 (Tsuge et al., 2011), such as 2,4-dimethyl-1-heptene, 2,4,6-trimethyl-1-nonene, and 2,4,6,8-tetramethyl-1-undecene. Beyond the 2,4-ditert-butylphenol additive at 10.45 minutes, no other additives were detected. It is common and expected to see polypropylene samples with a 2,4-ditert-butylphenol additive (Oliveira et al., 2020). This sample was ultimately placed in the polypropylene category.

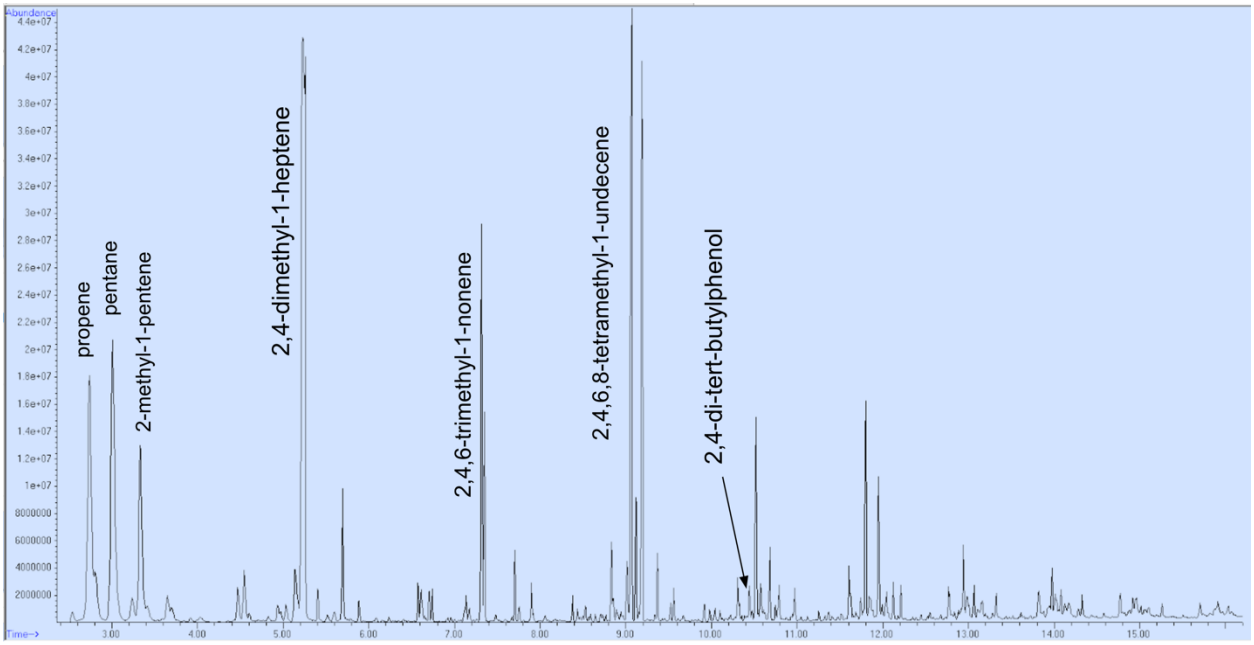

Figure 43: Labeled pyro-gram peaks of sample NS4, which was determined to be polypropylene.

Sample NS5, which is shown in figure 44, was another clear fragment of a plastic cup. This fragment had many marker compounds relevant to polypropylene (Tsuge et al., 2011), such as 2,4-dimethyl-1-heptene, 2,4,6-trimethyl-1-nonene, and 2,4,6,8-tetramethyl-1-undecene, which are shown in the chromatogram in figure 45. Plastic cups are often comprised of polypropylene, so this identification was expected (Andrady, 2011). The sample contained the 2,4-ditert-butylphenol additive at 10.45 minutes, which was not unusual in a polypropylene sample. No bisphenol A, methyl methacrylate, phthalate, or styrene additives were detected. Following a straightforward analysis, the sample was determined to be polypropylene with a 2,4-ditert-butylphenol additive and was placed in the polypropylene category.

Figure 44: An image of sample NS5.

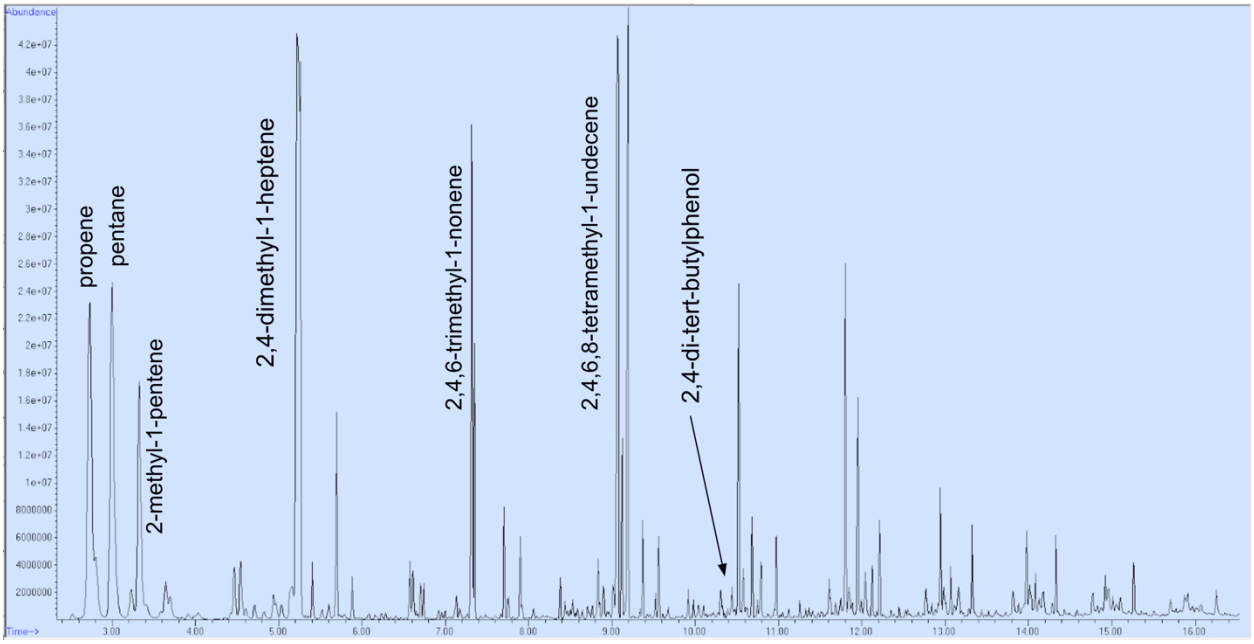

Figure 45: Labeled pyro-gram peaks of sample NS5, which was determined to be polypropylene.

c) Outer Cape

From the Outer Cape collection location, six samples were analyzed, numbered OC1 through OC6. As shown by the chart in figure 46, the sample pool from this location consisted of the following polymer characterizations: 33.33% polyethylene, 16.67% polypropylene, 16.67% resin, 16.67% PET, and 16.67% cellulose.

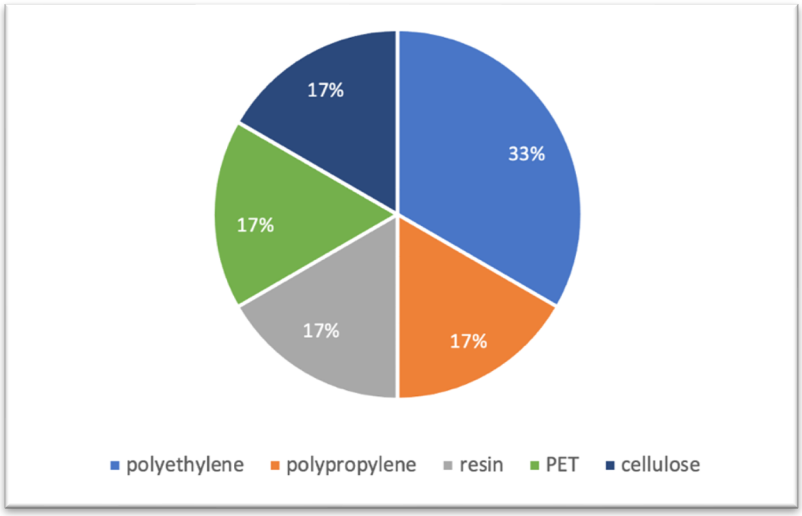

Figure 46: Polymer characterization of the Outer Cape samples.

The first sample from the Outer Cape was a fragment of a Poland Spring water bottle label, which is shown in figure 47. This fragment, sample OC1, was characterized as polypropylene due to the recognition of its' expected 2,4-dimethyl-1-heptene marker peak, at 5.30 minutes (Tsuge et al., 2011). Other standard polypropylene peaks were present in the ion chromatogram shown in figure 48, including propene, pentane, 2-methyl-1-pentene, 2,4,6-trimethyl-1-nonene, and 2,4,6,8-tetremethyl-1-undecene (Tsuge et al., 2011). These peaks confirmed the initial polypropylene identification. No bisphenol A, methyl methacrylate, phthalate, or styrene additives were detected. The 2,4-ditert-butylphenol additive was present at 10.45 minutes, which is common in polypropylene samples

Figure 47: An image of sample OC1.

(Oliveira et al., 2020). The abundance of unlabeled peaks is the result of extra noise during the analysis (Fialkov et al., 2007; Wenig, 2011). These peaks were various hydrocarbon chains that did not indicate any copolymer or unmentioned additives. The sample was determined to be polypropylene with a 2,4-ditert-butylphenol additive and was placed in the polypropylene category.

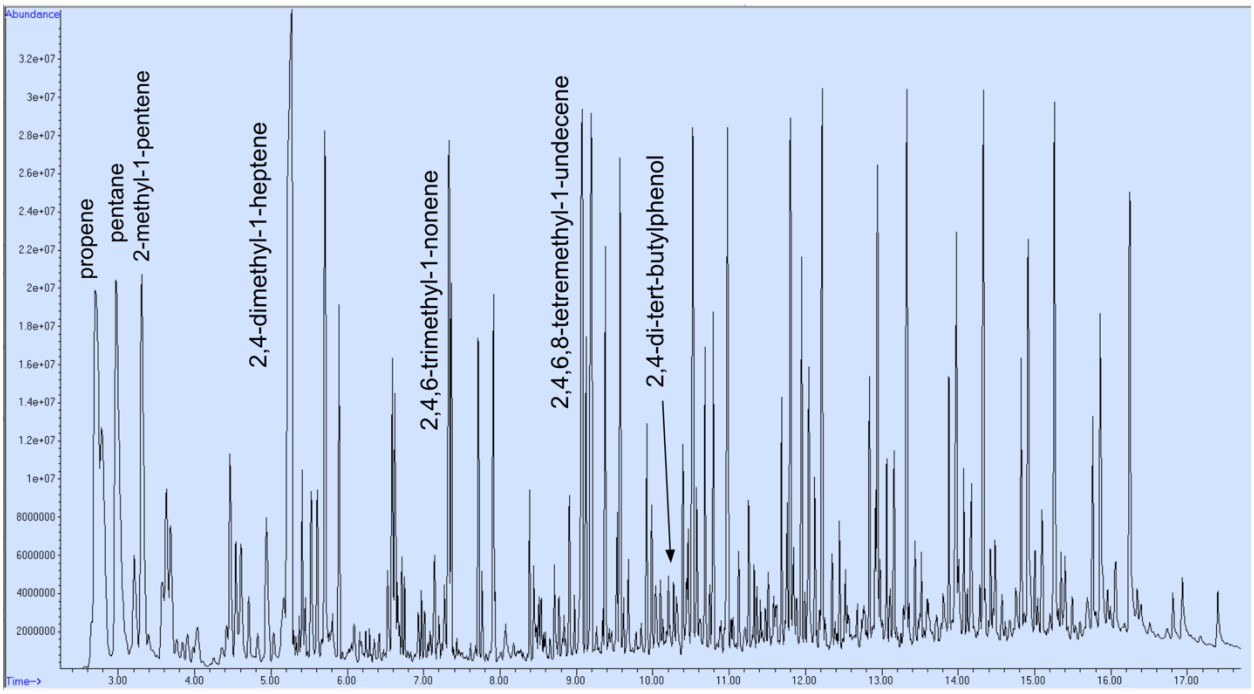

Figure 48: Labeled pyro-gram peaks of sample OC1, which was determined to be polypropylene.

Figure 49: An image of sample OC2.

Sample OC2 was a flimsy piece of clear plastic wrap that is pictured in figure 49. It was determined to be polyethylene due to its peak pattern of triplet hydrocarbon clusters of increasing carbon chain length, which is displayed by the chromatogram in figure 50. As expected, each triplet contained a single bonded, double bonded, and saturated hydrocarbon with its specified number of carbons (Tsuge et al.,

2011). There were no bisphenol A, methyl methacrylate, phthalate, or styrene additives detected. The 2,4-ditert-butylphenol additive was detected at 10.45 minutes. This sample was ultimately categorized as polyethylene with a 2,4-ditert-butylphenol additive and was placed in the polyethylene category.

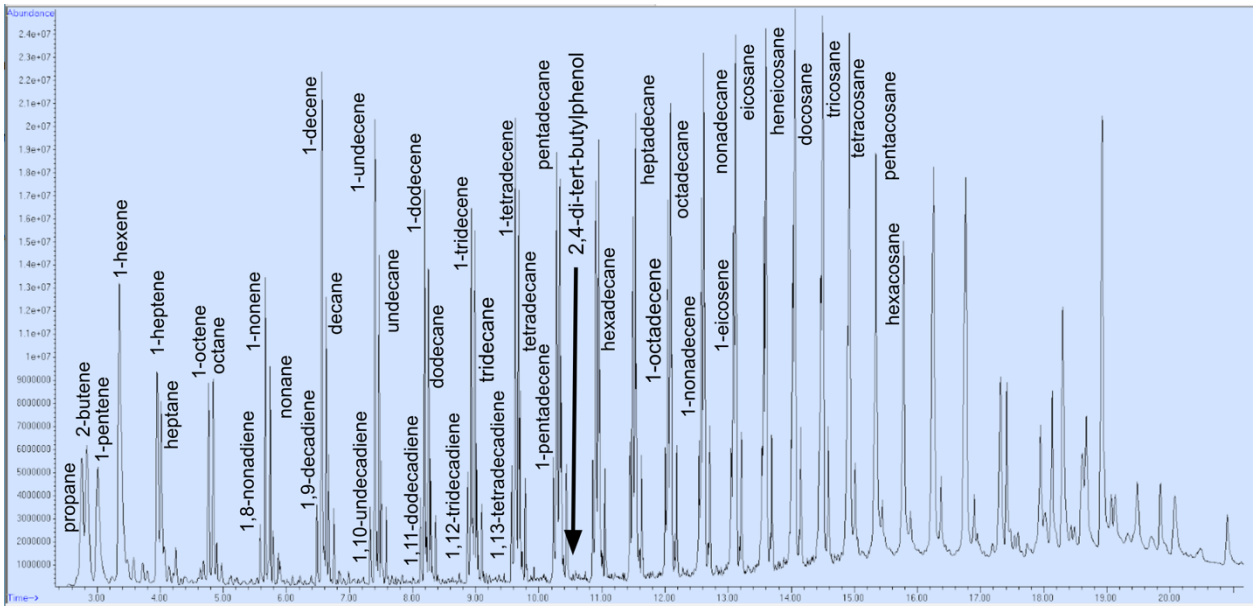

Figure 50: Labeled pyro-gram peaks of sample OC2, which was determined to be polyethylene.

Sample OC3, which is shown in figure 51, was a cigarette butt. This sample was determined to be cellulose acetate based on the presence of the expected marker compound, acetic acid, at 3.84 minutes (Tsuge et al., 2011). This result was expected, since it is known that a significant component of cigarette butts is cellulose acetate (Andrady, 2011; Araújo, Maria Christina Barbosa de and Costa, 2021; Belzagui et al., 2021; Shen et al., 2021). Additionally, other relevant marker compounds for cellulose acetate were present in its' ion chromatogram that is shown in figure 52 (Tsuge et al., 2011), including carbon dioxide (2.69 minutes), acetic anhydride (4.21 minutes), 2-hydroxyethyl acetate (4.64 minutes), and 4,6-

Figure 51: An image of sample OC3.

dimethyl-2*H*-pyran-2-one (9.08 minutes). The tall peaks at the end of the spectra are long carbon chains that do not indicate any copolymer or additive. There were no 2,4-ditert-butylphenol, bisphenol A, methyl methacrylate, phthalate, or styrene additives detected. The sample was characterized as cellulose acetate and placed in the cellulose category.

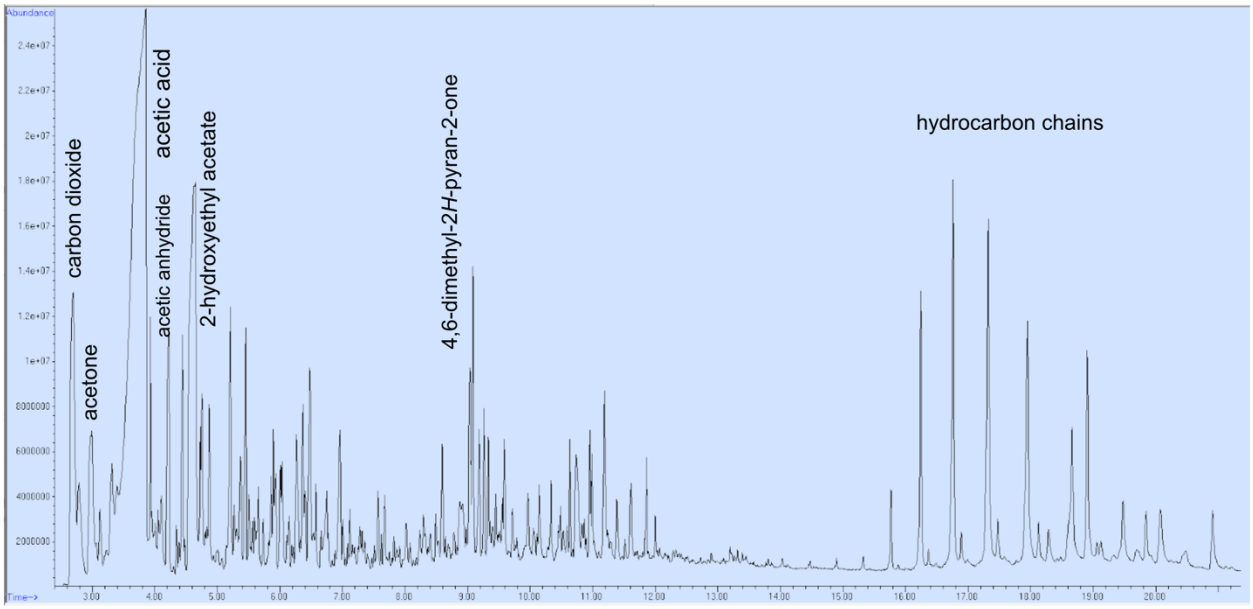

Figure 52: Labeled pyro-gram peaks of sample OC3, which was determined to be cellulose acetate.

Figure 53: An image of sample OC4.

Sample OC4, pictured in figure 53, was determined to be Poly(ethylene terephthalate), or PET. This flimsy clear plastic consisted of many marker compounds expected of PET (Tsuge et al., 2011), including acetaldehyde (2.72 minutes), benzene (3.79 minutes), vinyl benzoate (7.84 minutes), divinyl terephthalate (10.85 minutes), 4-(vinyloxycarbonyl) benzoic acid (11.25 minutes), ethan-1,2-diyldibenzoate (14.04 minutes), 2-(benzoyloxy)ethyl vinyl terephthalate (16.02 minutes), and ethan-1,2-diyl divinyl diterephthalate (18.85 minutes). These markers are shown in the ion

chromatogram in figure 54. Many additives were detected in the spectra. Methyl methacrylate was identified at 4.09 minutes. A styrene additive was present at 5.73 minutes and a 2,4-ditert-butylphenol additive was present at 10.45 minutes. There was no bisphenol A detected. Since the expected spectra contained phthalates (Tsuge et al., 2011), these compounds were not categorized as additives. This sample was ultimately characterized as PET with various additives, and it was placed in the PET category. This identification was expected since flimsy plastic films are typically comprised of PET (Hatami et al., 2021).

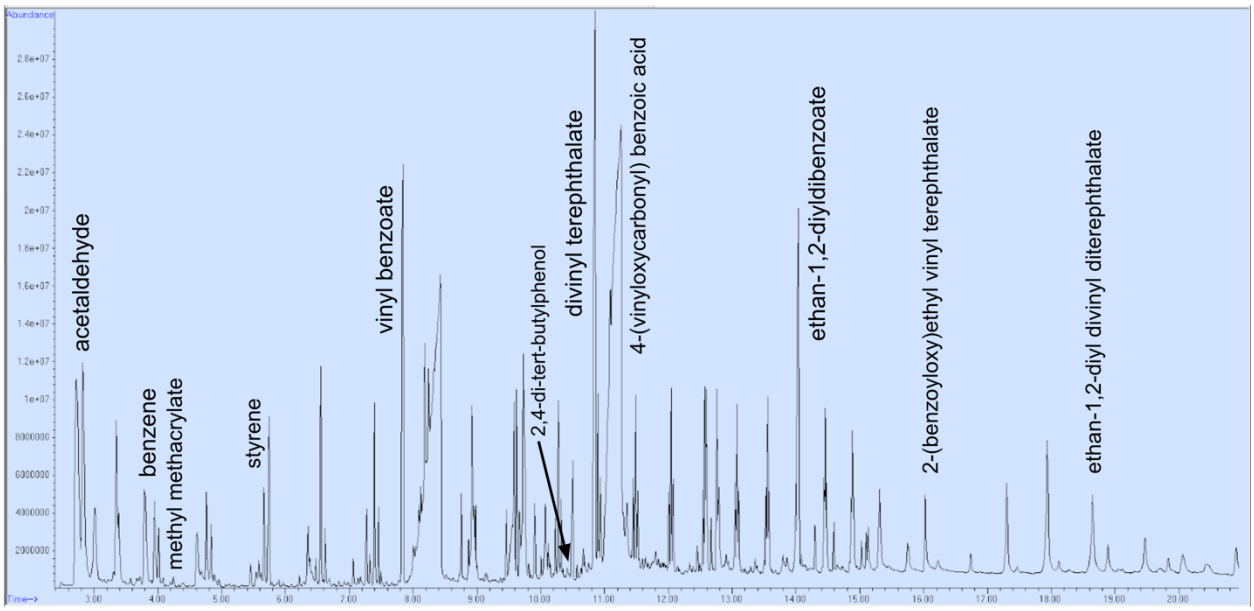

Figure 54: Labeled pyro-gram peaks of sample OC4, which was determined to be Poly(ethylene terephthalate), or PET.

Sample OC5 was a pliable blue fragment that is shown in figure 55. This sample was characterized as polyethylene due to the pattern of triplet hydrocarbon clusters with increasing carbon chain length (Tsuge et al., 2011). These clusters are shown in the ion chromatogram in figure 56. As per a typical polyethylene polymer, each triplet contained a single bonded, double bonded, and saturated hydrocarbon with its

Figure 55: An image of sample OC5.

specified number of carbons (Tsuge et al., 2011). The sample contained a 2-(benzoyloxy)ethyl vinyl terephthalate additive. There were no 2,4-ditert-butylphenol, bisphenol A, methyl methacrylate, or styrene additives detected. This sample was ultimately categorized as polyethylene with additives and was placed in the polyethylene category.

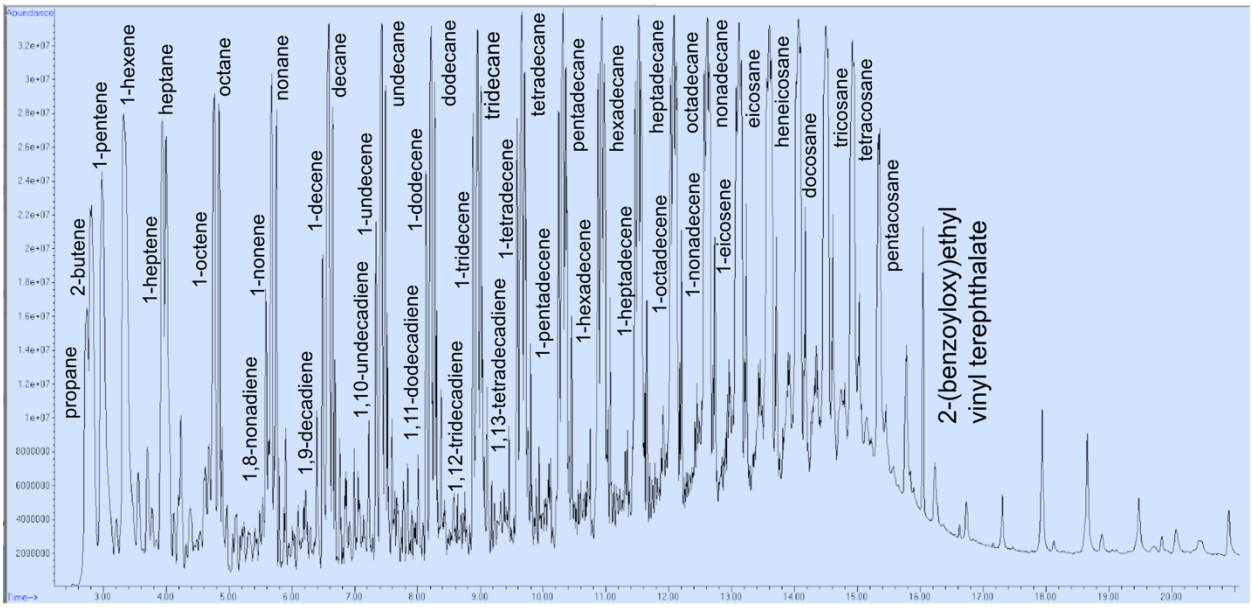

Figure 56: Labeled pyro-gram peaks of sample OC5, which was determined to be polyethylene.

Figure 57: An image of sample OC6.

Sample OC6, which was a white and rubbery blob that is shown in figure 57, provided interpretational challenges. It was ultimately determined to be a plastic containing non-typical polymer, such as chewing gum (Farber et al., 2010; Palabiyik et al., 2020). Some compounds expected in a polystyrene standard were present (Tsuge et al., 2011), including toluene (4.56 minutes) and styrene (5.71 minutes). However, there was no styrene dimer or trimer present, so these compounds were likely additive components of a different polymer

base. For example, chlorosulfonated polyethylene, or CSM, was another possibility. Some expected compounds from the standard were present in the ion chromatogram in figure 58 (Tsuge et al., 2011), including previously mentioned and styrene, in addition to phenol (6.40 minutes). However, this polymer does not account for the cresol that was present at 7.23 minutes. Some polymers with both phenol and cresol expected include phenol formaldehyde resin and cresol formaldehyde resin (Tsuge et al., 2011). The brominated epoxy resin, however, typically contains toluene and phenol (Tsuge et al., 2011). Since there are various components of the listed examples, this sample likely contained a mixture of these polymers as additives in a chewing gum product. Chewing gum is manufactured using an insoluble gum base that typically consists of synthetic polymer elastomers, which give the gum its desired physical properties (Farber et al., 2010). The various components that make up gum are complicated, including various amounts of sugars, aromatic compounds, colors, additives, emulsifiers, plasticizers, and resins (Farber et al., 2010; Palabiyik et al., 2020). Based on this information, it makes sense that indicators of various resins were present in this sample. For statistical purposes, this sample was

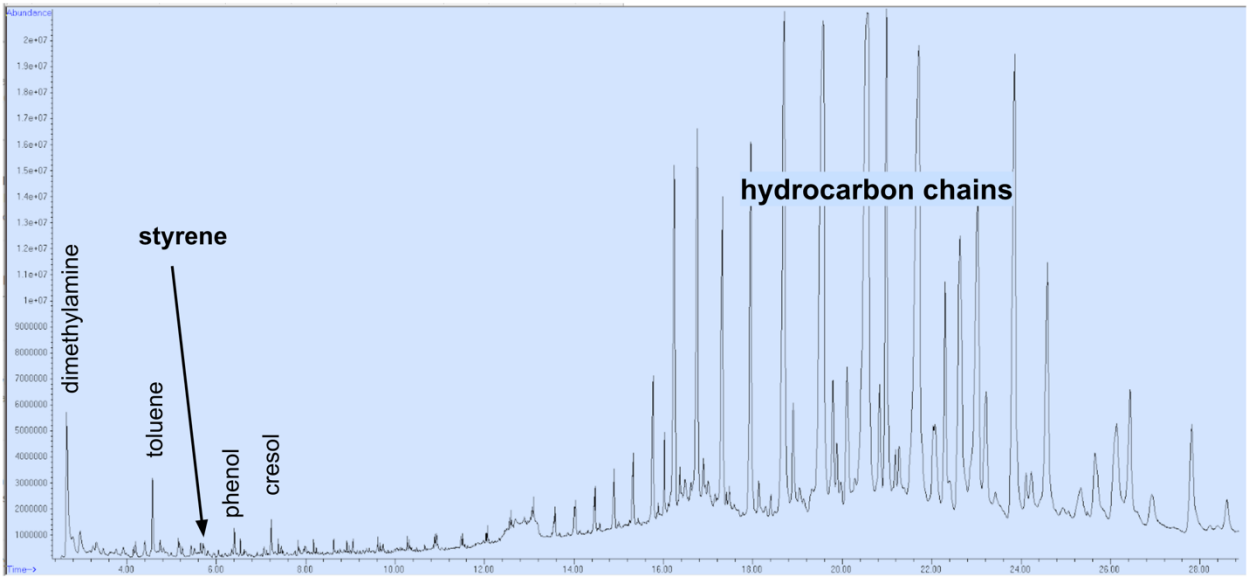

Figure 58: Labeled pyro-gram peaks of sample OC6, which was determined to be an atypical mixed polymer.

considered resin, since this characterization most accurately represented its mixture of additives. Phthalate and styrene additives were present. No bisphenol A, methyl methacrylate, or 2,4-ditert-butylphenol were present.

---

d) Cape Cod Bay

From the Bay Side collection location, nineteen samples were analyzed, numbered CCB1 through CCB19. The sample pool from this location consisted of the following polymer characterizations: 31.58% polypropylene, 21.05% polyethylene, 21.05% resins, 10.53% PET, 5.26% PVC, 5.26% cellulose, and 5.26% polyamide. These proportions are shown in figure 59.

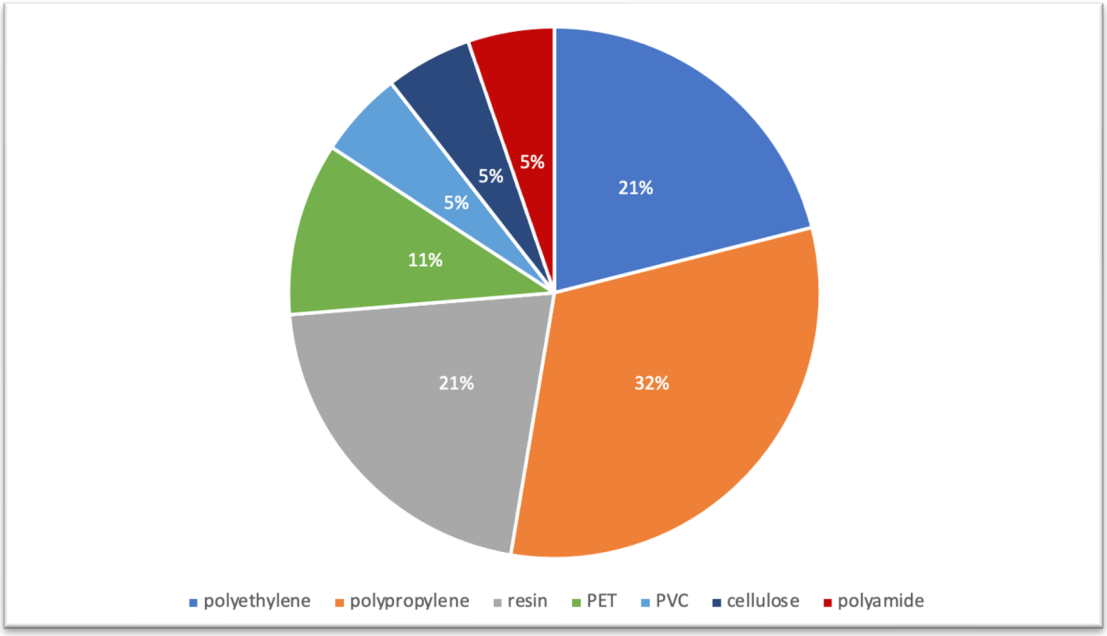

Figure 59: Polymer characterization of the Cape Cod Bay samples.

Sample CCB1 was a paper-thin neon green fragment that is shown in figure 60. It was hard and crumbly and resembled a paint chip. The ion chromatogram shown in figure 61 consisted of phenol, cresol, p-isopropyl phenol, p-isopropenyl phenol, BPA, which led to the

characterization of an epoxy resin (Tsuge et al., 2011). Additionally, the presence of benzene, diphenyl, and methyl methacrylate indicated some potential Poly(n-butyl methacrylate), or PBMA (Tsuge et al., 2011). Styrene (104 m/z) was detected at 5.72 minutes. These compounds could also indicate polystyrene, but this characterization does not account for the methyl methacrylate. Additionally, the lack of styrene dimer or trimer compounds reduced the likelihood of this possibility. This sample was likely a mixture containing the PBMA and epoxy resin polymers and was ultimately placed in the resin category. Since BPA was expected in the prominent epoxy resin polymer (Tsuge et al., 2011), this compound was not considered an additive. If polystyrene was not a polymer present in the mixture, then the styrene compound was likely an additive. There were no 2,4-ditert-butylphenol or phthalate additives present.

Figure 60: An image of sample CCB1.

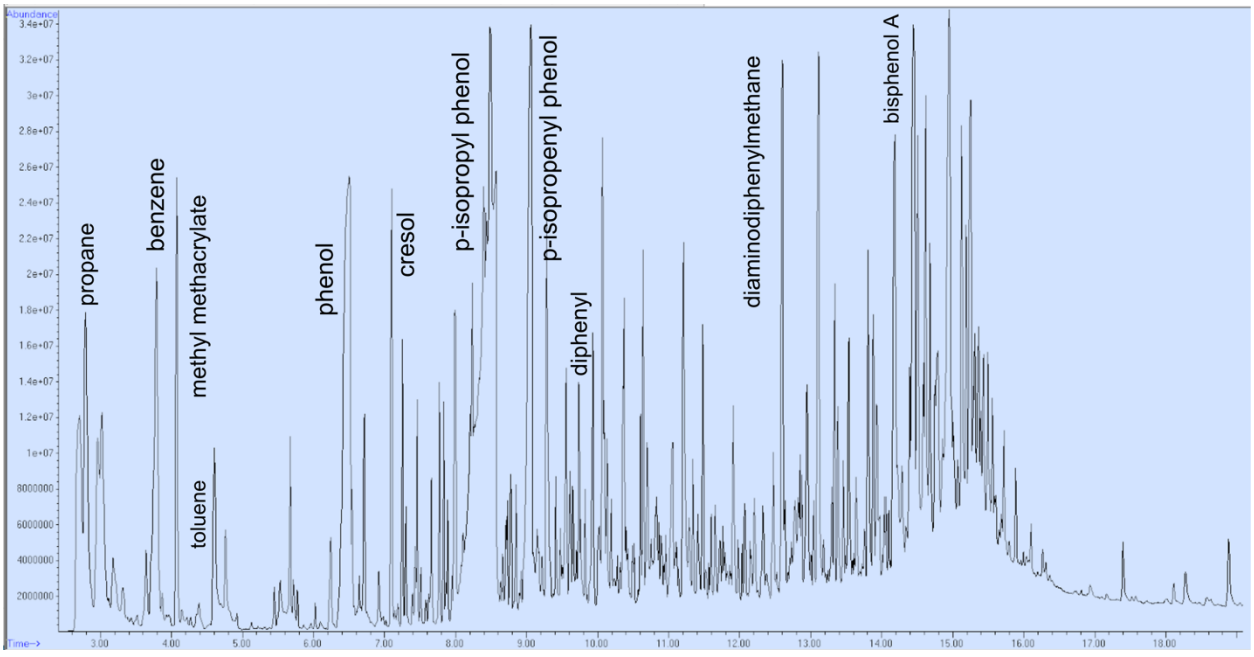

Figure 61: Labeled pyro-gram peaks of sample CCB1, which was determined to be an epoxy resin.

Sample CCB2, which was part of a plastic food wrapper, is shown in figure 62. This sample was determined to be polypropylene based on the presence of 2,4-dimethyl-1-heptene at 5.23 minutes in the ion chromatogram, which is shown in figure 63. Many other expected polypropylene markers were present (Tsuge et al., 2011), including propene (2.74 minutes), pentane (3.01 minutes), 2-methyl-1-pentene (3.33 minutes), 2,4,6-trimethyl-1-nonene (7.33 minutes), and 2,4,6,8-tetramethyl-1-undecene (9.07 minutes). It was expected for food wrappers to be composed of polypropylene (Andrady, 2011). There were no 2,4-ditert-butylphenol, bisphenol A, methyl methacrylate, phthalate, or styrene additives detected. The sample was ultimately placed in the polypropylene category.

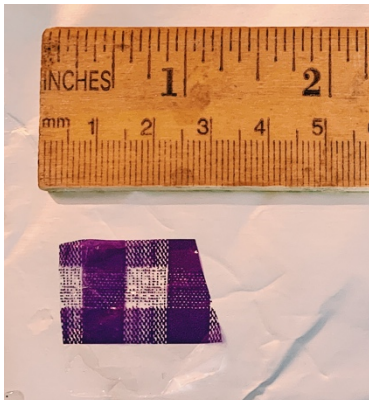

Figure 62: An image of sample CCB2.

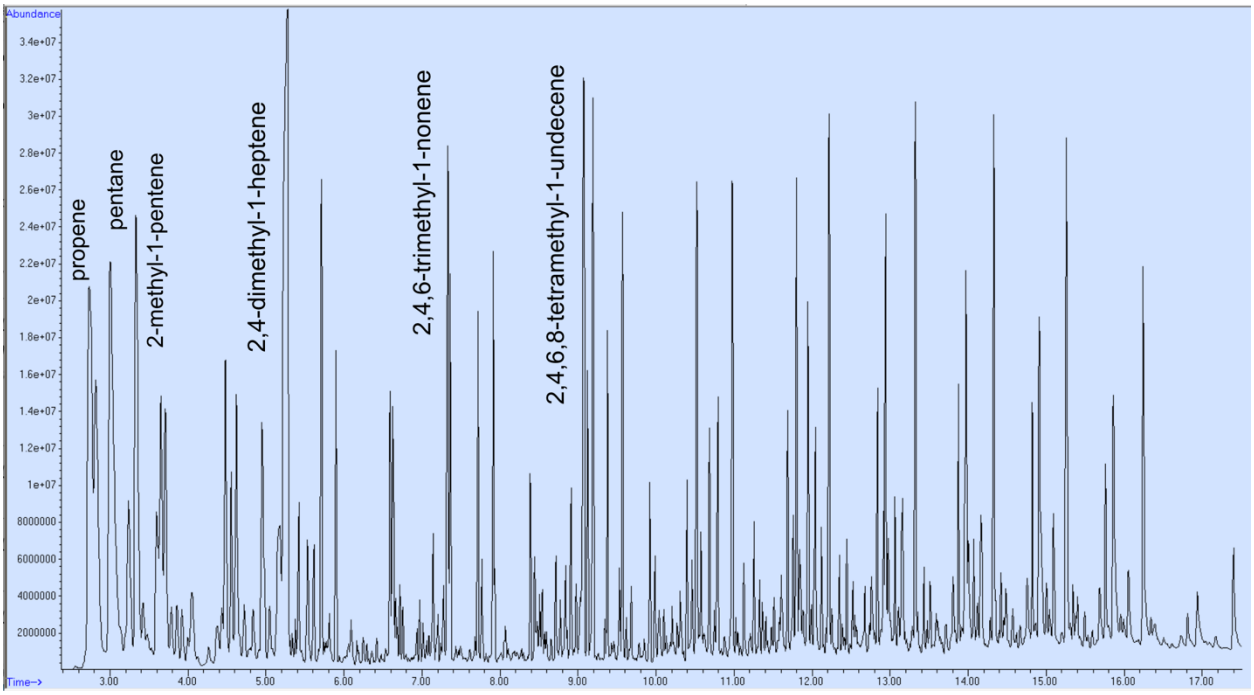

Figure 63: Labeled pyro-gram peaks of sample CCB2, which was determined to be polypropylene.

Figure 64: An image of sample CCB3.

Sample CCB3, which is shown in figure 64, was more of the thin neon green fragment. As displayed by the chromatogram in figure 65, this sample contained many relevant marker compounds for an epoxy resin (Tsuge et al., 2011), including phenol (6.43 minutes), cresol (7.07 minutes), p-isopropylphenol (8.47 minutes), p-isopropenylphenol (9.01 minutes) and bisphenol A (14.13 minutes). As described in the section on resins, it makes sense that fragments resembling paint chips would be pieces of resin coating. There were no 2,4-ditert-butylphenol, phthalate, or styrene additives detected. The methyl methacrylate additive was identified at 4.07 minutes. Since bisphenol A is part of the epoxy resin fragmentation, it is not considered an additive. The sample was ultimately characterized as an epoxy resin and was placed in the resin category. Since the additive composition in this sample differs from the epoxy resin described in sample CCB1, they may have originated from different sources.

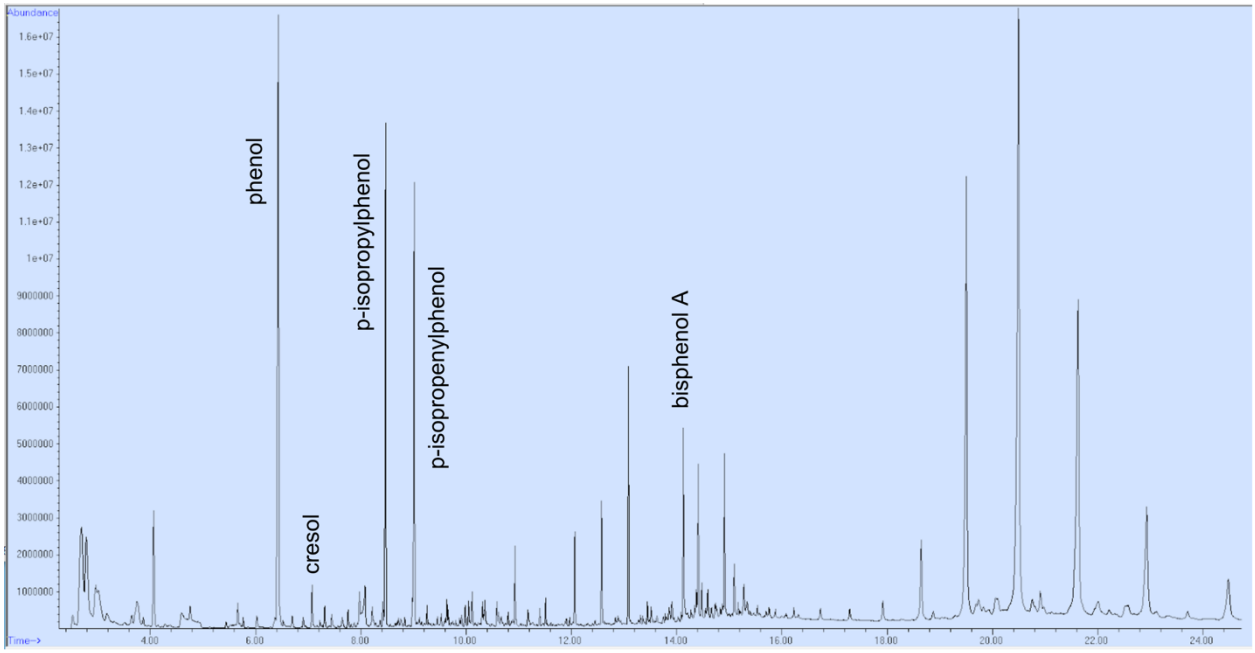

Figure 65: Labeled pyro-gram peaks of sample CCB3, which was determined to be an epoxy resin.

Sample CCB4 was a darker green thin fragment, shown in figure 66, that contained phthalic anhydride. It contained many compounds relevant to diallyl phthalate resin (DAP), including benzene (3.73 minutes), benzoic acid (7.99 minutes), and phthalic anhydride (9.32 minutes). This sample also had some relevant markers of cellulose acetate-propionate (CAP) in its ion chromatogram in figure 67, including carbon dioxide (2.63 minutes), acrolein (2.92 minutes), and acetic acid (3.30 minutes). There were no 2,4-ditert-butylphenol, phthalate, or styrene additives detected. Methyl methacrylate was present at 4.07 minutes and bisphenol A was present at 14.13 minutes. The sample was characterized as a mixed polymer likely containing diallyl phthalate resin, cellulose acetate-propionate, and a variety of additives. The sample was placed in the resin category.

Figure 66: An image of sample CCB4.

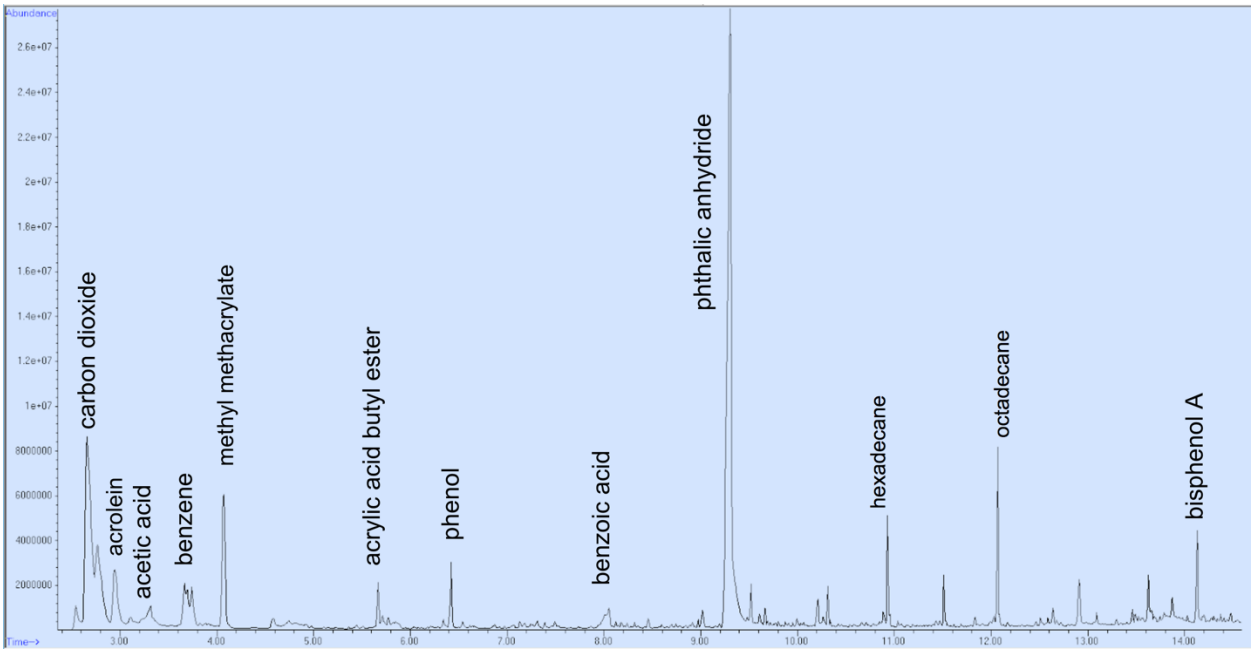

Figure 67: Labeled pyro-gram peaks of sample CCB4, which was determined to be a mixed resin polymer containing DAP and CAP.

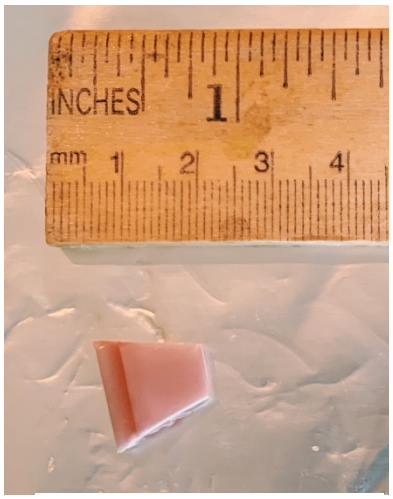

Figure 68: An image of sample CCB5.

Sample CCB5 was a fragment of a pink sandcastle beach toy which is shown in figure 68. The ion chromatogram, shown in figure 69, contained many relevant marker compounds for polypropylene (Tsuge et al., 2011), including propene (2.74 minutes), pentane (2.99 minutes), 2-methyl-1-pentene (3.35 minutes), 2,4-dimethyl-1-heptene (5.26 minutes), 2,4,6-trimethyl-1-nonene (7.35 minutes), and 2,4,6,8-tetramethyl-1-undecene (9.08 minutes). There were no 2,4-ditert-butylphenol, methyl methacrylate, phthalate, or styrene additives detected. The bisphenol A additive was detected at 14.16 minutes. The abundance of unlabeled peaks is the result of extra noise during the analysis (Fialkov et al., 2007; Wenig, 2011). These peaks were various hydrocarbon chains that did not indicate any copolymer or unmentioned additives. The sample was characterized as polypropylene with additives and placed in the polypropylene category.

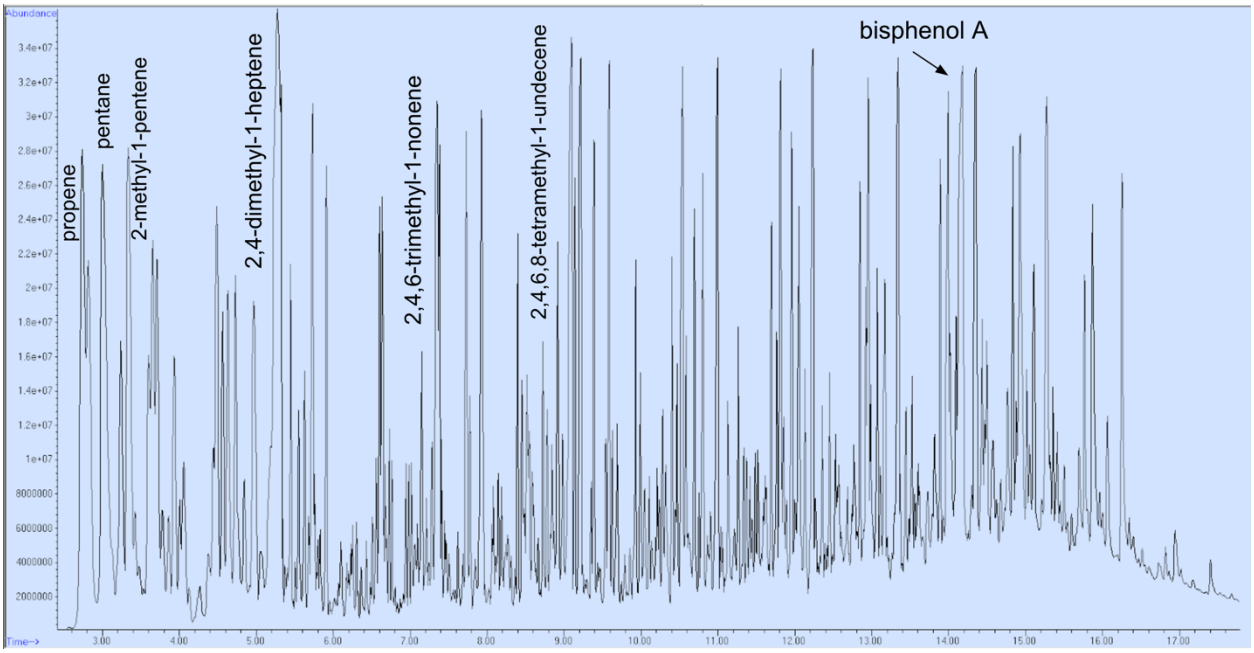

Figure 69: Labeled pyro-gram peaks of sample CCB5, which was determined to be polypropylene.

Sample CCB6 was a fragment of a clear plastic wrapper, as shown in figure 70. This sample contained many relevant indicators of the polypropylene polymer in its ion chromatogram (Tsuge et al., 2011), including propene (2.74 minutes), pentane (3.01 minutes), 2-methyl-1-pentene (3.33 minutes), 2,4-dimethyl-1-heptene (5.21 minutes), 2,4,6-trimethyl-1-nonene (7.32 minutes), and 2,4,6,8-tetramethyl-1-undecene (9.06 minutes). The peaks for these fragmentation products are shown in the chromatogram in figure 71. There were no methyl methacrylate or styrene additives detected. The bisphenol A additive was present at 14.13 minutes and the 2,4-ditert-butylphenol additive was present at 10.45 minutes. Terephthalate was also present. The sample was characterized as polypropylene with additives and placed in the polypropylene category.

Figure 70: An image of sample CCB6.

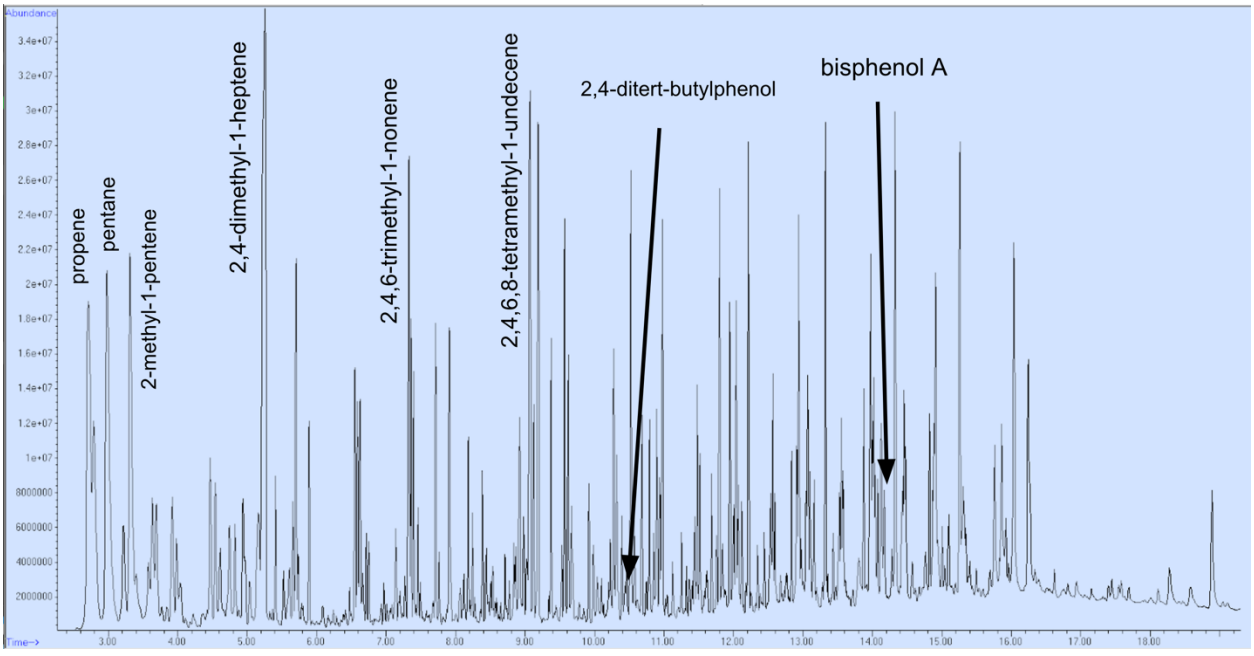

Figure 71: Labeled pyro-gram peaks of sample CCB6, which was determined to be polypropylene.

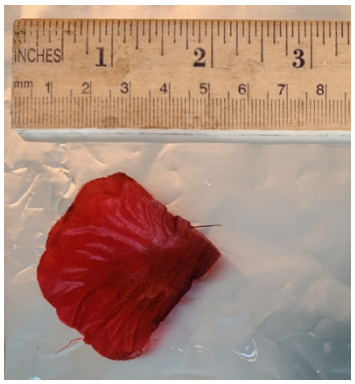

Figure 72: An image of sample CCB7.

Sample CCB7 was a portion of a synthetic red rose petal, just like the sample from the Dennis Bay. An image of this sample is shown in figure 72. This sample contained many relevant marker compounds for the PET polymer (Tsuge et al., 2011), including carbon dioxide (2.65 minutes), acetaldehyde (2.77 minutes), benzene (3.78 minutes), benzoic acid (8.39 minutes), diphenyl (9.73 minutes), divinyl terephthalate (10.83 minutes), 4-(vinyloxycarbonyl) benzoic acid (11.17 minutes), and ethan-1,2-diyldibenzoate (14.02 minutes). These markers are shown in the ion chromatogram in figure 73. The bisphenol A additive was present at 14.16 minutes and a styrene additive was present at 5.71 minutes. There were no 2,4-ditert-butylphenol or methyl methacrylate additives detected. Since phthalates were a component of the polymer, they were not considered an additive. The sample was characterized as PET with additives and was placed in the PET category.

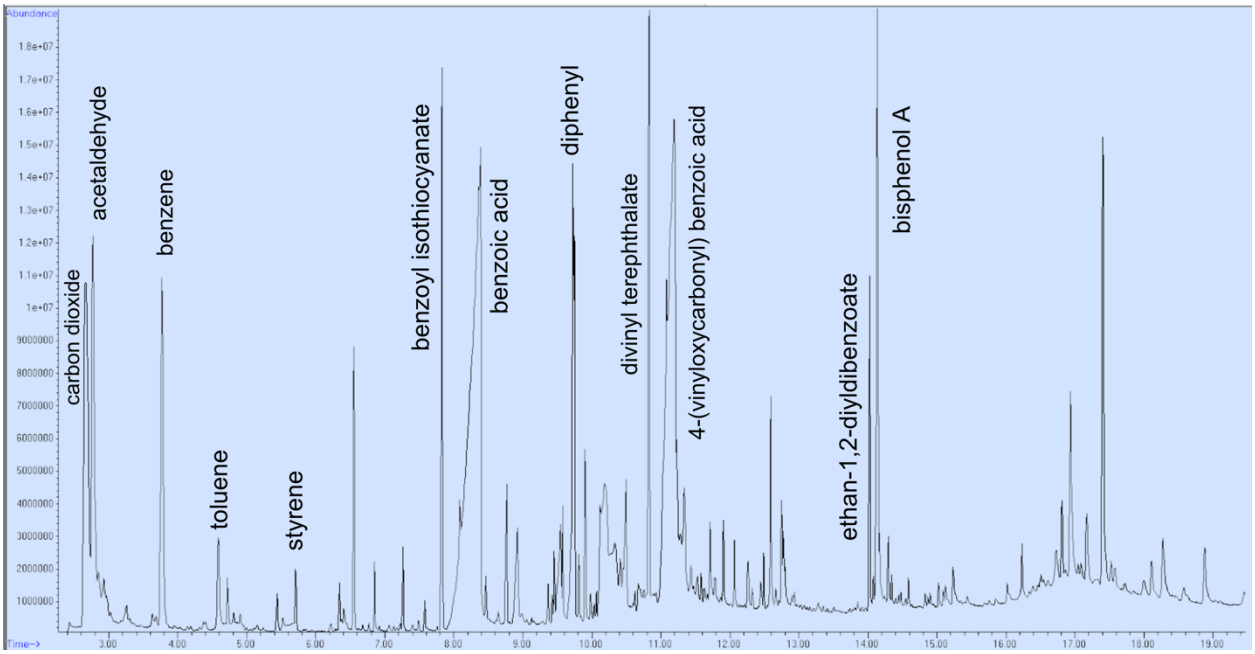

Figure 73: Labeled pyro-gram peaks of sample CCB7, which was determined to be PET.

Sample CCB8 came from a plastic clothing size label sticker. An image of this sample is shown in figure 74. It's ion chromatogram consisted of many marker compounds for the PET polymer (Tsuge et al., 2011), including carbon dioxide (2.68 minutes), benzene (3.78 minutes), benzoic acid (8.54 minutes), diphenyl (9.73 minutes), divinyl terephthalate (10.85 minutes), and 4-(vinyloxycarbonyl) benzoic acid (11.30 minutes). These marker peaks are shown in the ion chromatogram in figure 75. The methyl methacrylate additive was present at 4.07 minutes and the styrene additive was present at 5.73 minutes. The bisphenol A additive as present at 14.18 minutes. There were no 2,4-ditert-butylphenol or phthalate additives detected. This sample was characterized as PET with additives and placed in the PET category. This identification was expected since flimsy plastic films are typically comprised of PET (Hatami et al., 2021).

Figure 74: An image of sample CCB8.

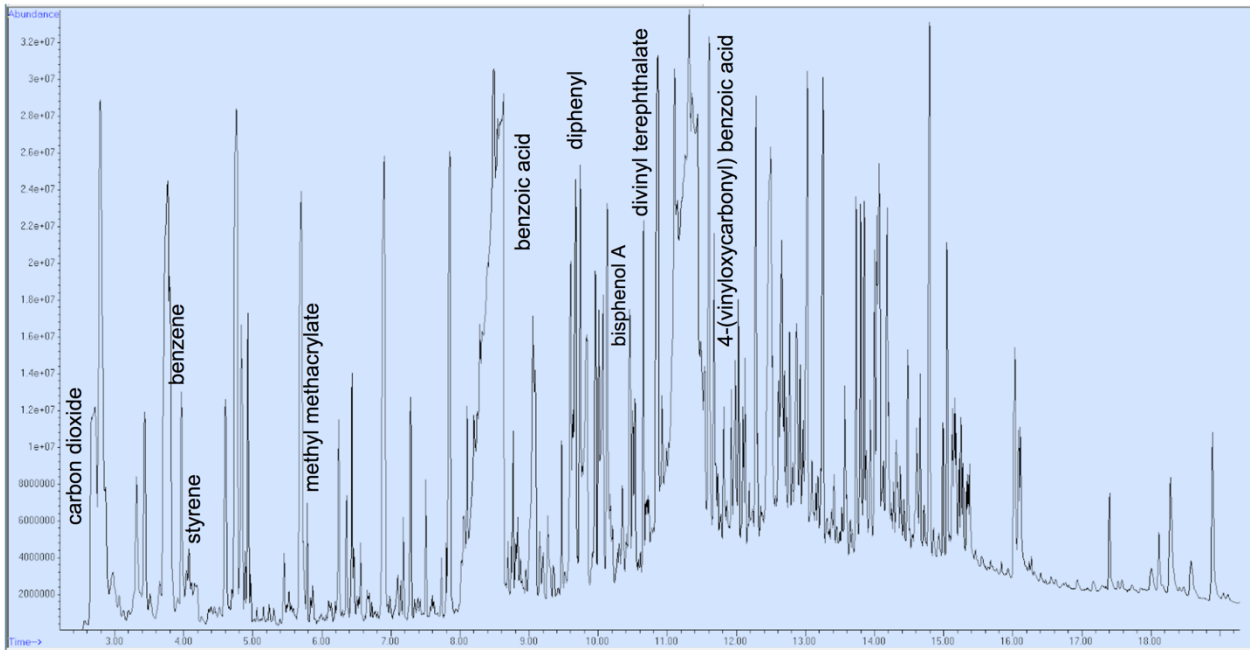

Figure 75: Labeled pyro-gram peaks of sample CCB8, which was determined to be PET.

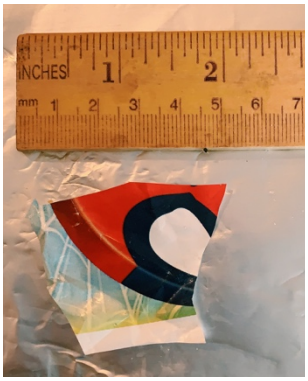

Figure 76: An image of sample CCB9.

Sample CCB9 was a portion of a plastic food wrapper that is shown in figure 76. It's ion chromatogram contained many relevant marker compounds for polypropylene (Tsuge et al., 2011), including propane (2.74 minutes), pentane (3.01 minutes), 2-methyl-1-pentene (3.33 minutes), 2,4-dimethyl-1-heptene (5.26 minutes), 2,4,6-trimethyl-1-nonene (7.35 minutes), and 2,4,6,8-tetramethyl-1-undecene (9.12 minutes). These marker compounds are labeled in the ion chromatogram in figure 77. The 2,4-ditert-butylphenol additive was detected at 10.45 minutes. As previously mentioned, it is common for this additive to be used in polypropylene manufacturing. There were no bisphenol A, methyl methacrylate, phthalate, or styrene additives detected. Following a straightforward analysis, the sample was characterized and categorized as polypropylene.

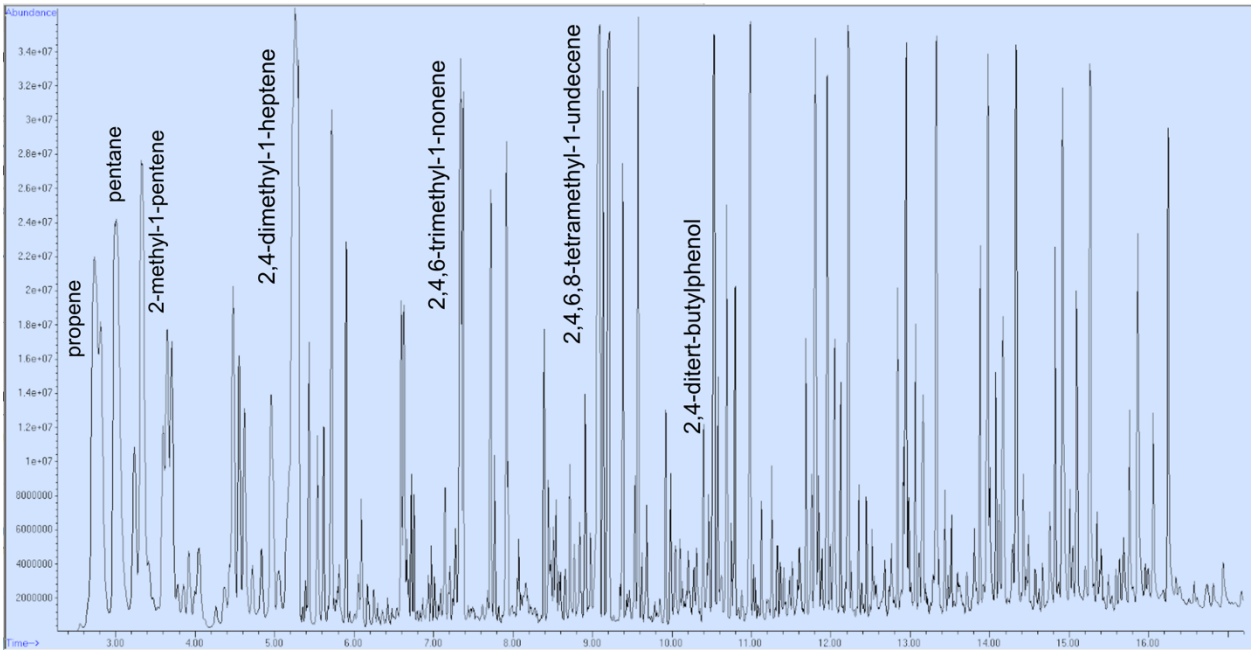

Figure 77: Labeled pyro-gram peaks of sample CCB9, which was determined to be polypropylene.

Sample CCB10 was a clear, pliable yet stiff fragment. This sample is shown in figure 78 and was breaking down at the time of collection. It contained many relevant marker peaks of PVC (Tsuge et al., 2011), including hydrogen chloride (2.68 minutes), benzene (3.73 minutes), toluene (4.59 minutes), xylene (5.44 minutes), styrene (5.71 minutes), indene (7.12 minutes), naphthalene (8.34 minutes), acenaphthene (9.73 minutes), fluorene (11.12 minutes) and anthracene (12.31 minutes)). These marker compounds are shown in the ion chromatogram in figure 79. The methyl methacrylate additive was present at 4.07 minutes. The bisphenol A additive was present at 14.13 minutes. The 2,4-ditert-butylphenol additive was not detected. Although the above-mentioned markers alluded to a PVC characterization, the presence of methyl methacrylate in conjunction with PVC markers correlated with the expected fragmentation components for methyl acrylate-vinyl chloride copolymer, or P(MA-VC), which is a copolymer of PVC (Tsuge et al., 2011). The most prominent marker compounds for this copolymer include hydrogen chloride, benzene, methyl methacrylate, toluene, and diethyl phthalate (Tsuge et al., 2011), which closely align with the spectra for this sample. Diethyl phthalate was not identified in the spectra, but other phthalates, such as phthalic anhydride (9.28 minutes), dibutyl phthalate (13.01 minutes) and bis(2-ethylhexyl) phthalate (15.66 minutes) were present. Since methyl methacrylate and styrene appear to be components of the polymer fragmentation in this sample, they were not considered additives. The sample was characterized as copolymer of PVC and P(MA-VC) and was placed in the PVC category.

Figure 78: An image of sample CCB10.

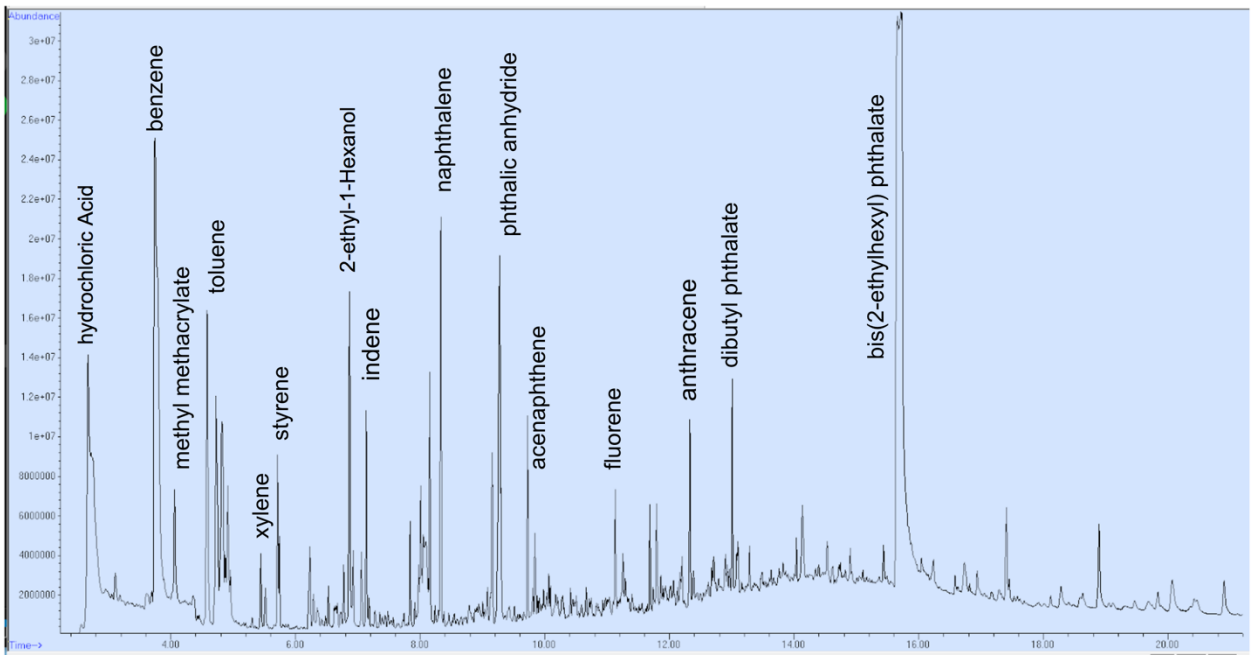

Figure 79: Labeled pyro-gram peaks of sample CCB10, which was determined to be a copolymer of PVC and P(MA-VC).

Figure 80: An image of sample CCB11.

Sample CCB11 was a light green hard plastic fragment that is shown in figure 80. It was less than 3 mm when collected, but it appeared to be a fragment of some other larger plastic, making it a secondary microplastic. It was unclear what the original plastic product may have been. The sample's ion chromatogram, shown in figure 81, contained many compounds relevant to the expected fragmentation of polypropylene (Tsuge et al., 2011), including propene (2.74 minutes), pentane (3.02 minutes), 2-methyl-1-pentene (3.34 minutes), 2,4-dimethyl-1-heptene (5.25 minutes), 2,4,6-trimethyl-1-nonene (7.32 minutes), and 2,4,6,8-tetramethyl-1-undecene (9.07 minutes). The BPA additive was present at 14.11 minutes. There were no 2,4-ditert-butylphenol, methyl methacrylate, phthalate, or styrene additives detected. The sample was characterized and categorized as polypropylene.

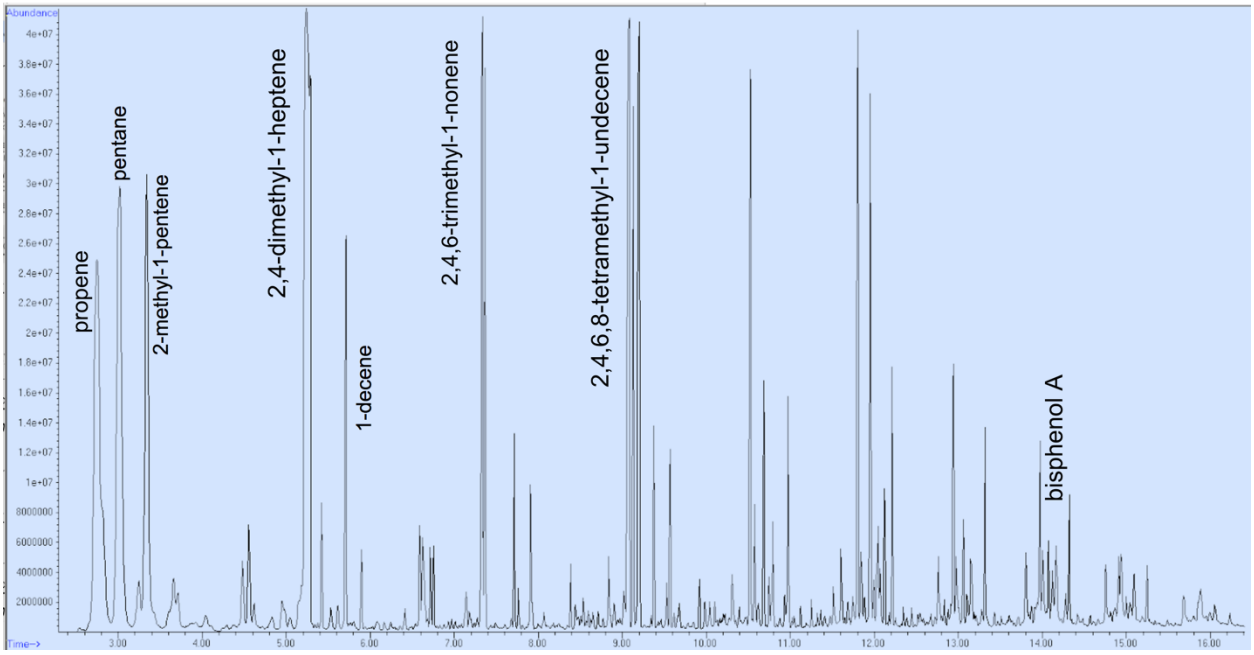

Figure 81: Labeled pyro-gram peaks of sample CCB11, which was determined to polypropylene.

Figure 82: An image of sample CCB12.

Sample CCB12 was a small white plastic cap that was already less than 5 mm when collected. It was also very brittle and was clearly breaking apart to release secondary microplastics, as seen by its image in figure 82. Its ion chromatogram, shown in figure 83, revealed a pattern of hydrocarbon clusters, which alluded to the polyethylene polymer (Tsuge et al., 2011). There were no 2,4-ditert-butylphenol, bisphenol A, methyl methacrylate, phthalate, or styrene additives detected. However, acetic acid was present at 3.52 minutes. The acetic acid compound is not typically part of the polyethylene fragmentation pattern (Tsuge et al., 2011), so this peak indicated a copolymer. Some common polymers that contain acetic acid include polyvinyl alcohol, or PVA, which contains acetic acid and various aromatic compounds that would be found in PVC and cellulose acetate (Tsuge et al., 2011). However, neither of these polymers matched up with the spectra of this sample aside from the acetic acid peak. The more

likely characterization was an ethylene-vinyl acetate copolymer, or EVA. This copolymer essentially consists of the expected polyethylene fragmentation with the addition of acetic acid (Tsuge et al., 2011), which is what was displayed in the spectra. The sample was ultimately characterized as EVA and placed in the polyethylene category.

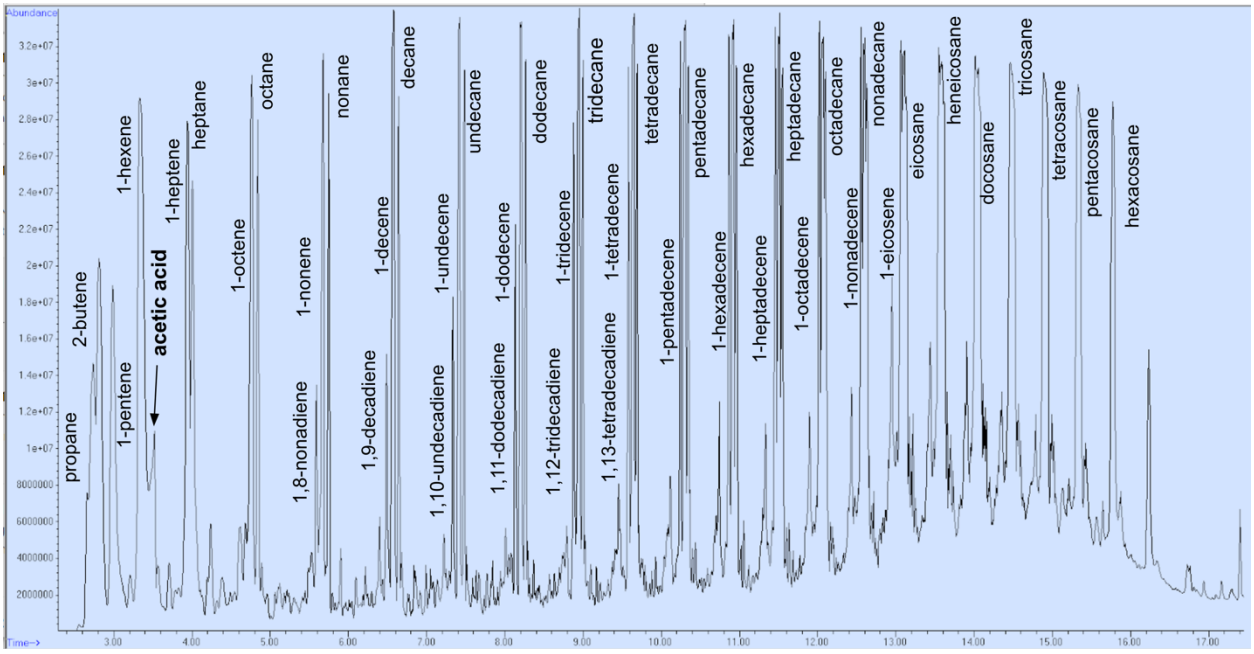

Figure 83: Labeled pyro-gram peaks of sample CCB12, which was determined to EVA.

Figure 84: An image of sample CCB13.

Sample CCB13 was an orange synthetic thread from some sort of rope, as seen in figure 84. Its ion chromatogram, shown in figure 85, revealed a series of hydrocarbons, which alluded to polyethylene (Tsuge et al., 2011). This sample was within the definable microplastic size range at the point of collection, but it appeared to be initially from a larger rope, making it a secondary microplastic. It was also already deteriorating in the environment and releasing small secondary microplastic threads. The signal was not very strong, so the triplets were not very clear, but the pattern and the markers were there. There was a prominent peak for the expected single bonded

hydrocarbon from each length carbon chain. There were no 2,4-ditert-butylphenol, bisphenol A, methyl methacrylate, phthalate, or styrene additives detected. The sample was characterized and categorized as polyethylene.

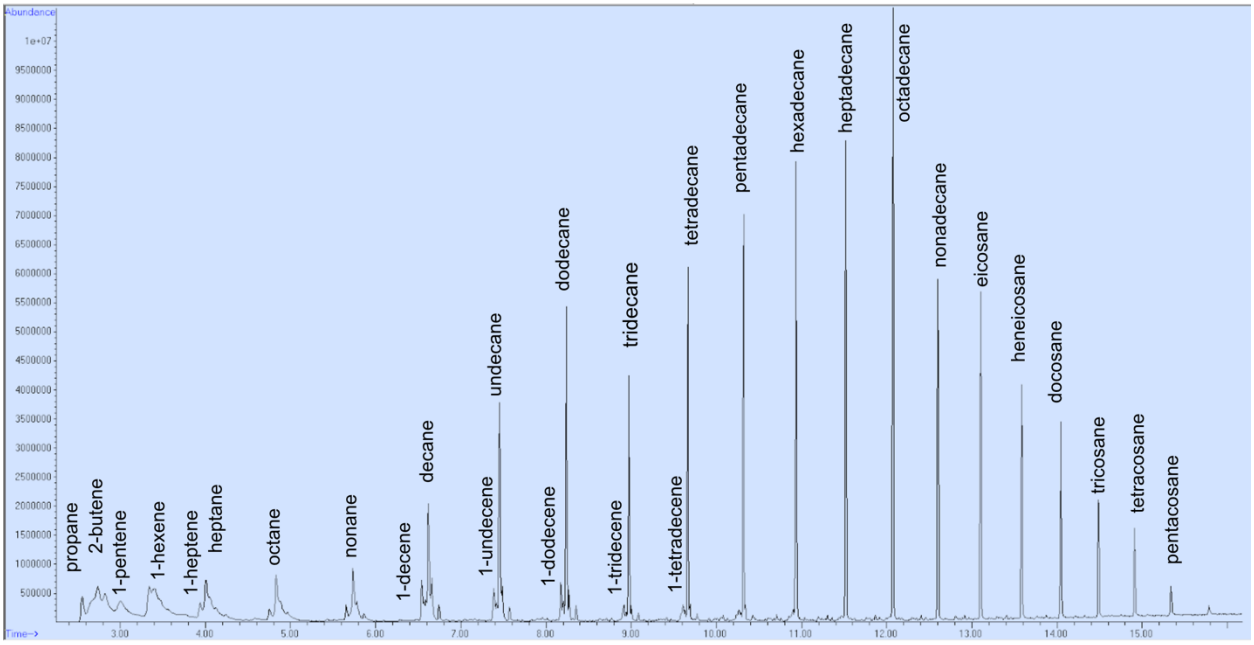

Figure 85: Labeled pyro-gram peaks of sample CCB13, which was determined to polyethylene.

Sample CCB14 was a fragment of a food wrapper and is shown in figure 86. The part of the wrapper that was collected was larger than 5 mm, but it was expected to degrade into secondary microplastics. Its ion chromatogram, shown in figure 87, consisted of many hydrocarbons, so it was initially thought to be polyethylene. For example, the first few peaks consisted of propane (2.80 minutes), 2-pentene (3.00 minutes), and 1-hexene (3.33 minutes). However, after these first few peaks, the hydrocarbons were not aligning with the expected pattern for polyethylene. Additionally, a prominent peak at 4.76 minutes was determined to be cyclopentanone, which is a known marker for nylon (Tsuge et al., 2011). Various polymers contain this compound in their expected

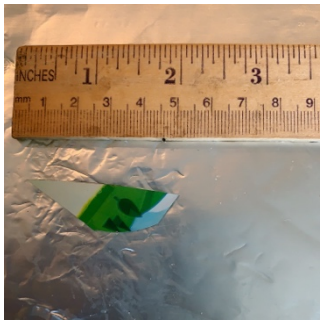

Figure 86: An image of sample CCB14.

fragmentation patters. A likely match could be poly(dodecamethylene adipamide), otherwise known as nylon-12,6. This polymer consists of cyclopentane and various hydrocarbons that were present in the fragmentation of this sample (Tsuge et al., 2011), such as 1-decene (6.53 minutes), 1-decanamine (7.39 minutes), undec-10-en-1-amine (8.17 minutes), dodec-11-en-1-amine (8.92 minutes), 1-dodecanamine (9.61 minutes), 1,12-dodecanediamine (12.04 minutes), 5-cyano-N-(undec-10-enyl)pentanamide (14.50 minutes), and 1,8-diazacycloicosane-2,7-dione (16.75 minutes). One peak did stand out from this characterization: ethan-1,2-diyldibenzoate at 14.03 minutes was an indicator of PET (Tsuge et al., 2011). There were no other standard peaks for PET, so this compound was likely an additive or misinterpreted. The 2,4-ditert-butylphenol additive was present at 10.45 minutes and the styrene additive was present at 5.71 minutes. There were no bisphenol A, methyl methacrylate, or phthalate additives detected. The sample was ultimately characterized as nylon and placed in the polyamide category. Polyamides consist of amide (CO-NH) linkages, which allow for successful hydrogen bonding to occur on the surface (Rabel, 2000; Rodgers and Waddell, 2013). Polyamides are typically formed by polycondensation and ring opening polymerization reactions (Agrawal and Jassal, 2008). Polycondensation reactions, which have not been previously discusses, proceed via a carbonyl addition elimination that can be catalyzed (Agrawal and Jassal, 2008). There are a wide variety of nylon polymers that are manufactured and marketed under different names (Rodgers and Waddell, 2013). Nylon-6 and nylon-6,6 are two of the most common ((Deopura, 2008; Rodgers and Waddell, 2013). Between these two, this sample was more like nylon-6,6 due to its expected cyclopentanone peak (Tsuge et al., 2011). However, most of the peaks aligned better with the previously mentioned nylon-12,6. Given the scope of this study, the nylon classification and polyamide characterization thoroughly differentiated this sample from the rest.

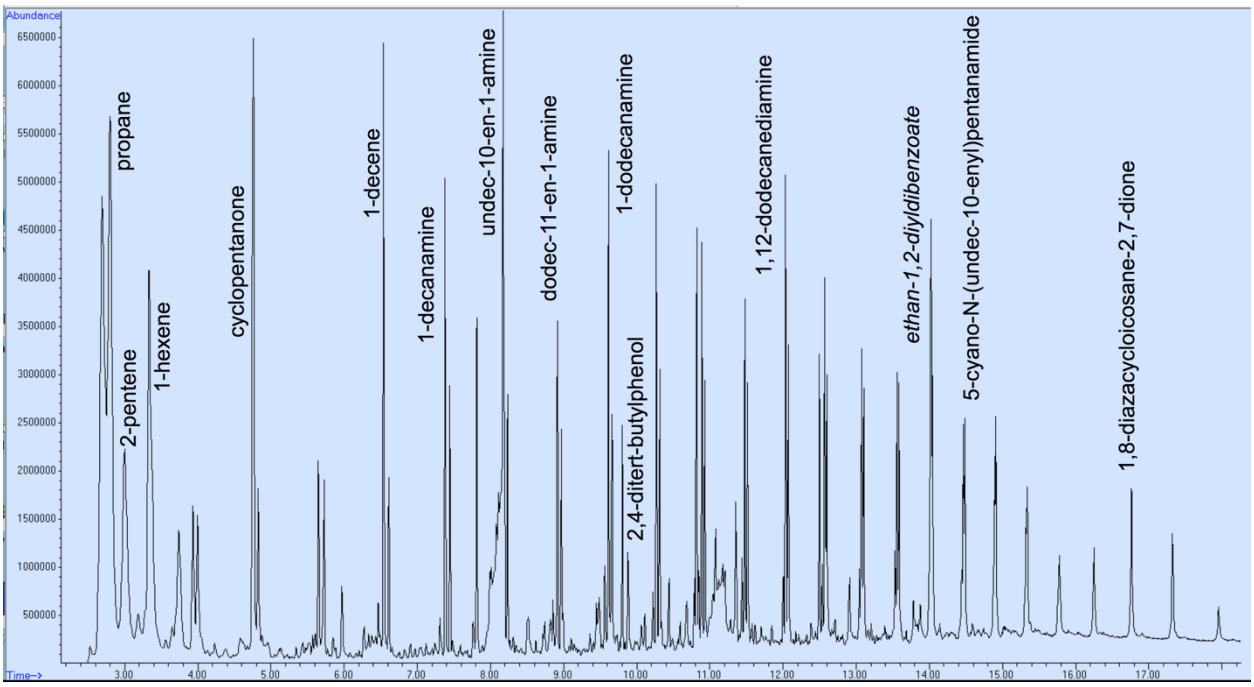

Figure 87: Labeled pyro-gram peaks of sample CCB14, which was determined to nylon-12,6.

Figure 88: An image of sample CCB15.

Sample CCB15, was a part of a plastic drink bottle that is shown in figure 88. The ion chromatogram for this sample, which is shown in figure 89, consisted of a pattern of hydrocarbon clusters that indicated polyethylene (Tsuge et al., 2011). This characterization is expected since plastic bottles are typically made of polyethylene (Andrady, 2011). This sample was relatively intact when collected, but over time would have been expected to break down into secondary microplastics. The 2,4-di-tert-butylphenol additive was present in the spectra at 10.45 minutes. There were no bisphenol A, methyl methacrylate, phthalate, or styrene additives detected. Following a straightforward analysis, the sample was characterized and categorized as polyethylene.

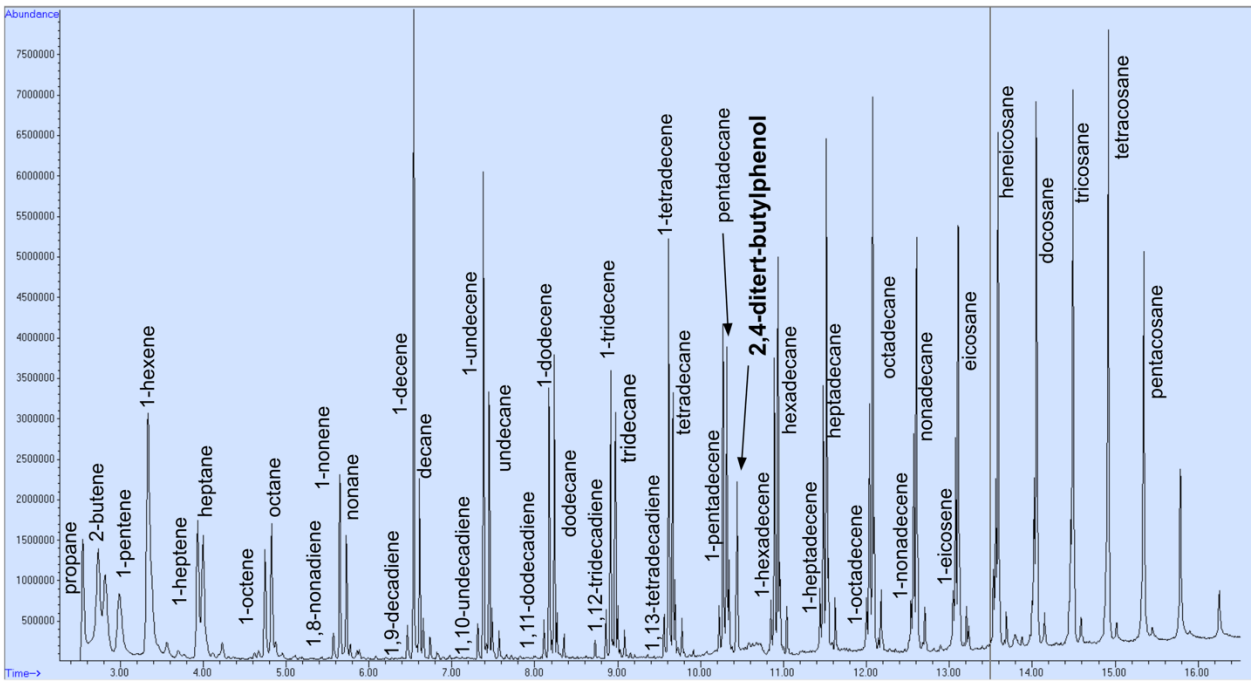

Figure 89: Labeled pyro-gram peaks of sample CCB15, which was determined to polyethylene.

Sample CCB16 was a dark green plastic fragment that was about 2 mm wide when collected. It was also visibly deteriorating and releasing secondary microplastics at the time of collection, which can be seen in figure 90. It is unclear where this sample came from or what product it could be attributed to. The fragmentation pattern of this sample's ion chromatogram contained many compounds relevant to the polypropylene polymer standard (Tsuge et al., 2011), such as propene (2.75 minutes), pentane (3.01 minutes), 2-methyl-1pentene (3.34 minutes), 2,4-dimethyl-1-heptene (5.24 minutes), 2,4,6-trimethyl-1-nonene (7.32 minutes), and 2,4,6,8-tetramethyl-1-undecene (9.07 minutes). These marker peaks can be seen in figure 91. The 2,4-ditert-butylphenol additive was present in the spectra at 10.45 minutes and the bisphenol A additive was present at 14.11

Figure 90: An image of sample CCB16.

minutes. There were no methyl methacrylate, phthalate, or styrene additives detected. The sample was characterized and categorized as polypropylene.

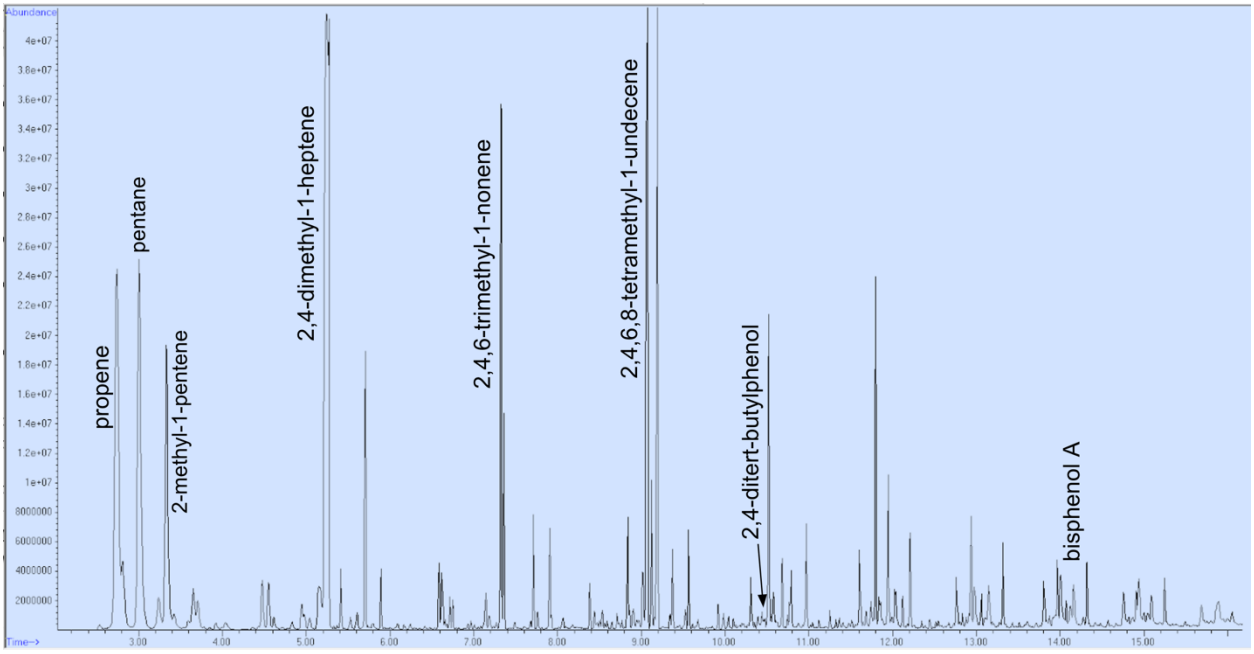

Figure 91: Labeled pyro-gram peaks of sample CCB16, which was determined to polypropylene.

Figure 92: An image of sample CCB17.

Sample CCB17 was a small red sphere that appeared to be a nurdle, or pre-production industry pellet, making it a primary microplastic. An image of this sample is shown in figure 92. Its ion chromatogram, shown in figure 93, contained indicators of cellulose (Tsuge et al., 2011), including carbon dioxide (2.73 minutes), pyruvic acid (3.23 minutes), hydroxyacetaldehyde (3.76 minutes), acetone alcohol (4.02 minutes), 2-furfural (5.16 minutes), 5-methylfuran-2(3H)-one (5.45 minutes), 5-(hydroxymethyl)dihydro-2(3H)-furanone (6.37), 3,6-dianhydro-α -glucopyranose (8.42 minutes), levoglucosenone (8.71 minutes), 2-hydroxy-6,8-dioxabicyclo[3.2.1]octan-4-one (9.59 minutes), and levoglucosan (13.93 minutes). This fragmentation pattern of furans, pyrans, and levoglucosan is expected in the cellulose standard

(Tsuge et al., 2011). There were no 2,4-ditert-butylphenol, bisphenol A, methyl methacrylate, phthalate, or styrene additives detected. The sample was characterized and categorized as cellulose.

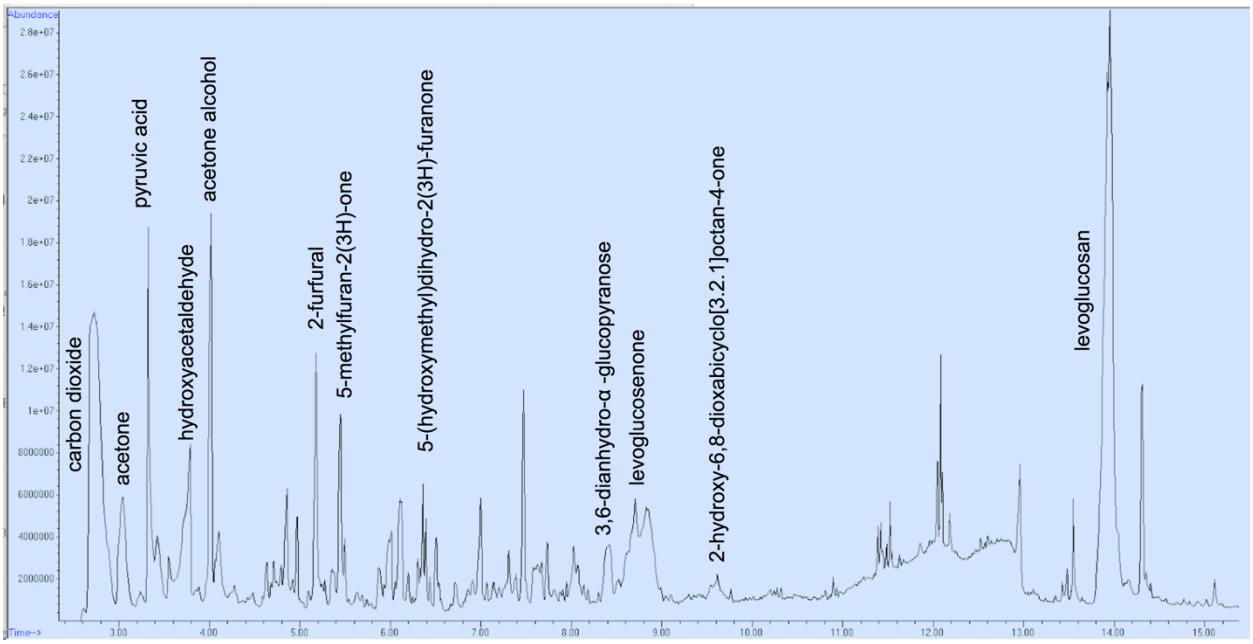

Figure 93: Labeled pyro-gram peaks of sample CCB17, which was determined to be cellulose.

Sample CCB18 consisted of tiny blue specs of plastic that are shown in figure 94. It is unclear whether this sample was a primary or secondary microplastic, but it was within the definable size range when collected. It's ion chromatogram, pictured in figure 95, contained many hydrocarbons and did not have a lot of prominent peaks. The presence of oxalic acid at 2.67 minutes, toluene at 4.58 minutes, and bisphenol A at 14.12 minutes were the most prominent indicators. These compounds are markers for various resins. The epoxy resin and the bismaleimide triazine resin are expected to contain bisphenol A in their standard spectral fragmentation (Tsuge et al., 2011), while the diallyl phthalate resin and the brominated epoxy resin are expected to contain toluene (Tsuge et al., 2011). However, the

Figure 94: An image of sample CCB18.

spectra for this sample did not align perfectly with any specific resin. There were no 2,4-ditert-butylphenol, methyl methacrylate, phthalate, or styrene additives detected. Since toluene and BPA are both found in various resins, the sample was characterized and categorized as a resin. One likely possibility for this sample is that it may have been one of the resins indicated by toluene with a BPA additive present.

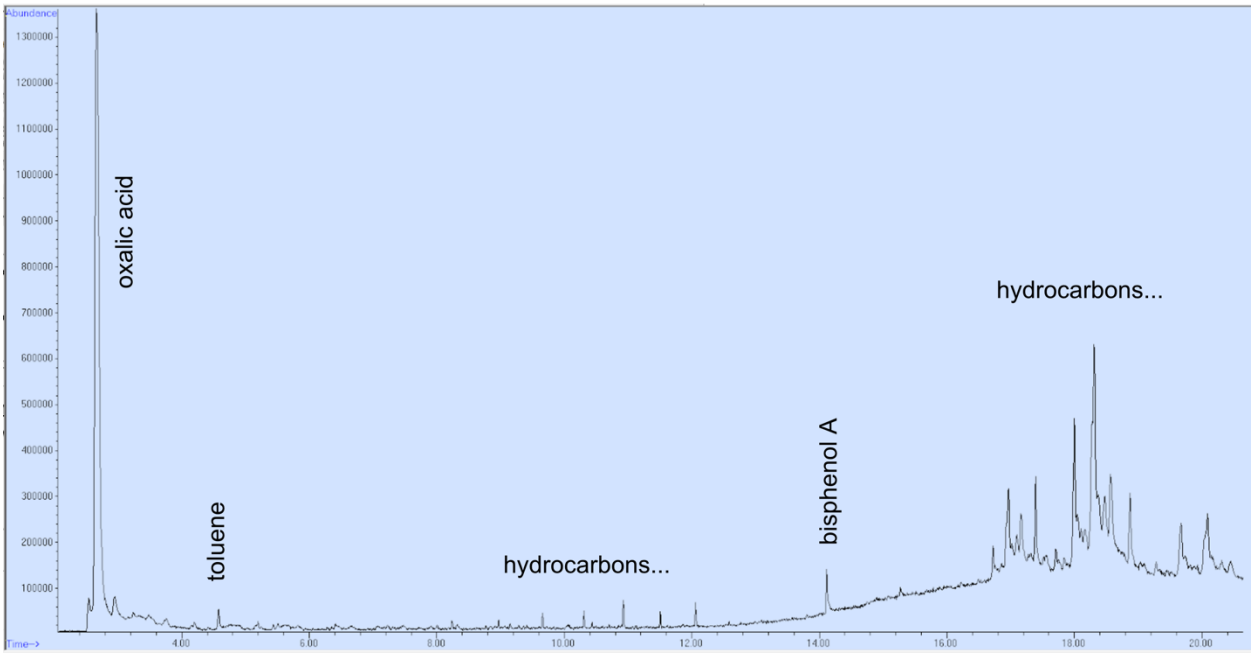

Figure 95: Labeled pyro-gram peaks of sample CCB18, which was determined to be a resin.

Figure 96: An image of sample CCB19.

Sample CCB19, which was a water bottle cap, is shown in figure 96. Its chromatogram contained a pattern of hydrocarbon clusters that resembled polyethylene (Tsuge et al., 2011), as seen in figure 97. This result is expected since water bottle caps are typically made of polyethylene (Andrady, 2011). The cap was less than 5 mm on all sides, so it technically qualified as a microplastic at the point of collection. In the littoral environment where it was found, it would likely continue to break down and produce more secondary microplastics. The 2,4-Di-tert-butylphenol was present

in the spectra at 10.45 minutes. There were no bisphenol A, methyl methacrylate, phthalate, or styrene additives detected. The sample was characterized and categorized as polyethylene.

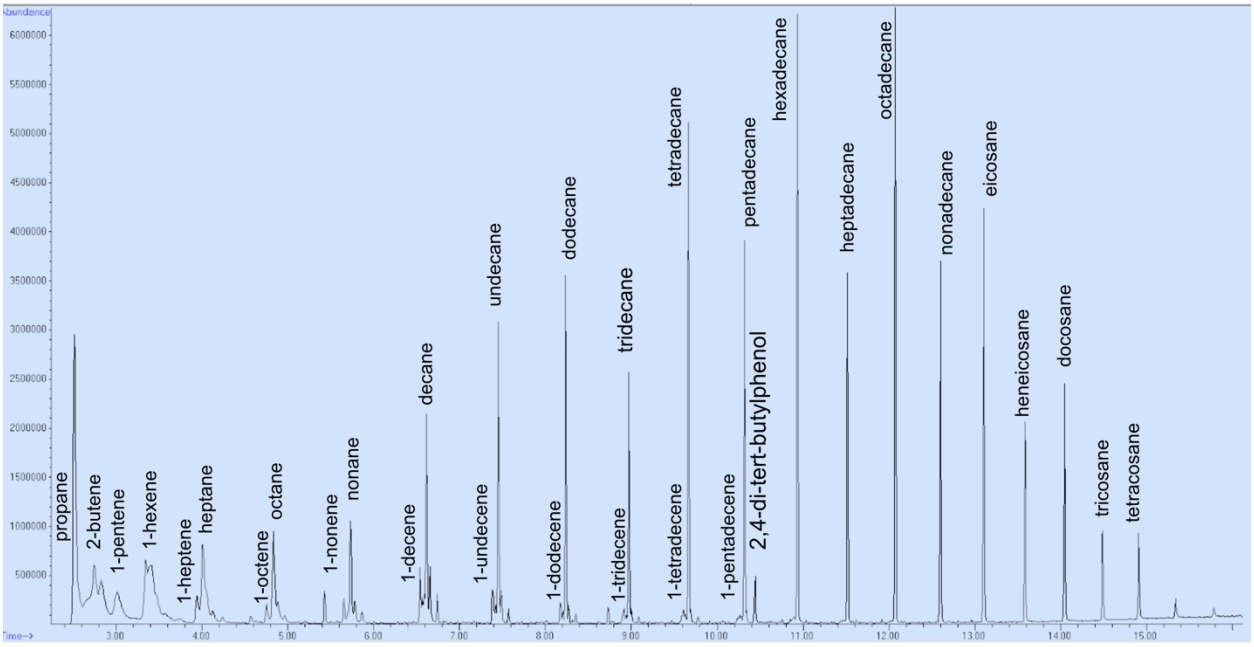

Figure 97: Labeled pyro-gram peaks of sample CCB19, which was determined to polyethylene.

---

e) Additives

Each sample was checked for the presence of bisphenol A, 2,4-ditertbutylphenol, phthalate, methyl methacrylate, and styrene additives. Bisphenol A was found in 9 samples as an additive, impacting making about 26% of the samples. 2,4-ditertbutylphenol was the most common additive, as it was found in 12 samples and thus was incorporated in about 34% of the samples. Eleven of these samples were polypropylene or polyethylene, and only one was PET. It is notable that 2,4-ditertbutylphenol is commonly and frequently added to the two most simple and abundantly produced polymers. Phthalate and styrene additives were found in 7 samples, each impacting 20% of the samples. Methyl methacrylate was found in 8 samples, impacting about 23% of the total analyzed. As described in the “relevant plastic additives” section of the

introduction, these five types of additives each have dangerous and toxic effects associated with them. The fact that they were identified in so many the samples analyzed is a cause for concern. As previously described, when these littoral plastics break down, they can enter the food web and even make it into human's blood (Leslie et al., 2022). These dangerous additives can leach from the plastics once inside the body and pose a serious public health threat. The development of safer polymers and materials that mimic the desirable properties these additives allow would be beneficial in moving away from the use of such threatening compounds.

Conclusion

The characterization of microplastic polymers from various locations on Cape Cod, Massachusetts provides a glimpse into what types of plastics and additives are polluting certain coastal environments. The scope and scale of this project did not allow for the complete examination of every microplastic sample present in these locations, so the results cannot be extrapolated to the full population of microplastic pollution with 100% certainty. However, this research did enable the analysis of representative samples and a subsequent increased understanding of plastic polymer composition in these areas, which offered insight to a newly studied field and built a basis for future research. As microplastic research is a developing field, this component of polymer identification will add to the understanding of potential sources and risks of plastic pollution, paving the way for more in-depth hypotheses to be tested, and allowing for better plastic management. The chemical characterization of these microplastics will lead to understanding the types, and possibly the products, that are polluting various environments. This information can be used to encourage personal and legislative action to minimize and prevent microplastic pollution.

The results of this study revealed a greater variety of polymers than initially predicted. It was expected that most samples would fall within the polyethylene and polypropylene categories, since these polymers are produced most abundantly and can float in seawater. The samples characterized consisted of a wide range of densities, which contradicts with the hypothesis: low density-floating polymers were expected to wash up on the Cape Cod shorelines and significantly outnumber the occurrence of high-density polymers. The prevalence of various densities may be accounted for by the sampling methods carried out in this study. Since many of the samples collected were macroplastics on the shore that would eventually break down into secondary microplastics, it makes sense that the source of this pollution could be coming from litter on the land instead of the ocean. It further connects that litter on the beach would consist of a wider range of samples than solely low density/floating polymers.

The implication of these results suggests that proper disposal of plastic products should limit the ability of microplastics to enter the environment. This expectation, however, is quite idealistic. The idea of implementing more trash and recycling bins on the beaches seems productive, but it is common for such bins to overflow and lead to further pollution of plastic productions. Additionally, there are many serious problems with the recycling system. There are specific recycling codes that are assigned to various polymers based on their toxicity and recyclability, which indicate how they should be disposed of. These codes are displayed in figure 98. However, as this research has shown, plastic products are not consistently manufactured with the

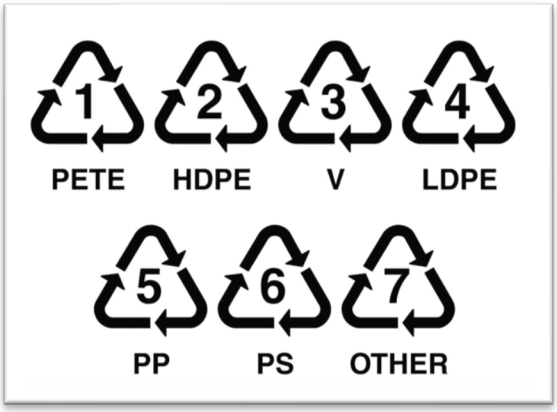

Figure 98: Recycling codes for various types of plastic polymers. These codes are based on the polymer type and alert consumers of the recyclability and potential health risks associated with the product.

exact same compositions. Different companies utilize various mixtures of polymers and additives to obtain their desired product, which diminishes the validity of the recycling codes. Consequently, recycling plants struggle to separate and organize plastic products.

The majority of "recycled" plastics are shipped overseas to be processed (Chen et al., 2021; Ferronato and Torretta, 2019). For a long time, China was the primary importer of plastic. They recently banned these imports due to the recycling challenges mentioned and the sheer abundance of waste. Now, the largest importer is Malaysia, followed by other developing nations (Chen et al., 2021; Ferronato and Torretta, 2019). The importers of this waste have no easier time recycling it, leading to a large amount of incineration, and dumping of the plastic (Ferronato and Torretta, 2019). While recycling is good in theory, the abundance and complexities of plastic products inhibit its success. It is critical that new solutions are sought. For example, a group at the University of Michigan is working on developing adhesives that can leech microplastics out of water and could potentially be applied to water filter systems (McNeil, 2021). Additionally, many labs are working on the synthesis of new materials and bioplastics that are less toxic or more easily recycled than traditional synthetic polymers. The development of safer and more durable plastics polymers that do not rely as heavily on additives would also be beneficial. No single solution can fully address the plastic problem, but holistic thinking and integrated approaches can make a positive difference. In the meantime, it is important to continue to learn more about how plastic particles behave in the environment and the human body to better assess their risks, in addition to realizing where improvements need to be made. The described work is relevant since it can be utilized to determine where future research efforts should be focused, in addition to educating the public about the dangers of plastic pollution and informing policy makers about the compositions of various forms of pollution.

References

1. National Institute of Standards and Technology Libraries, Tools, Service. *https://chemdata.nist.gov/dokuwiki/doku.php?id=chemdata%3Astart* (accessed April 11, 2022).

2. Ferronato, N.; Torretta, V. Waste Mismanagement in Developing Countries: A Review of Global Issues. *International Journal of Environmental Research and Public Health* **2019***, 16*.

3. Chen, H. L.; Nath, T. K.; Chong, S.; Foo, V.; Gibbins, C.; Lechner, A. M. The plastic waste problem in Malaysia: management, recycling and disposal of local and global plastic waste. *SN Applied Sciences* **2021***, 3*, 437.

4. McNeil, A. Microplastics Capture & Repurposing . *https://mcneilgroup.chem.lsa.umich.edu/chemical-research/* (accessed April 7, 2022).

5. Leslie, H. A.; van Velzen, Martin J. M.; Brandsma, S. H.; Vethaak, A. D.; Garcia-Vallejo, J. J.; Lamoree, M. H. Discovery and quantification of plastic particle pollution in human blood. *Environ. Int.* **2022**, 107199.

6. AGRAWAL, A. K.; JASSAL, M. In *4 - Manufacture of polyamide fibres;* Deopura, B. L., Alagirusamy, R., Joshi, M. and Gupta, B., Eds.; Polyesters and Polyamides; Woodhead Publishing: 2008; pp 97-139.

7. DEOPURA, B. L. In *2 - Polyamide fibers;* Deopura, B. L., Alagirusamy, R., Joshi, M. and Gupta, B., Eds.; Polyesters and Polyamides; Woodhead Publishing: 2008; pp 41-61.

8. Palabiyik, I.; Güleri, T.; Gunes, R.; Öner, B.; Toker, O. S.; Konar, N. A fundamental optimization study on chewing gum textural and sensorial properties: The effect of ingredients. *Food Structure* **2020***, 26*, 100155.

9. Farber, T. M.; Clewell, A. E.; Endres, J. R.; Hauswirth, J.; Van Gemert, M.; Schauss, A. G.; Sheane, C. A. Safety assessment of a novel ingredient for removable chewing gum. *Food and Chemical Toxicology* **2010***, 48*, 831-838.

10. Ouellette, R. J.; Rawn, J. D. In *28 - Synthetic Polymers;* Ouellette, R. J., Rawn, J. D., Eds.; Organic Chemistry Study Guide; Elsevier: Boston, 2015; pp 587-601.

11. Rabel, F. In *CHROMATOGRAPHY: THIN-LAYER (PLANAR) | Layers;* Wilson, I. D., Ed.; Encyclopedia of Separation Science; Academic Press: Oxford, 2000; pp 853-860.

12. Rodgers, B.; Waddell, W. In *Chapter 14 - Tire Engineering;* Mark, J. E., Erman, B. and Roland, C. M., Eds.; The Science and Technology of Rubber (Fourth Edition); Academic Press: Boston, 2013; pp 653-695.

13. Lloret, J. Correspondence with Marine Biological Laboratory Research Scientist. **2022**.

14. Mallick, P. K. In *5 - Thermoplastics and thermoplastic–matrix composites for lightweight automotive structures;* Mallick, P. K., Ed.; Materials, Design and Manufacturing for Lightweight Vehicles; Woodhead Publishing: 2010; pp 174-207.

15. Lanaro, M.; Booth, L.; Powell, S. K.; Woodruff, M. A. In *3 - Electrofluidodynamic technologies for biomaterials and medical devices: melt electrospinning;* Guarino, V., Ambrosio, L., Eds.; Electrofluidodynamic Technologies (EFDTs) for Biomaterials and Medical Devices; Woodhead Publishing: 2018; pp 37-69.

16. Centers for Disease Control and Prevention Glossary of Volatile Organic Compounds. *Department of Health and Human Services* **2003**.

17. Mögel, I.; Baumann, S.; Böhme, A.; Kohajda, T.; von Bergen, M.; Simon, J.; Lehmann, I. The aromatic volatile organic compounds toluene, benzene and styrene induce COX-2 and prostaglandins in human lung epithelial cells via oxidative stress and p38 MAPK activation. *Toxicology* **2011***, 289*, 28-37.

18. National Toxicology Program Report on Carcinogens, Twelfth Edition. *National Toxicology Program, Department of Health and Human Services* **2011**.

19. Gonçalves, J. M.; Sousa, V. S.; Teixeira, M. R.; Bebianno, M. J. Chronic toxicity of polystyrene nanoparticles in the marine mussel Mytilus galloprovincialis. *Chemosphere* **2022***, 287*, 132356.

20. Xu, B.; Liu, F.; Cryder, Z.; Huang, D.; Lu, Z.; He, Y.; Wang, H.; Lu, Z.; Brookes, P. C.; Tang, C.; Gan, J.; Xu, J. Microplastics in the soil environment: Occurrence, risks, interactions and fate – A review. *Crit. Rev. Environ. Sci. Technol.* **2020***, 50*, 2175-2222.

21. Sarker, A.; Deepo, D. M.; Nandi, R.; Rana, J.; Islam, S.; Rahman, S.; Hossain, M. N.; Islam, M. S.; Baroi, A.; Kim, J. A review of microplastics pollution in the soil and terrestrial ecosystems: A global and Bangladesh perspective. *Sci. Total Environ.* **2020***, 733*, 139296.

22. Wang, W.; Ge, J.; Yu, X.; Li, H. Environmental fate and impacts of microplastics in soil ecosystems: Progress and perspective. *Sci. Total Environ.* **2020***, 708*, 134841.

23. Liu, J.; Qin, J.; Zhu, L.; Zhu, K.; Liu, Z.; Jia, H.; Lichtfouse, E. The protective layer formed by soil particles on plastics decreases the toxicity of polystyrene microplastics to earthworms (Eisenia fetida). *Environ. Int.* **2022***, 162*, 107158.

24. Shang, Y.; Wang, S.; Jin, Y.; Xue, W.; Zhong, Y.; Wang, H.; An, J.; Li, H. Polystyrene nanoparticles induced neurodevelopmental toxicity in Caenorhabditis elegans through regulation of dpy-5 and rol-6. *Ecotoxicol. Environ. Saf.* **2021***, 222*, 112523.

25. Silverstein, R. M.; Webster, F. X.; Kiemle, D. J. *Spectrometric Identification of Organic Compounds;* John Wiley & Sons, INC.: 2005; .

26. Fadare, O. O.; Okoffo, E. D. Covid-19 face masks: A potential source of microplastic fibers in the environment. *Sci. Total Environ.* **2020***, 737*, 140279.

27. Anonymous *Advanced Fibre-Reinforced Polymer (FRP) Composites for Structural Applications;* Woodhead Publishing Series in Civil and Structural Engineering "; Woodhead Publishing: 2013; , pp xix-xxii.

28. Chapiro, A. In *Radiation Effects in Polymers;* Buschow, K. H. J., Cahn, R. W., Flemings, M. C., Ilschner, B., Kramer, E. J., Mahajan, S. and Veyssière, P., Eds.; Encyclopedia of Materials: Science and Technology; Elsevier: Oxford, 2004; pp 1-8.

29. Kim, Y.; Lee, S.; Yoon, H. Fire-Safe Polymer Composites: Flame-Retardant Effect of Nanofillers. *Polymers* **2021***, 13*, 540.

30. Diaz, L.; Zhang, K.; Phan, A. Monomer recovery through advanced pyrolysis of waste high density polyethylene (HDPE). *RSC Green Chemistry* **2018***, 20*.

31. Slade, J. Research. *https://sites.google.com/ucsd.edu/slade-lab/research?authuser=0* (accessed March 2, 2022).

32. Free, C. M.; Jensen, O. P.; Mason, S. A.; Eriksen, M.; Williamson, N. J.; Boldgiv, B. High-levels of microplastic pollution in a large, remote, mountain lake. *Mar. Pollut. Bull.* **2014***, 85*, 156-163.

33. Bian, P.; Liu, Y.; Zhao, K.; Hu, Y.; Zhang, J.; Kang, L.; Shen, W. Spatial variability of microplastic pollution on surface of rivers in a mountain-plain transitional area: A case study in the Chin Ling-Wei River Plain, China. *Ecotoxicol. Environ. Saf.* **2022***, 232*, 113298.

34. Padha, S.; Kumar, R.; Dhar, A.; Sharma, P. Microplastic pollution in mountain terrains and foothills: A review on source, extraction, and distribution of microplastics in remote areas. *Environ. Res.* **2022***, 207*, 112232.

35. Zhang, J.; Wang, L.; Trasande, L.; Kannan, K. Occurrence of Polyethylene Terephthalate and Polycarbonate Microplastics in Infant and Adult Feces. *Environ. Sci. Technol. Lett.* **2021***, 8*, 989-994.

36. MASSINGILL, J. L.; BAUER, R. S. EPOXY RESINS. *Applied Polymer Science: 21st Century* **2000**, 393-424.

37. Takeichi, T.; Furukawa, N. In *5.25 - Epoxy Resins and Phenol-Formaldehyde Resins;* Matyjaszewski, K., Möller, M., Eds.; Polymer Science: A Comprehensive Reference; Elsevier: Amsterdam, 2012; pp 723-751.

38. Du, Y.; Zhao, G.; Shi, G.; Wang, Y.; Li, W.; Ren, S. Effect of crosslink structure on mechanical properties, thermal stability and flame retardancy of natural flavonoid based epoxy resins. *European Polymer Journal* **2022***, 162*, 110898.

39. Xie, Y.; Li, H.; Ding, Y.; Zhang, C.; Huang, Q.; Chen, C.; Han, S.; Zhang, J. The effect of resins concentration and polarity on the viscosity and impedance of electrically-treated waxy oils. *Journal of Petroleum Science and Engineering* **2022***, 212*, 110359.

40. Speizer, F. E. Overview of the risk of respiratory cancer from airborne contaminants. *Environ. Health Perspect.* **1986***, 70*, 9-15.

41. Li, C.; Zhuang, H.; Hsieh, L.; Lee, W.; Tsao, M. PAH emission from the incineration of three plastic wastes. *Environ. Int.* **2001***, 27*, 61-67.

42. Lambert, S.; Sinclair, C.; Boxall, A. Occurrence, Degradation, and Effect of Polymer-Based Materials in the Environment. *Reviews of Environmental Contamination and Toxicology (Continuation of Residue Reviews)* **2014***, vol 227.*

43. Shaw, D. G.; Day, R. H. Colour- and form-dependent loss of plastic micro-debris from the North Pacific Ocean. *Mar. Pollut. Bull.* **1994***, 28*, 39-43.

44. Smits-van Prooije, A. E.; Lammers, J. H. C. M.; Waalkens-Berendsen, D. H.; Kulig, B. M.; Snoeij, N. J. Effects of the PCB 3,4,5,3′,4′,5′-hexachlorobiphenyl on the reproduction capacity of Wistar rats. *Chemosphere* **1993***, 27*, 395-400.

45. Daouk, T.; Larcher, T.; Roupsard, F.; Lyphout, L.; Rigaud, C.; Ledevin, M.; Loizeau, V.; Cousin, X. Long-term food-exposure of zebrafish to PCB mixtures mimicking some environmental situations induces ovary pathology and impairs reproduction ability. *Aquatic Toxicology* **2011***, 105*, 270-278.

46. Koelmans, A. A.; Besseling, E.; Wegner, A.; Foekema, E. M. Plastic as a carrier of POPs to aquatic organisms: a model analysis. *Environ. Sci. Technol.* **2013***, 47*, 7812-7820.

47. da Costa, J. P.; Santos, P. S. M.; Duarte, A. C.; Rocha-Santos, T. (Nano)plastics in the environment – Sources, fates and effects. *Sci. Total Environ.* **2016***, 566-567*, 15-26.

48. Auta, H. S.; Emenike, C. U.; Fauziah, S. H. Distribution and importance of microplastics in the marine environment: A review of the sources, fate, effects, and potential solutions. *Environ. Int.* **2017***, 102*, 165-176.

49. Lares, M.; Ncibi, M. C.; Sillanpää, M.; Sillanpää, M. Occurrence, identification and removal of microplastic particles and fibers in conventional activated sludge process and advanced MBR technology. *Water Res.* **2018***, 133*, 236-246.

50. Calhoun, A. In *3 - Polypropylene;* Wagner, J. R., Ed.; Multilayer Flexible Packaging (Second Edition); William Andrew Publishing: 2016; pp 35-45.

51. McKeen, L. In *3 - Introduction to the Physical, Mechanical, and Thermal Properties of Plastics and Elastomers;* McKeen, L., Ed.; The Effect of Sterilization on Plastics and Elastomers (Third Edition); William Andrew Publishing: Boston, 2012; pp 57-84.

52. Kusch, P. Chapter 7 - Application of Pyrolysis-Gas Chromatography/Mass Spectrometry (Py-GC/MS). *Comprehensive Analytical Chemistry* **2017***, 75*, 169-207.

53. Costa, M. F.; Duarte, A. C. Chapter 2 - Microplastics Sampling and Sample Handling. *Comprehensive Analytical Chemistry* **2017***, 75*, 25-47.

54. da Costa, J. P.; Duarte, A. C.; Rocha-Santos, T. A. P. Chapter 1 - Microplastics – Occurrence, Fate and Behaviour in the Environment. *Comprehensive Analytical Chemistry* **2017***, 75*, 1-24.

55. Rodríguez-Seijo, A.; Pereira, R. Chapter 3 - Morphological and Physical Characterization of Microplastics. *Comprehensive Analytical Chemistry* **2017***, 75*, 49-66.

56. Rios Mendoza, L. M.; Taniguchi, S.; Karapanagioti, H. K. Chapter 8 - Advanced Analytical Techniques for Assessing the Chemical Compounds Related to Microplastics. *Comprehensive Analytical Chemistry* **2017***, 75*, 209-240.

57. Ahmed, R.; Hamid, A. K.; Krebsbach, S. A.; He, J.; Wang, D. Critical review of microplastics removal from the environment. *Chemosphere* **2022***, 293*, 133557.

58. Meeker, J. D.; Sathyanarayana, S.; Swan, S. H. Phthalates and other additives in plastics: human exposure and associated health outcomes. *Philosophical transactions of the Royal Society of London.Series B, Biological sciences* **2009***, 364*, 2097-2113.

59. Bach, C.; Dauchy, X.; Severin, I.; Munoz, J.; Etienne, S.; Chagnon, M. Effect of temperature on the release of intentionally and non-intentionally added substances from polyethylene terephthalate (PET) bottles into water: Chemical analysis and potential toxicity. *Food Chem.* **2013***, 139*, 672-680.

60. Zhao, F.; Wang, P.; Lucardi, R. D.; Su, Z.; Li, S. Natural Sources and Bioactivities of 2,4-Di-Tert-Butylphenol and Its Analogs. *Toxins* **2020***, 12*.

61. Green, T.; Toghill, A.; Foster, J. R. The role of cytochromes P-450 in styrene induced pulmonary toxicity and carcinogenicity. *Toxicology* **2001***, 169*, 107-117.

62. Simmonds, M. S. J. IARC Monographs on the Evaluation of Carcinogenic Risks to Humans. Vol. 82, Some Traditional Herbal Medicines, Some Mycotoxins, Naphthalene and Styrene: World Health Organisation, IARC Press, Lyon France, 2002, 590 pp., ISBN 92 832 1282 7, US$40. *Phytochemistry* **2004***, 65*, 139.

63. Kogevinas, M.; Gwinn, W. M.; Kriebel, D.; Phillips, D. H.; Sim, M.; Bertke, S. J.; Calaf, G. M.; Colosio, C.; Fritz, J. M.; Fukushima, S.; Hemminki, K.; Jensen, A. A.; Kolstad, H.; Mráz, J.; Nesnow, S.; Nylander-French, L. A.; Parent, M.; Sandy, M.; Smith-Roe, S. L.; Stoner, G.; Suzuki, T.; Teixeira, J. P.; Vodicka, P.; Tornero-Velez, R.; Guyton, K. Z.; Grosse, Y.; El Ghissassi, F.; Bouvard, V.; Benbrahim-Tallaa, L.; Guha, N.; Vilahur, N.; Driscoll, T.; Hall, A.; Middleton, D.; Jaillet, C.; Mattock, H.; Straif, K. Carcinogenicity of quinoline, styrene, and styrene-7,8-oxide. *The Lancet Oncology* **2018***, 19*, 728-729.

64. Bereznowski, Z. In vivo assessment of methyl methacrylate metabolism and toxicity. *Int. J. Biochem. Cell Biol.* **1995***, 27*, 1311-1316.

65. Mainwaring, G.; Foster, J. R.; Lund, V.; Green, T. Methyl methacrylate toxicity in rat nasal epithelium: studies of the mechanism of action and comparisons between species. *Toxicology* **2001***, 158*, 109-118.

66. Liu, R.; Mabury, S. A. Unexpectedly high concentrations of 2,4-di-tert-butylphenol in human urine. *Environmental Pollution* **2019***, 252*, 1423-1428.

67. Andrady, A. L. Microplastics in the marine environment. *Mar. Pollut. Bull.* **2011***, 62*, 1596-1605.

68. Geyer, R.; Jambeck, J. R.; Kara, L. L. Production, use, and fate of all plastics ever made. *Sci. Adv.* **2017***, 3*, e1700782.

69. Lebreton, L.; Egger, M.; Slat, B. A global mass budget for positively buoyant macroplastic debris in the ocean. *Scientific Reports* **2019***, 9*, 12922.

70. Stevens, E. S. In *The Age of Plastics;* Green Plastics; Princeton University Press: 2002; pp 3-9.

71. AnonymousThe New Plastics Economy: Rethinking the future of plastics. **2016**.

72. Cwszot, K. File:Electron Ionization GC-MS.png. **2018**.

73. Fischer, M.; Scholz-Böttcher, B. M. Simultaneous Trace Identification and Quantification of Common Types of Microplastics in Environmental Samples by Pyrolysis-Gas Chromatography–Mass Spectrometry. *Environ. Sci. Technol.* **2017***, 51*, 5052-5060.

74. Rochman, C. M. In *The Complex Mixture, Fate and Toxicity of Chemicals Associated with Plastic Debris in the Marine Environment;* Bergmann, M., Gutow, L. and Klages, M., Eds.; Marine Anthropogenic Litter; Springer International Publishing: Cham, 2015; pp 117-140.

75. Rillig, M. C. Microplastic in Terrestrial Ecosystems and the Soil? *Environ. Sci. Technol.* **2012***, 46*, 6453-6454.

76. Belzagui, F.; Buscio, V.; Gutiérrez-Bouzán, C.; Vilaseca, M. Cigarette butts as a microfiber source with a microplastic level of concern. *Sci. Total Environ.* **2021***, 762*, 144165.

77. Shen, M.; Li, Y.; Song, B.; Zhou, C.; Gong, J.; Zeng, G. Smoked cigarette butts: Unignorable source for environmental microplastic fibers. *Sci. Total Environ.* **2021***, 791*, 148384.

78. Araújo, Maria Christina Barbosa de; Costa, M. F. d. Cigarette butts in beach litter: Snapshot of a summer holiday. *Mar. Pollut. Bull.* **2021***, 172*, 112858.

79. Fialkov, A. B.; Steiner, U.; Lehotay, S. J.; Amirav, A. Sensitivity and noise in GC–MS: Achieving low limits of detection for difficult analytes. *International Journal of Mass Spectrometry* **2007***, 260*, 31-48.

80. Wenig, P. Post-optimization of Py-GC/MS data: A case study using a new digital chemical noise reduction filter (NOISERA) to enhance the data quality utilizing OpenChrom mass spectrometric software. *J. Anal. Appl. Pyrolysis* **2011***, 92*, 202-208.

81. Hatami, M.; Sharifi, A.; Karimi-Maleh, H.; Agheli, H.; Karaman, C. Simultaneous improvements in antibacterial and flame retardant properties of PET by use of bio-nanotechnology for fabrication of high performance PET bionanocomposites. *Environ. Res.* **2021**, 112281.

82. Jafferson, J. M.; Chatterjee, D. A review on polymeric materials in additive manufacturing. *Materials Today: Proceedings* **2021***, 46*, 1349-1365.

83. Kang, J. S.; Baek, J. H.; Jung, S.; Chung, H. J.; Lee, D. K.; Kim, H. J. Ingestion of Bis(2-ethylhexyl) phthalate (DEHP) during adolescence causes depressive-like behaviors through hypoactive glutamatergic signaling in the medial prefrontal cortex. *Environmental Pollution* **2021***, 289*, 117978.

84. Oliveira, W. d. S.; Monsalve, J. O.; Nerin, C.; Padula, M.; Godoy, H. T. Characterization of odorants from baby bottles by headspace solid phase microextraction coupled to gas chromatography-olfactometry-mass spectrometry. *Talanta* **2020***, 207*, 120301.

85. Zhang, T.; Lin, L.; Li, D.; Wu, S.; Kong, L.; Wang, J.; Shi, H. The microplastic pollution in beaches that served as historical nesting grounds for green turtles on Hainan Island, China. *Mar. Pollut. Bull.* **2021***, 173*, 113069.

86. Fok, L.; Cheung, P. K.; Tang, G.; Li, W. C. Size distribution of stranded small plastic debris on the coast of Guangdong, South China. *Environmental Pollution* **2017***, 220*, 407-412.

87. Canesi, L.; Ciacci, C.; Bergami, E.; Monopoli, M. P.; Dawson, K. A.; Papa, S.; Canonico, B.; Corsi, I. Evidence for immunomodulation and apoptotic processes induced by cationic polystyrene nanoparticles in the hemocytes of the marine bivalve Mytilus. *Mar. Environ. Res.* **2015***, 111*, 34-40.

88. Chiu, H.; Xia, T.; Lee, Y.; Chen, C.; Tsai, J.; Wang, Y. Cationic polystyrene nanospheres induce autophagic cell death through the induction of endoplasmic reticulum stress. *Nanoscale* **2015***, 7*, 736-746.

89. Barshtein, G.; Livshits, L.; Shvartsman, L. D.; Shlomai, N. O.; Yedgar, S.; Arbell, D. Polystyrene Nanoparticles Activate Erythrocyte Aggregation and Adhesion to Endothelial Cells. *Cell Biochem. Biophys.* **2016***, 74*, 19-27.

90. Eben, M.; Cithuraj, K.; Justus, S.; Bhagavathsingh, J. Synthesis and characterization of stretchable IPN polymers from biodegradable resins incorporated with styrene and methyl methacrylate monomers for enhanced mechanical strength. *European Polymer Journal* **2020***, 138*, 109957.

91. Chen, C.; Kuo, P.; Lee, T.; Liu, C. Snow lines on shorelines: Solving Styrofoam buoy marine debris from oyster culture in Taiwan. *Ocean Coast. Manage.* **2018***, 165*, 346-355.

92. Mukai, Y.; Goto, A.; Tashiro, Y.; Tanabe, S.; Kunisue, T. Coastal biomonitoring survey on persistent organic pollutants using oysters (Saccostrea mordax) from Okinawa, Japan: Geographical distribution and polystyrene foam as a potential source of hexabromocyclododecanes. *Sci. Total Environ.* **2020***, 739*, 140049.

93. Gaylarde, C. C.; Neto, J. A. B.; da Fonseca, E. M. Paint fragments as polluting microplastics: A brief review. *Mar. Pollut. Bull.* **2021***, 162*, 111847.

94. Tsuge, S.; Ohtani, H.; Watanabe, C. *Pyrolysis - GC/MS Data Book of Synthetic Polymers;* 2011; .

95. Jeon, J.; Park, S.; Choi, T.; Park, J.; Yang, Y.; Yoon, J. Biodegradation of polyethylene and polypropylene by Lysinibacillus species JJY0216 isolated from soil grove. *Polym. Degrad. Stab.* **2021***, 191*, 109662.

96. Toapanta, T.; Okoffo, E. D.; Ede, S.; O'Brien, S.; Burrows, S. D.; Ribeiro, F.; Gallen, M.; Colwell, J.; Whittaker, A. K.; Kaserzon, S.; Thomas, K. V. Influence of surface oxidation on the quantification of polypropylene microplastics by pyrolysis gas chromatography mass spectrometry. *Sci. Total Environ.* **2021***, 796*, 148835.

97. Zhang, D.; Liu, X.; Huang, W.; Li, J.; Wang, C.; Zhang, D.; Zhang, C. Microplastic pollution in deep-sea sediments and organisms of the Western Pacific Ocean. *Environmental Pollution* **2020***, 259*, 113948.

98. Athey, S. N.; Erdle, L. M. Are We Underestimating Anthropogenic Microfiber Pollution? A Critical Review of Occurrence, Methods, and Reporting. *Environ. Toxicol. Chem.* **2021***, n/a*.

99. Rahman, A.; Sarkar, A.; Yadav, O. P.; Achari, G.; Slobodnik, J. Potential human health risks due to environmental exposure to nano- and microplastics and knowledge gaps: A scoping review. *Sci. Total Environ.* **2021***, 757*, 143872.

100. Huang, D.; Tao, J.; Cheng, M.; Deng, R.; Chen, S.; Yin, L.; Li, R. Microplastics and nanoplastics in the environment: Macroscopic transport and effects on creatures. *J. Hazard. Mater.* **2021***, 407*, 124399.

101. Avio, C. G.; Gorbi, S.; Regoli, F. Plastics and microplastics in the oceans: From emerging pollutants to emerged threat. *Mar. Environ. Res.* **2017***, 128*, 2-11.

102. Hayes, A.; Kirkbride, K. P.; Leterme, S. C. Variation in polymer types and abundance of microplastics from two rivers and beaches in Adelaide, South Australia. *Mar. Pollut. Bull.* **2021***, 172*, 112842.

103. Crawford, C. B.; Quinn, B. In *10 - Microplastic identification techniques;* Crawford, C. B., Quinn, B., Eds.; Microplastic Pollutants; Elsevier: 2017; pp 219-267.

104. Gola, D.; Kumar Tyagi, P.; Arya, A.; Chauhan, N.; Agarwal, M.; Singh, S. K.; Gola, S. The impact of microplastics on marine environment: A review. *Environmental Nanotechnology, Monitoring & Management* **2021***, 16*, 100552.

105. Choong, W. S.; Hadibarata, T.; Yuniarto, A.; Tang, K. H. D.; Abdullah, F.; Syafrudin, M.; Al Farraj, D. A.; Al-Mohaimeed, A. M. Characterization of microplastics in the water and sediment of Baram River estuary, Borneo Island. *Mar. Pollut. Bull.* **2021***, 172*, 112880.

106. Tongo, I.; Erhunmwunse, N. O. Effects of ingestion of polyethylene microplastics on survival rate, opercular respiration rate and swimming performance of African catfish (Clarias gariepinus). *J. Hazard. Mater.* **2022***, 423*, 127237.